Giant magnetoresistance

Magnetic materials in nanoelectronics

- properties and fabrication

Lecture

M.Urbaniak

Giant magnetoresistance

1. Introduction
2. Magnetoresistance
3. Giant magnetoresistance

Introduction

Normal metal resistance
intrinsic resistivity – due solely to phonons in a perfect lattice [5]

Bloch-Grüneisen formula [5]:

$$\rho_i(T) = \frac{C}{M\theta}\left(\frac{T}{\theta}\right)^5 \int_0^{\theta/T} \frac{z^5 e^z}{(e^z-1)^2}\,dz$$

θ – Debye temperature, M – atomic mass

- the formula was derived for monovalent metal with spherical Fermi surface and phonon spectrum from Debye model
- despite this the formula is useful for initial analysis of experimental results

Note the huge number of references used to create the diagram to the right

image from: R.A. Matula, J.Phys.Chem.Ref.Data **8**, 1147 (1979)

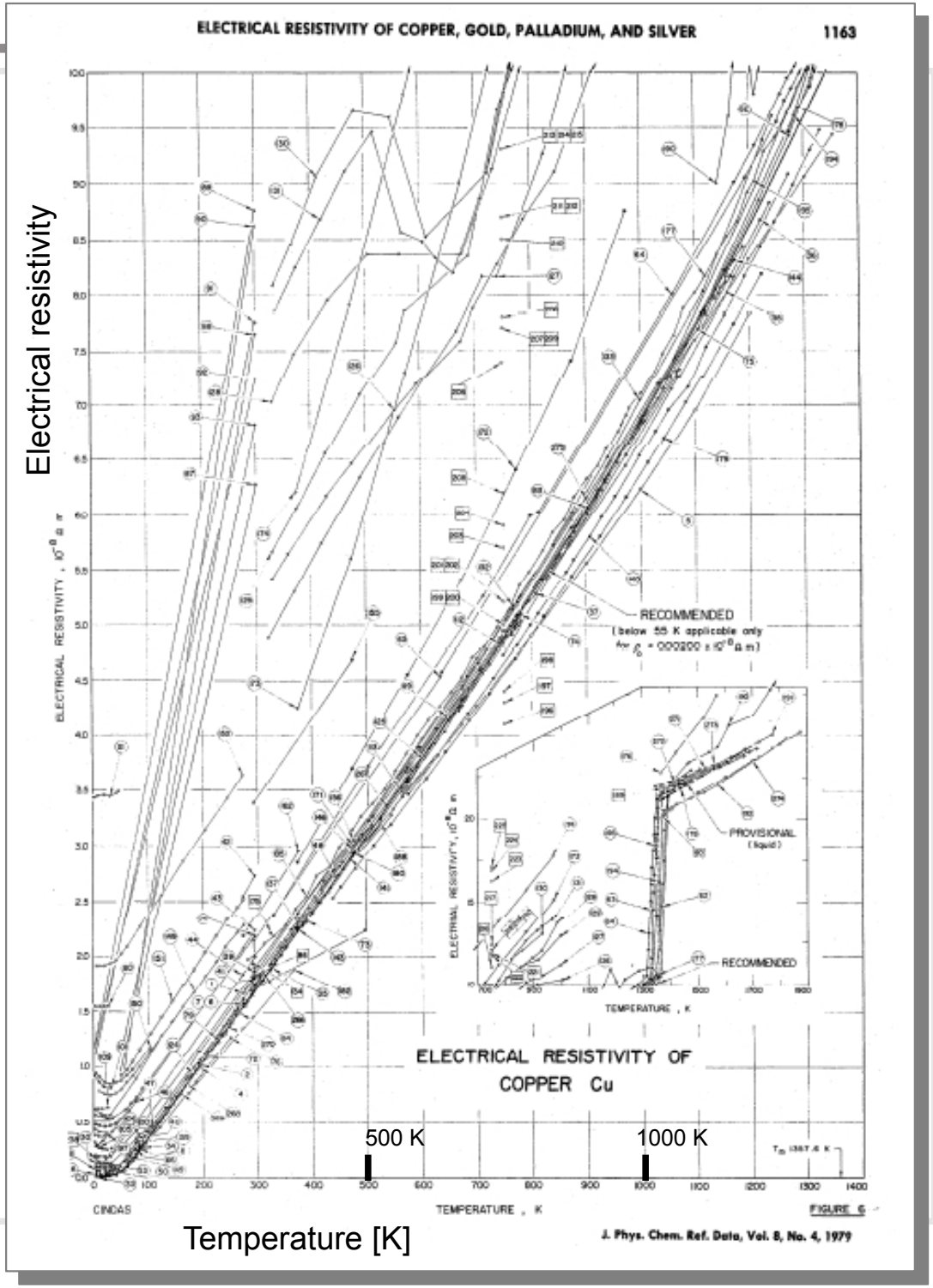

Introduction

Bloch-Grüneisen equation for limiting temperatures [5]:

$$T \to 0: \rho_i(T) \to 124.431 \left(\frac{T}{\theta}\right)^5$$

$$T \to \infty: \rho_i(T) \to \frac{C}{4M\theta}\left(\frac{T}{\theta}\right)$$

	θ at 298 K [K] [5,11]
Au	178±8
Ag	221
Cu	320
Fe	467 [11]
Co	445 [11]
Ni	450 [11]

image from: R.A. Matula, J.Phys.Chem.Ref.Data **8**, 1147 (1979)

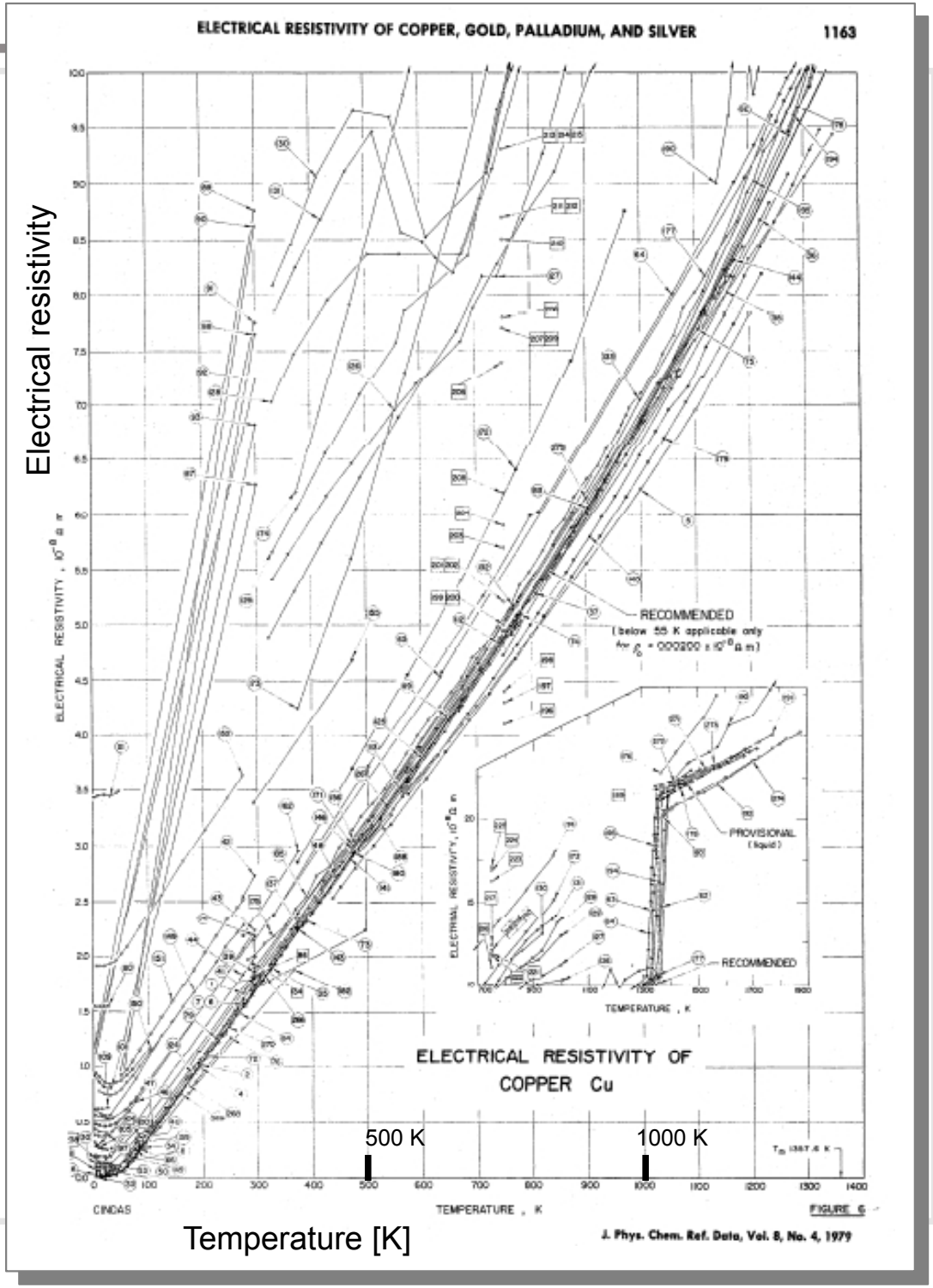

Introduction

Mathiessen rule (empirical) – the total resistivity of a specimen is a sum of resistivities due to phonons, impurities, defects, etc. (approx. valid if scattering events are independent)

$$\rho = \rho_{phonons} + \rho_{impurities} + \ldots$$

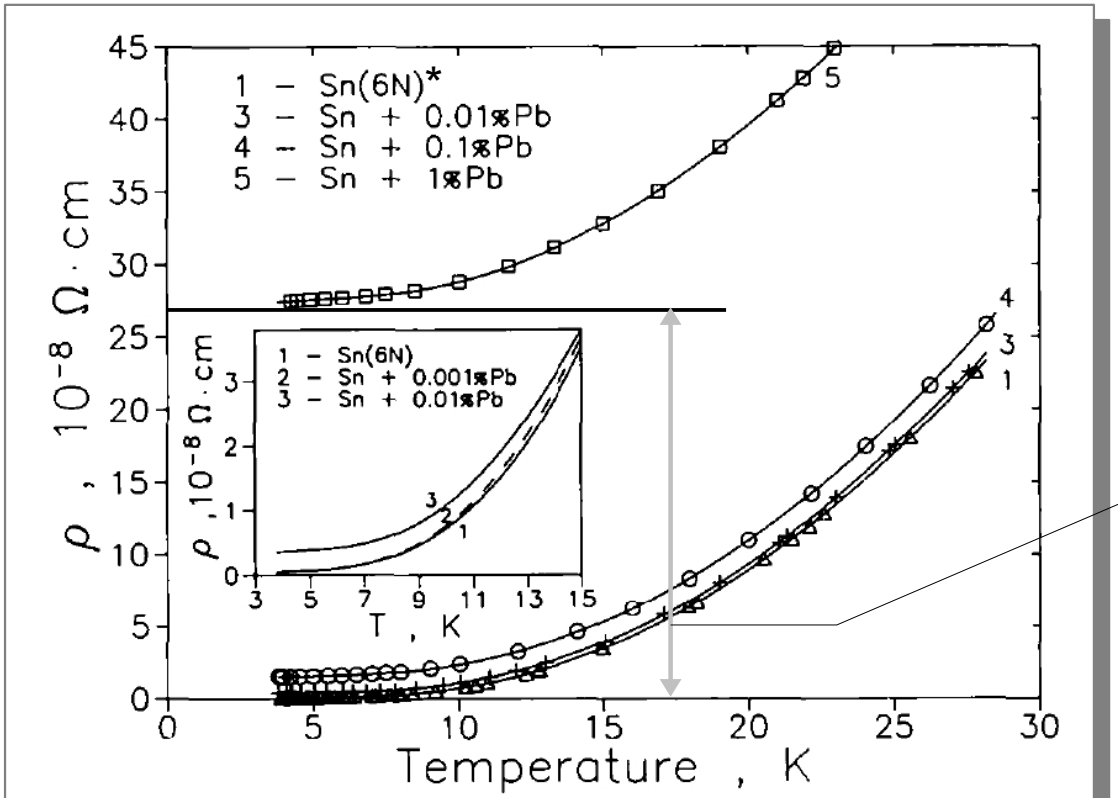

Fig. 1. Dependence of the electrical resistivity of lead-doped tin on temperature at various concentrations of lead admixtures.

- tin + lead, T≤28 K
- the resistivity of the Sn+Pb mixture increases with Pb concentration
- the dependence of a residual resistivity on Pb concentration is not linear

image from: R. Wawryk, J. Rafalowicz, Cz. Marucha, K. Balcerek, International Journal of Thermophysics **15**, 379 (1994)

*99.9999% purity; see “Why do we need high purity metals?” at https://www.ameslab.gov/mpc/purityFAQ for absolute and metals basis purity (retrieved on 2014.03.11)

Introduction

Size effect in resistivity

In thin films* the resistivity depends additionally on the thickness *t* of the layer

- in bulk samples only small fraction of electrons experiences the scattering at the outer boundaries
- in thin films (panel b) the contribution from surface scattering becomes important and the resistivity increases

The theoretical determination of the ρ(*t*) dependence is very difficult. The approximate Fuchs- Sondheimer theory predicts the following ρ(*t*) dependence [6,34]:

$$\frac{\sigma_0}{\sigma} = 1 + \frac{3}{8}\frac{\lambda}{t}(1-p) \qquad \left(\frac{t}{\lambda} \gg 1\right)$$

$$\frac{\sigma_0}{\sigma} = \frac{4\lambda}{3t(1+2p)\ln(\lambda/t)} \qquad \left(\frac{t}{\lambda} \ll 1\right)$$

λ – mean free path (mfp), p – fraction of electrons that are specularly** reflected at the outer boundaries, σ_0 – bulk conductivity

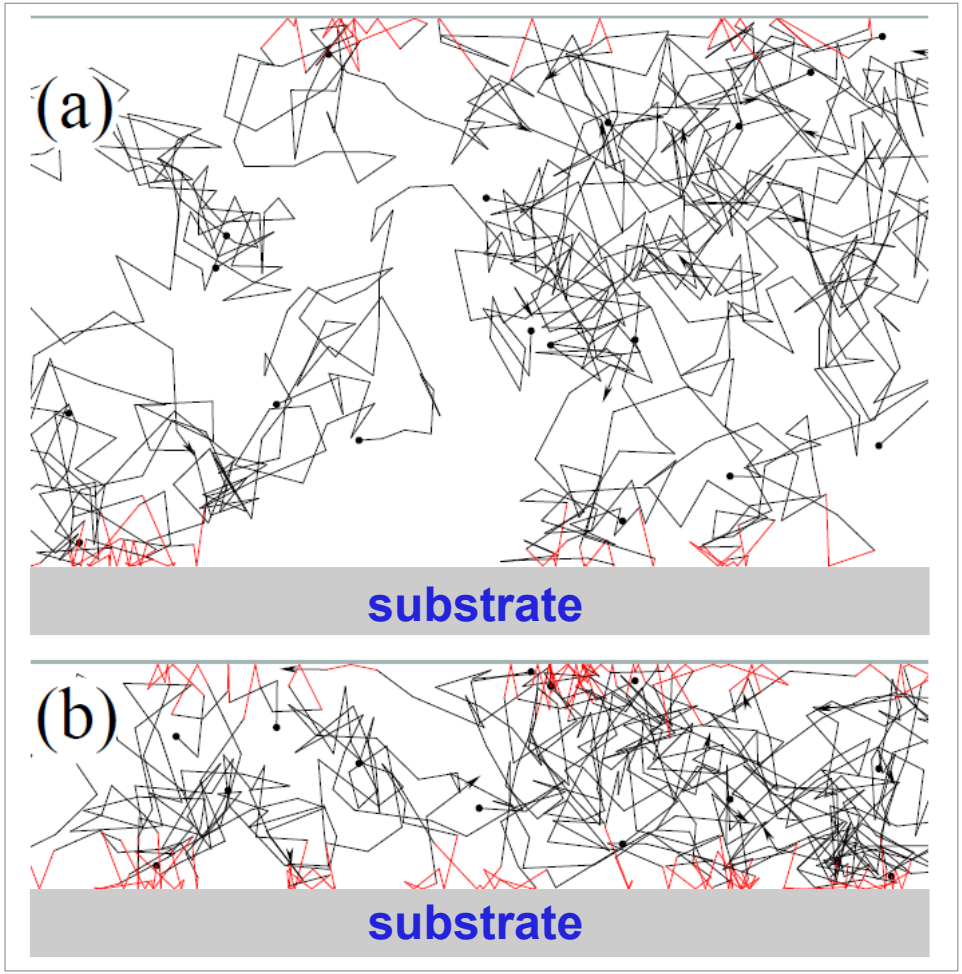

**speculum – Latin. mirror

*a film is said to be thin if the mean free path of current carriers is comparable with its thickness (compare the definition of magnetic thin film)

Introduction

Size effect in resistivity

In thin films* the resistivity depends additionally on the thickness *t* of the layer

- in bulk samples only small fraction of electrons experiences the scattering at the outer boundaries
- in thin films the contribution from surface scattering becomes important and the resistivity increases

The theoretical determination of the ρ(*t*) dependence is very difficult. The approximate Fuchs- Sondheimer theory predicts the following ρ(*t*) dependence [6,34]:

$$\frac{\sigma_0}{\sigma} = 1 + \frac{3}{8}\frac{\lambda}{t}(1-p) \qquad \left(\frac{t}{\lambda} \gg 1\right)$$

$$\frac{\sigma_0}{\sigma} = \frac{4\lambda}{3t(1+2p)\ln(\lambda/t)} \qquad \left(\frac{t}{\lambda} \ll 1\right)$$

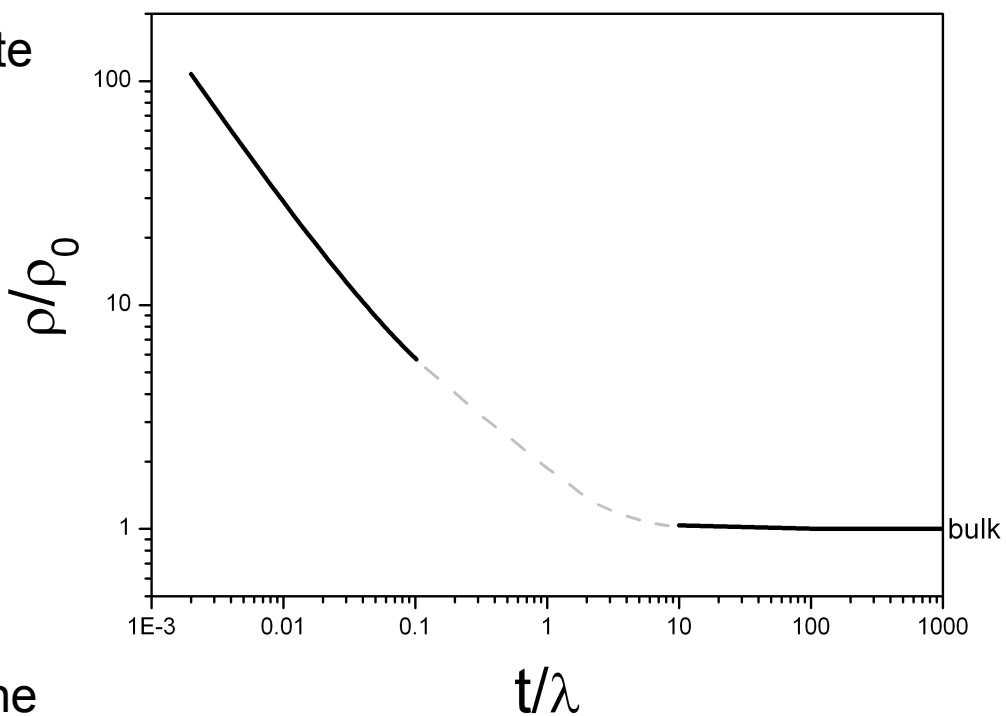

λ – mean free path (mfp), *p* – fraction of electrons that are specularly** reflected at the outer boundaries, σ_0 – bulk conductivity

**speculum – Latin. mirror

*a film is said to be thin if the mean free path of current carriers is comparable with its thickness (compare the definition of magnetic thin film)

Introduction

Size effect in resistivity

In thin films* the resistivity depends additionally on the thickness *t* of the layer

- in bulk samples only small fraction of electrons experiences the scattering at the outer boundaries
- in thin films the contribution from surface scattering becomes important and the resistivity increases

thermal evaporation onto 500-nm thick SiO_2 on Si(100) substrates in an ultra high vacuum UHV

- Note that the crystalline structure of the films can change with thickness too.

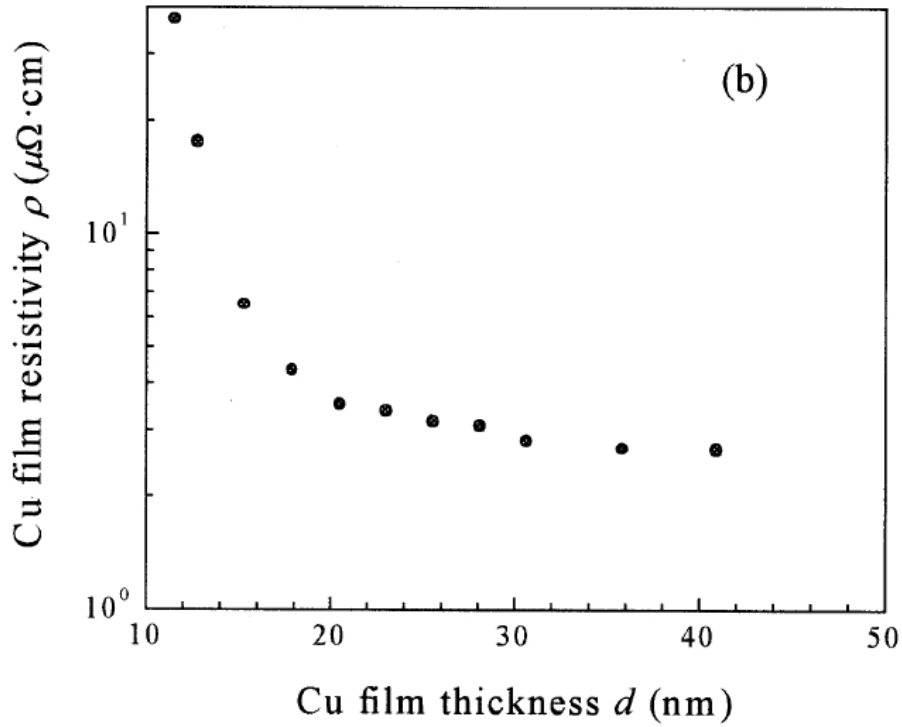

Fig. 2. (a) Sheet resistance R of Cu films vs. deposition time t_d plotted in semi-log scale. and (b) Cu film resistivity ρ plotted as a function of film thickness d on a semi-log scale. The error bars are less than the legend size.

image (fragment) from:
H.-D. Liu, Y.-P. Zhao, G. Ramanath, S.P. Murarka, G.-C. Wang, Thin Solid Films **384**, 151 (2001)

Introduction

Dependence of resistivity on temperature in magnetic metals:

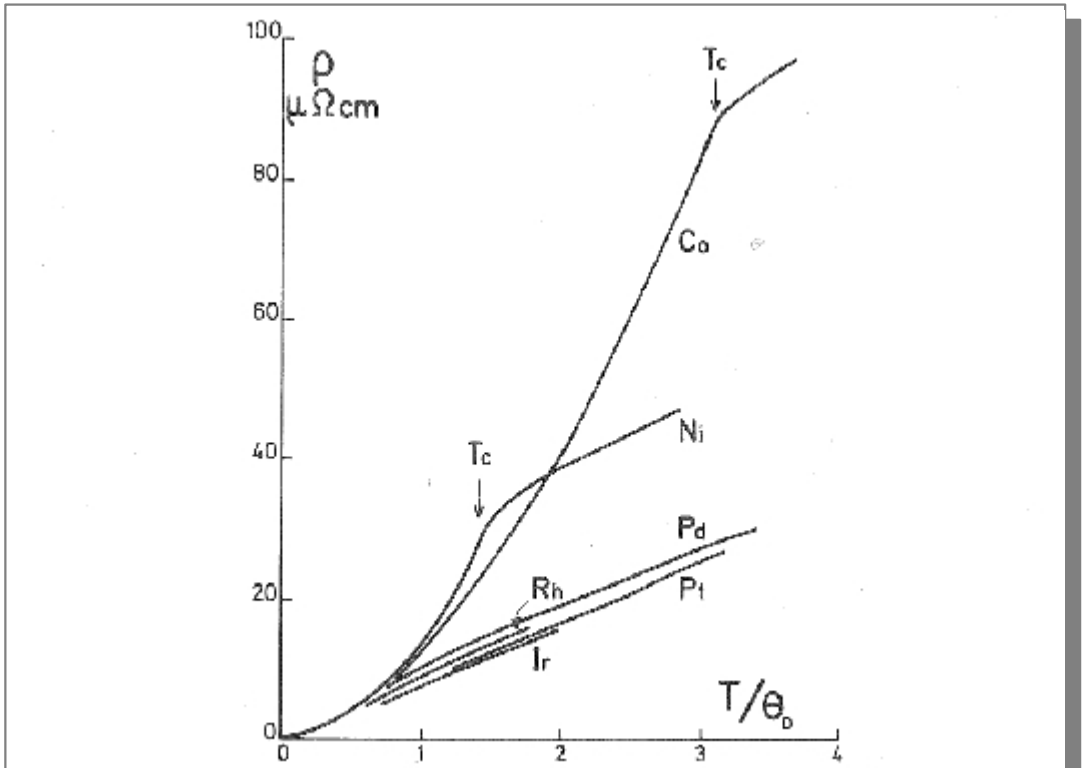

Fig. 10. Resistivity of several transition metals as a function of T/θ_D. θ_D is the Debye temperature.

image from: I.A. Campbell, A. Fert, in “Ferromagnetic Materials” 1982

- below Curie temperature T_c resistivity of a magnetic metals increases with temperature faster than above it
- below T_c temperature increase leads to increased magnetic disorder
- resistivity and magnetic order correlate

T_{Curie}:

Fe 1044 K

Co 1388 K

Ni 627 K

Introduction

Dependence of resistivity on temperature in magnetic metals:

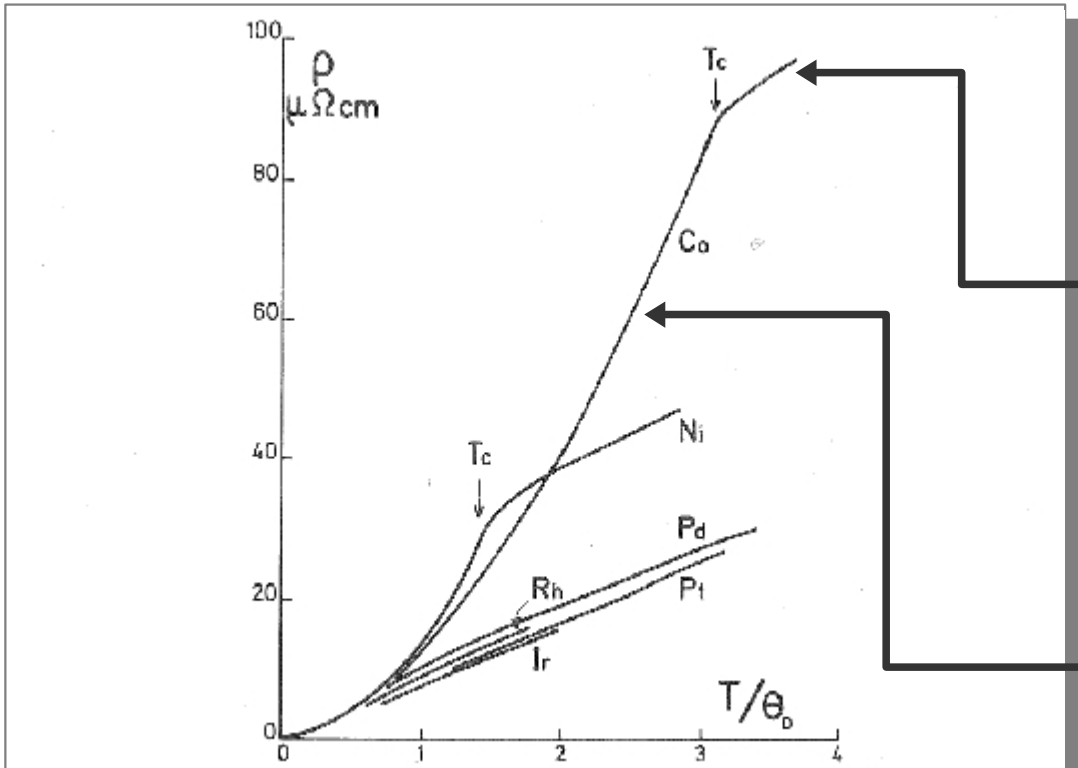

Fig. 10. Resistivity of several transition metals as a function of T/θ_D. θ_D is the Debye temperature.

image from: I.A. Campbell, A. Fert, in “Ferromagnetic Materials” 1982

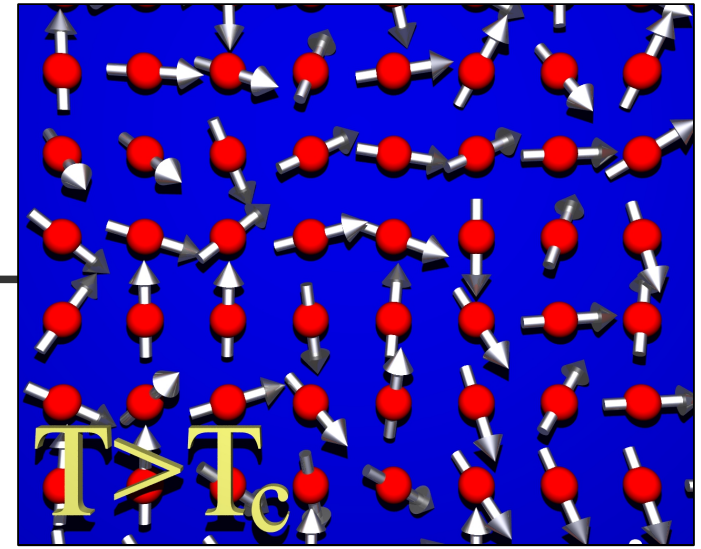

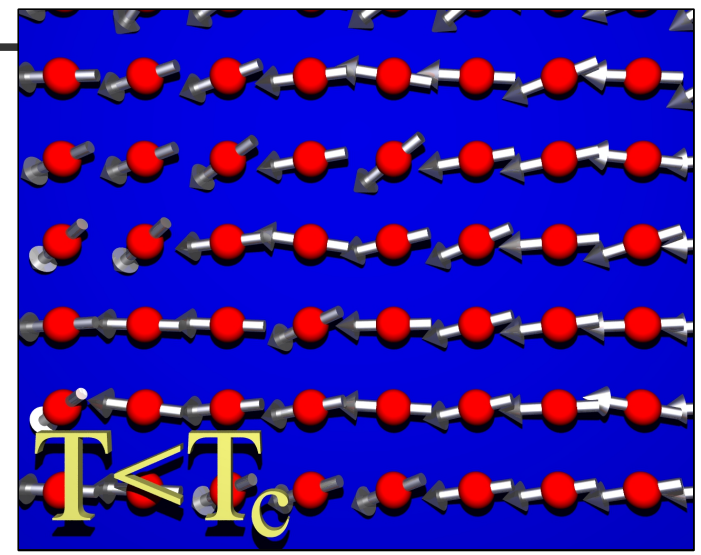

below Curie temperature magnetic moments are ordered

Introduction

Magnons

- at very low temperatures all spins point in almost exactly one direction* determined by the effective magnetic anisotropy

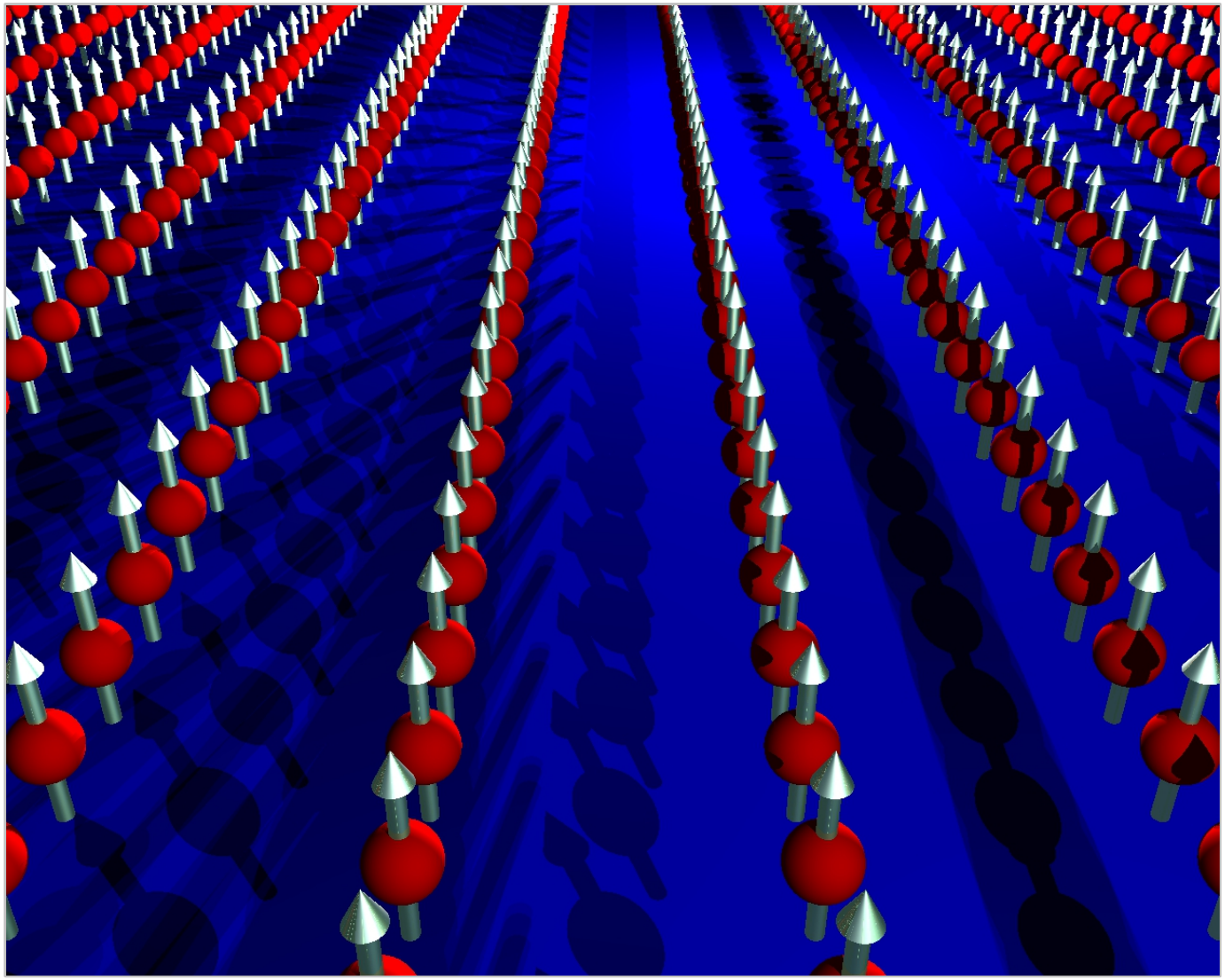

*we assume the bulk sample (negligible fraction of surface spins) and that there are no domain walls

Introduction

Magnons

- at higher temperatures the thermal energy coming from spin-phonon coupling must be accommodated by rearrangement of spins*

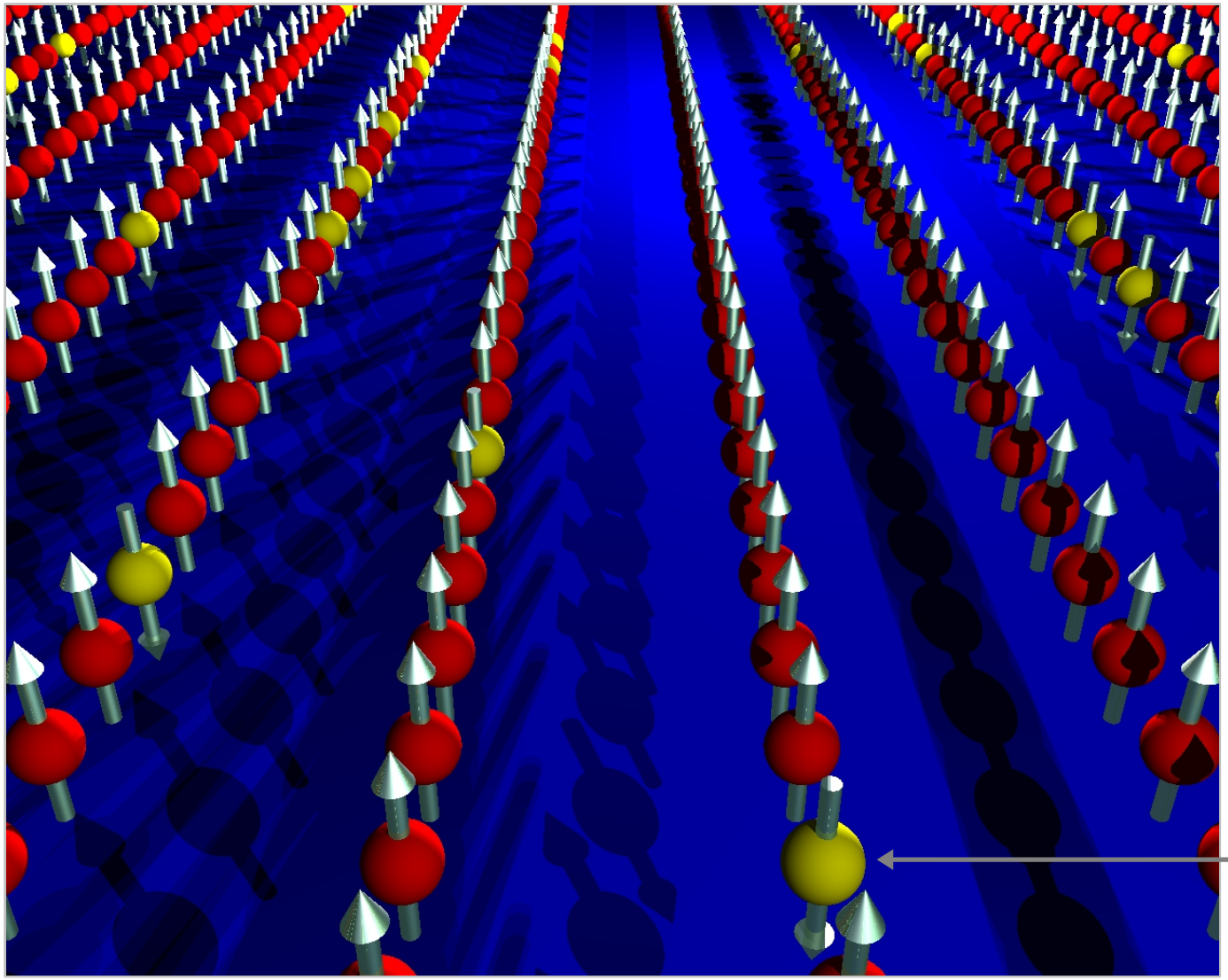

It is energetically costly to reverse single spins *S* [9]:

$$\Delta E = N_{nn} J_{ij} \vec{S}_i \cdot \vec{S}_j$$

N_{nn} - number of nearest neighbors

J_{ij} - exchange integral

...and a state with single flipped spin is not an eigenstate of Hamiltonian [35]

*the spins may be excited directly by magnetic field too.

Introduction

Magnons

- at higher temperatures the thermal energy coming from spin-phonon coupling must be accommodated by rearrangement of spins*

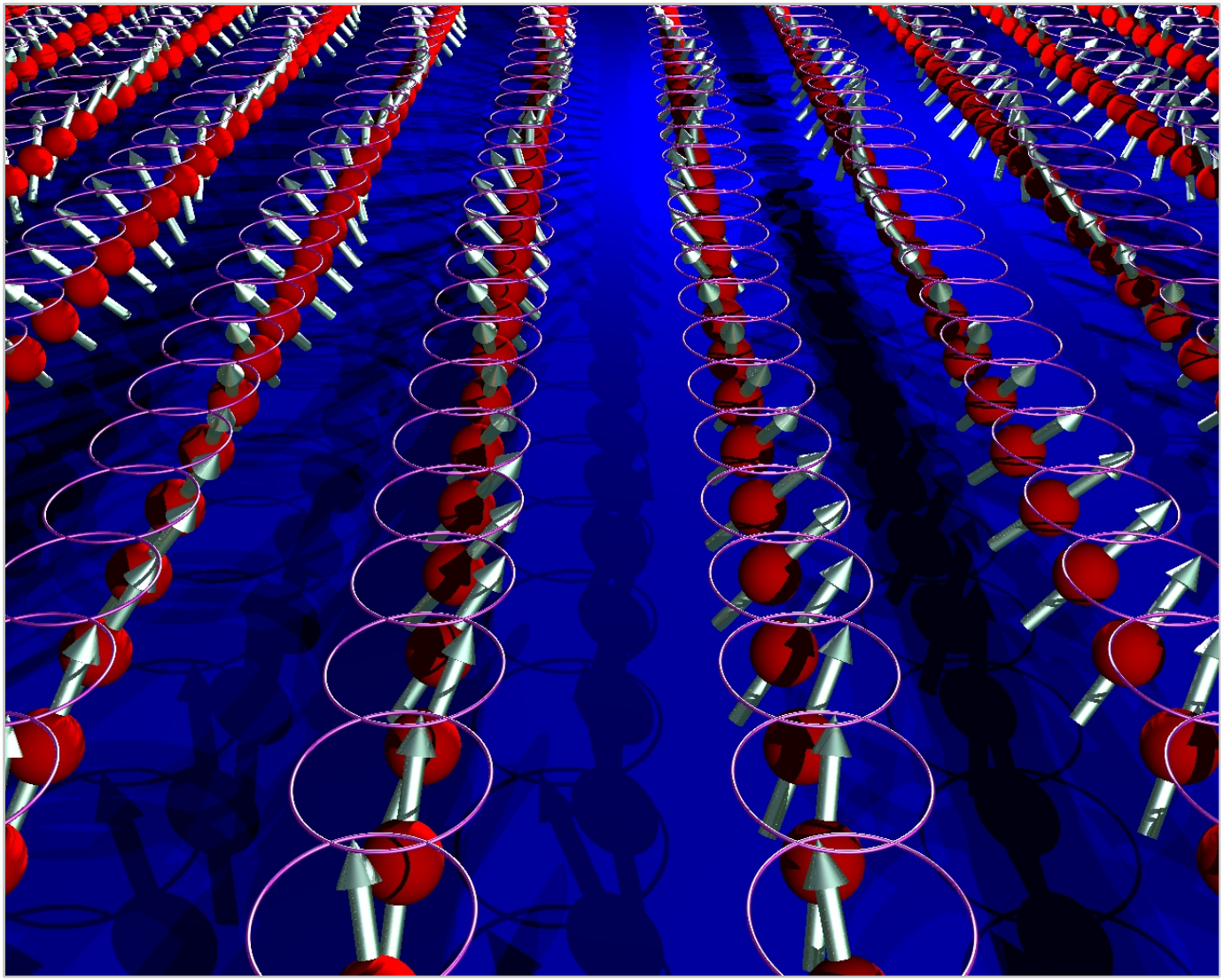

It is energetically costly to reverse single spins *S* [9]:

$$\Delta E = N_{nn} J_{ij} \vec{S}_i \cdot \vec{S}_j$$

N_{nn} - number of nearest neighbors

J_{ij} - exchange integral

Correlated movement/ precession of spins (pictured here as classical moments) reduces the energy of a spin system by [9]:

$$\Delta E = \left(\frac{h}{2\pi}\right)\omega_q \approx 2SJq^2a^2$$

*the spins may be excited directly by magnetic field too.

Introduction

Magnons

- at higher temperatures the thermal energy coming from spin-phonon coupling must be accommodated by rearrangement of spins*

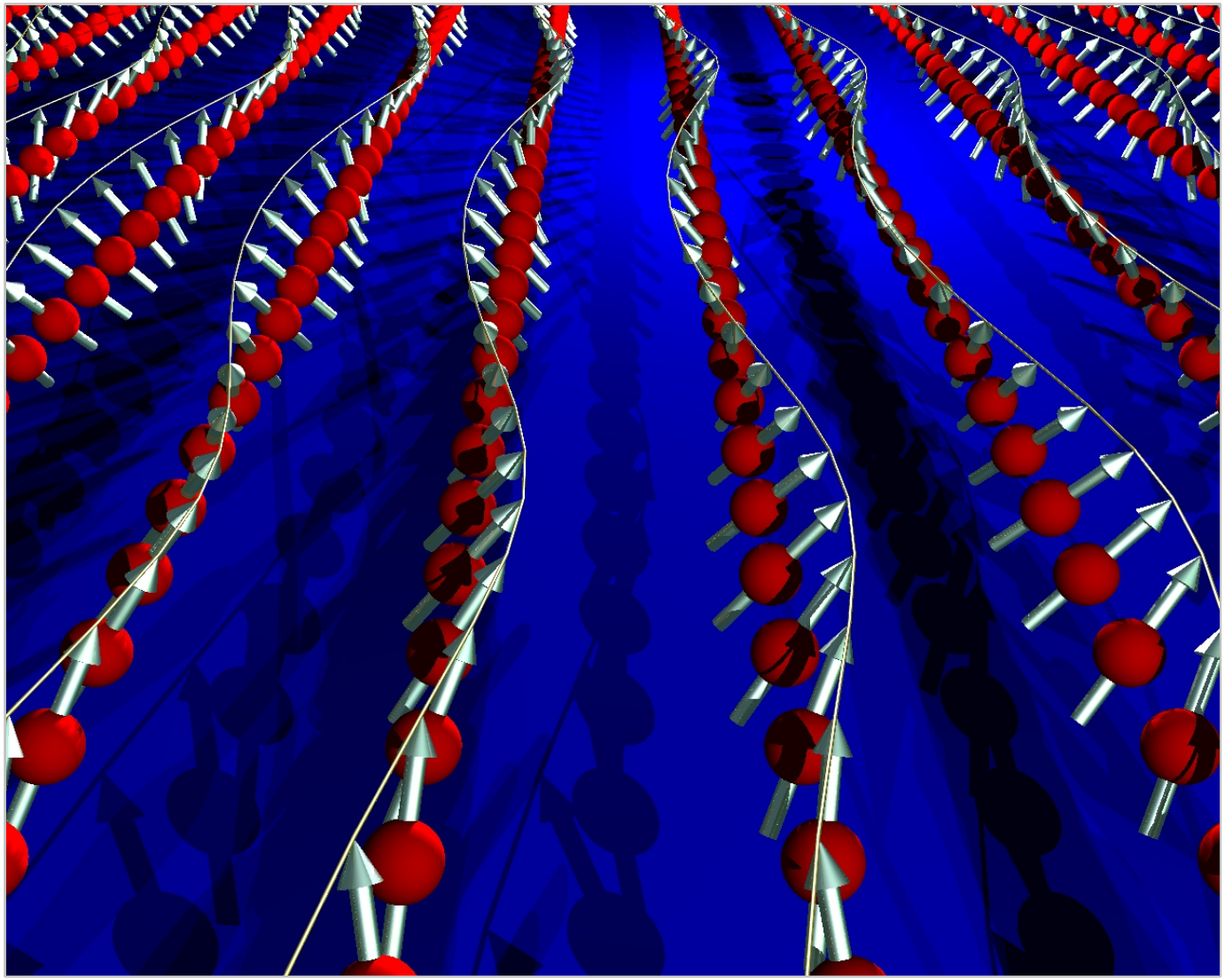

Correlated movement/ precession of spins (pictured here as classical moments) reduces the energy of a spin system by [9]:

$$\Delta E = \left(\frac{h}{2\pi}\right)\omega_q \approx 2SJq^2a^2$$

Each elementary excitation reduces the total spin NS of the system by one unit.

*the spins may be excited directly by magnetic field too.

Introduction

Magnon contribution to resistivity

- measurement in pulsed magnetic fields
- almost linear and non-saturating decrease of resistivity in fields above technical saturation (paraprocess)
- spin-flip and non-spin-flip (on phonons, other electrons [8]) scattering events are responsible for resistance
- spin-flip scattering on magnons (s-d interband transitions) is responsible for magnetoresistance
- “effect results from a reduction of electron-magnon scattering processes due to a damping of the spin waves at high fields” [8]
- magnon magnetoresistance is estimated to saturate at 80T at 50K and **2000 T** [sic] at 450 K

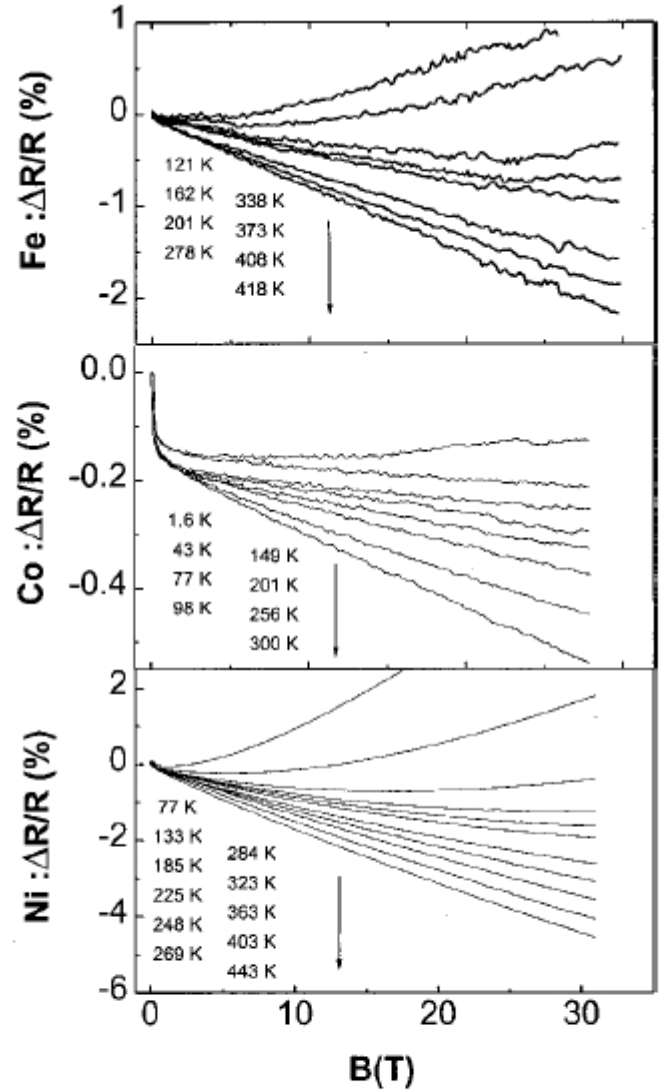

FIG. 1. Longitudinal high-field magnetoresistance ($B \| i$) at various temperatures for Fe, Co, and Ni epitaxial films – $Fe_{80\,nm}/MgO$, $Co_{7\,nm}/Al_2O_3$, and $Ni_{20\,nm}/MgO$. Note the extrinsic negative MR below the technical saturation of the magnetization for Co due to grain boundary effects.

image from: B. Raquet, M. Viret, E. Sondergard, O. Cespedes, R. Mamy, Phys. Rev. B **66**, 024433 (2002)

Introduction

Magnon contribution to resistivity

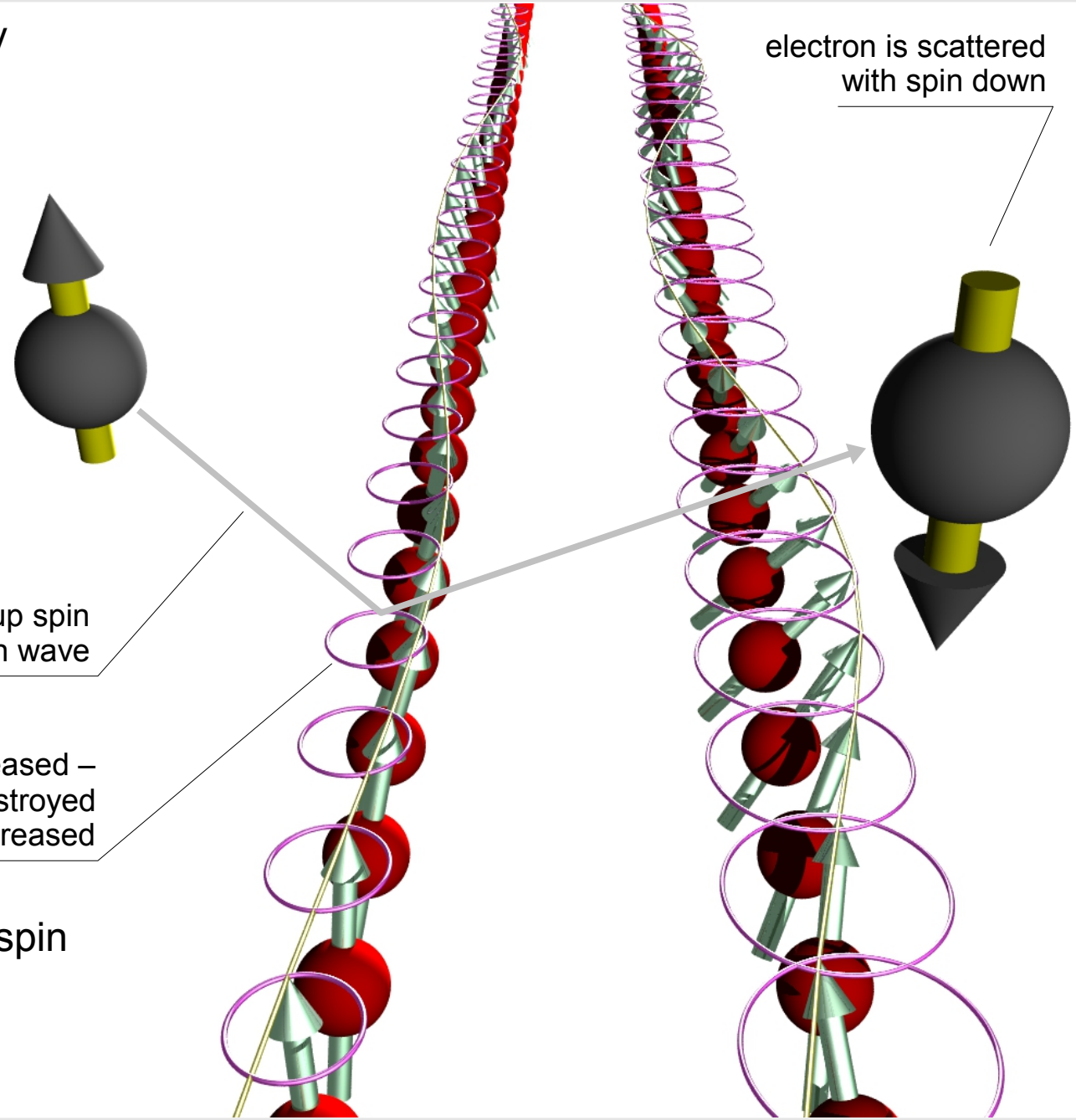

- In spin-flip scattering electron spin is transferred to quantized excitation of lattice spins – magnon. For electron $\Delta s = \pm 1$.

Introduction

Band splitting in ferromagnetic materials

normal metal (Cu, Au, etc.)

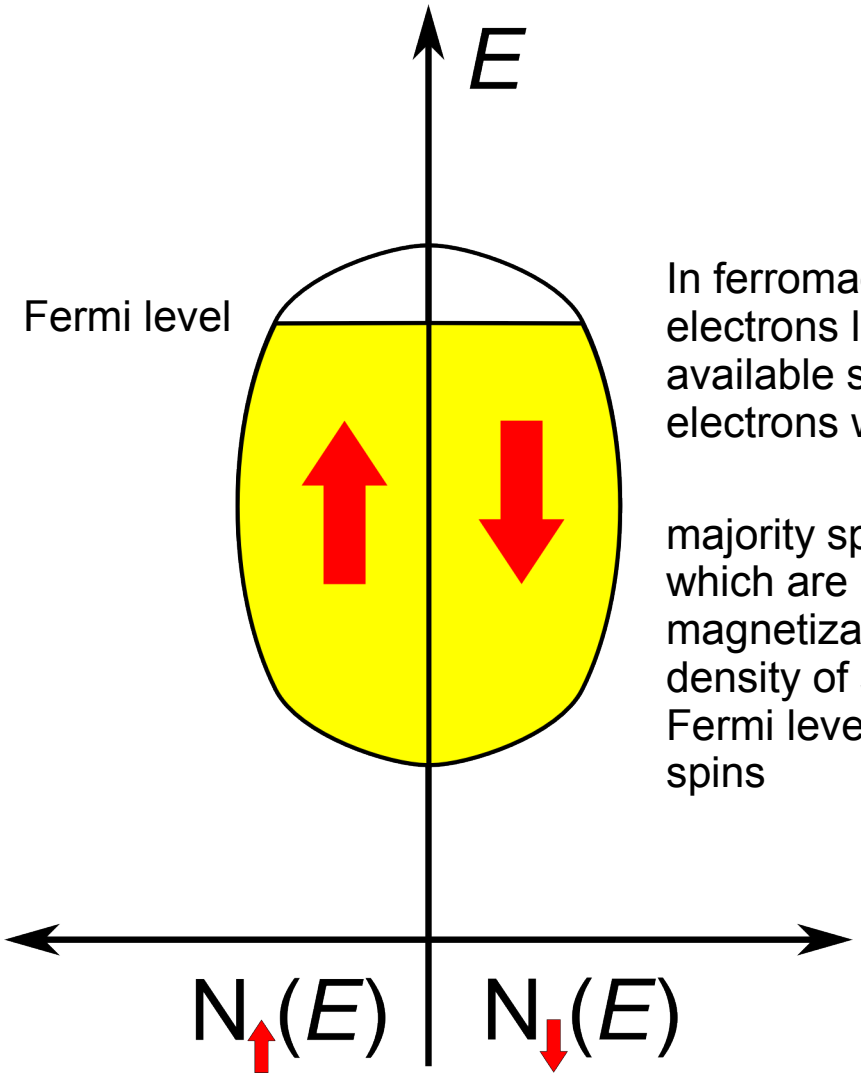

In ferromagnetic metals band splitting of d-electrons leads to different densities of available states at Fermi energy for electrons with opposite spins

majority spins (those which are parallel to magnetization) have lower density of states (DOS) at Fermi level than down spins

ferromagnetic metal (Fe, Co, etc.)

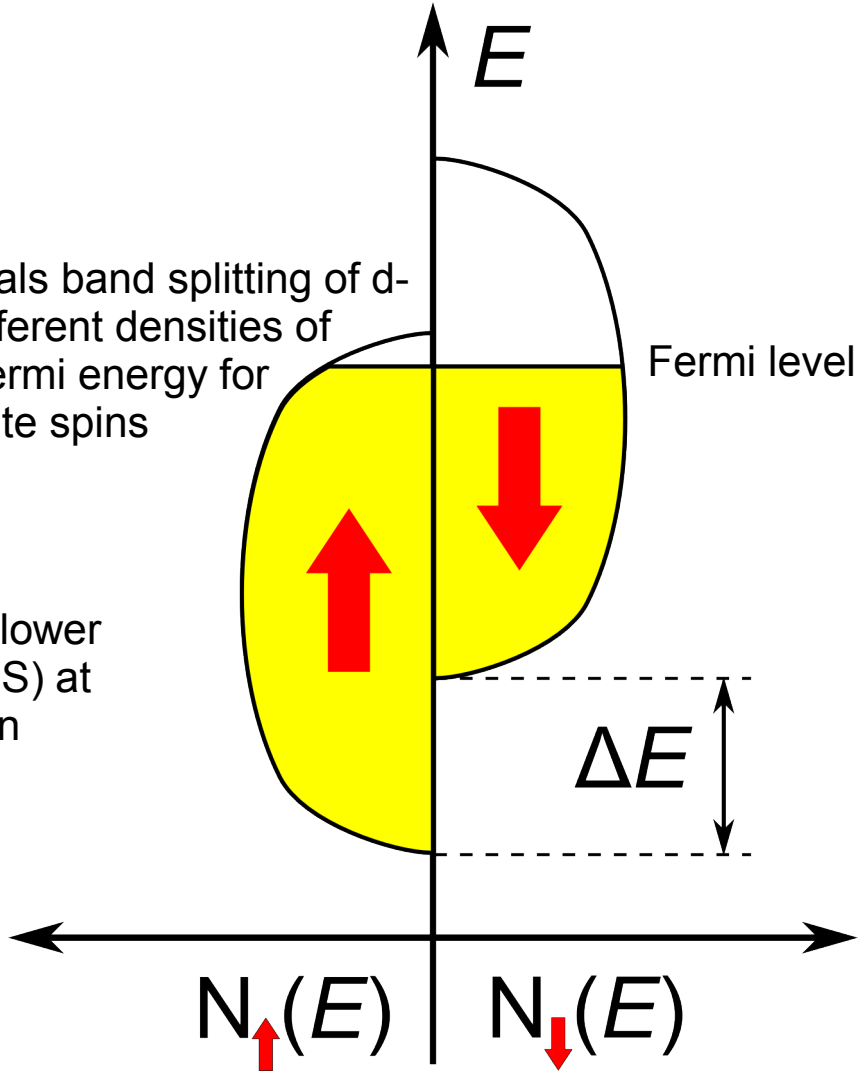

Introduction

Band splitting in ferromagnetic materials

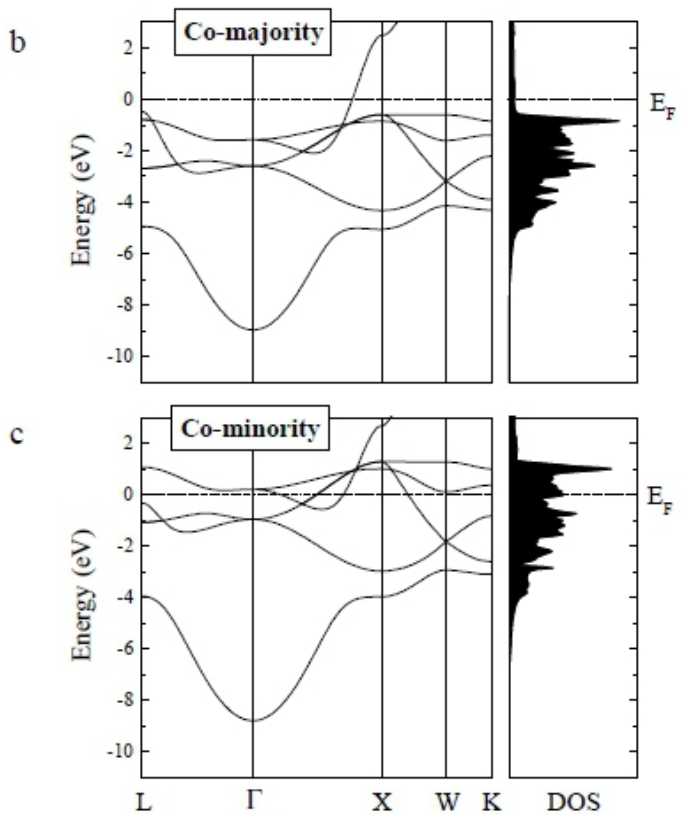

Electronic band structures (left panels) and the density of states (right panels) of Cu (a) and fcc Co for the majority-spin (b) and minority-spin (c) electrons. The band structure of non-magnetic Cu is same for the up-spin and down-spin electrons. It is characterized by the fully occupied *d* bands and the presence of a dispersive *sp* band at the Fermi energy, which result in high conductivity of Cu. The electronic structure of ferromagnetic Co is different for the two spin orientations and is characterized by the exchange-split *d* bands. The Fermi level lies within the *sp* band for the majority-spin electrons, which leads to high conductivity of majority-spin channel. The Fermi level lies, however, within the *d* band for the minority-spin electrons resulting in low conductivity of the minority-spin channel. In the latter case the *sp* electrons are strongly hybridized with the *d* electrons, which diminishes their contribution to conduction.

- in some ferromagnetic materials the density of states of up-spins may be close to zero
- in Co the d-band DOS for spin-up electrons is about 10 times lower than that of down-spin electrons

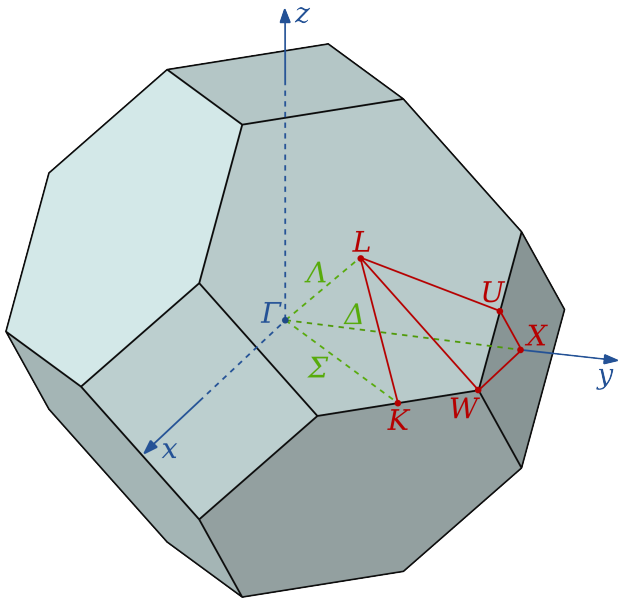

image from Wikimedia Commons; author Inductiveload

graphics from: Perspectives of Giant Magnetoresistance, E. Y. Tsymbal, D. G. Pettifor, published in Solid State Physics, ed. by H. Ehrenreich and F. Spaepen, Vol. 56 (Academic Press, 2001) pp.113-237

Introduction

Mott – two current model, 1936.

- mobile sp-electrons are responsible for electronic conductivity [3]
- s- electrons can be scattered to free states near Fermi level
- density of states of d-electrons in ferromagnetic metal is different for spin-up and spin-down electrons
- the conductivity of given type of carriers depends on the number of free states available as final states of scattering events
- probability of spin-flip scattering is much lower than the probability of scattering without the change of spin

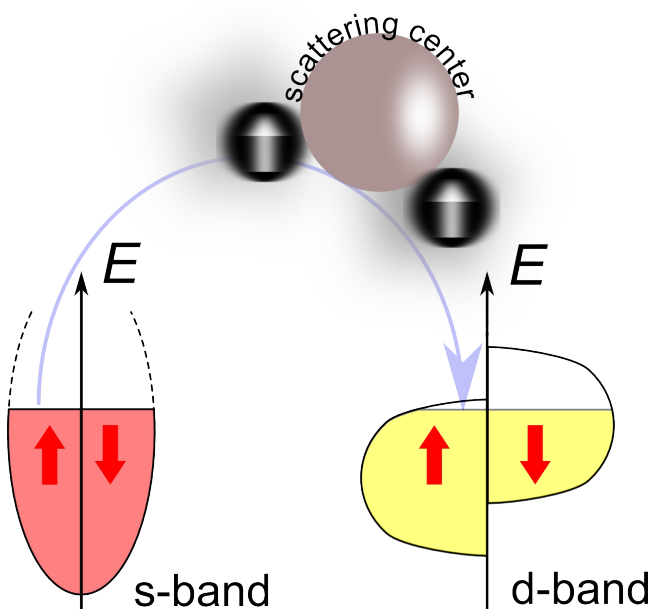

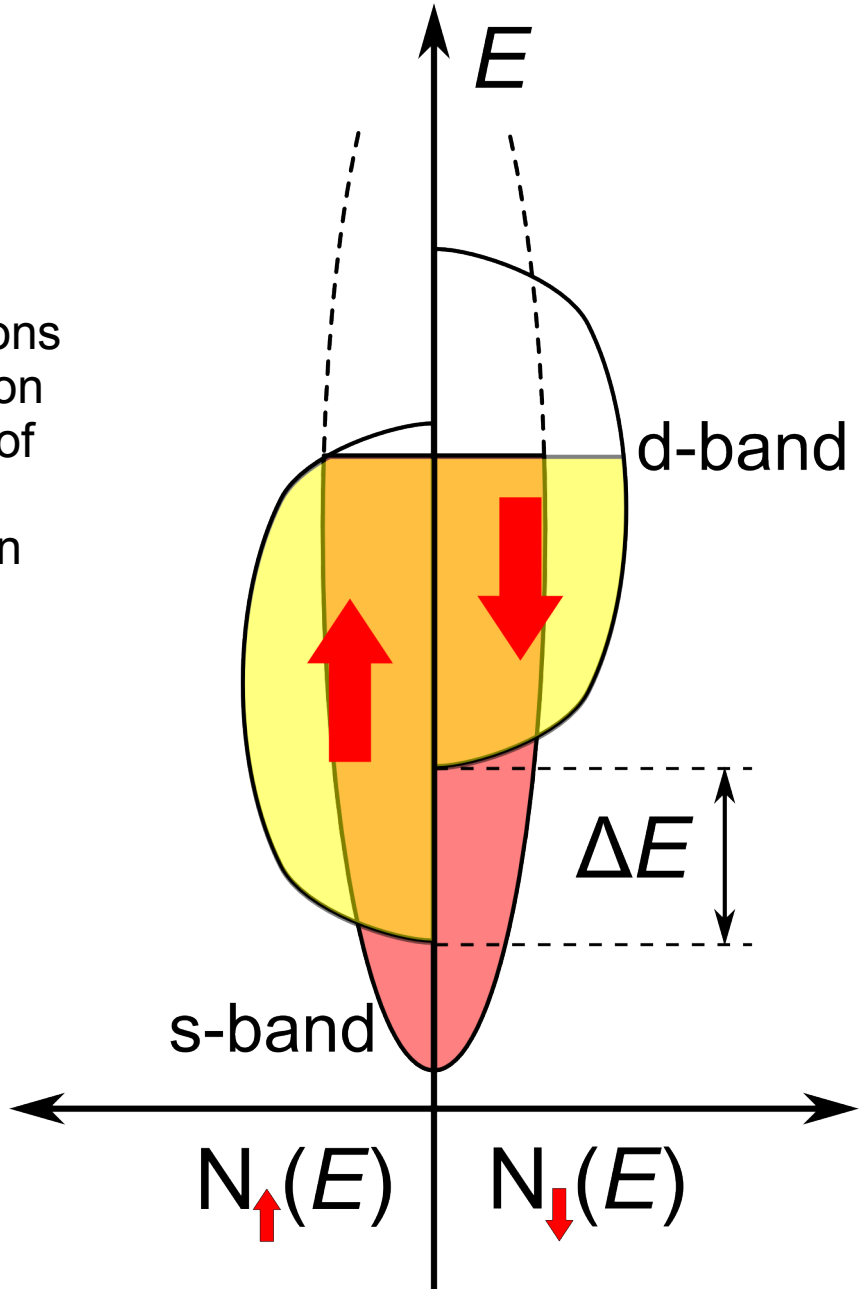

Introduction

Mott – two current model, 1936.

- the conductivity of a metal is a sum of independent conductivities of up and down-spins channels [3]

$$\sigma = \sigma_{\uparrow} + \sigma_{\downarrow}$$

- the relaxation time τ is given by Fermi golden rule (mean free path: $\lambda = \tau v_F$, v_F - Fermi velocity, of the order of 0.5×10^6m/s) [3,9]:

$$\tau^{-1} \propto \left\langle V_{scatt}^2 \right\rangle D(E_F)$$

average value of scattering potential

- the scattering potential needs not to be spin-dependent for resistivities of spin channels to be different – different DOS-es for opposite spins are enough

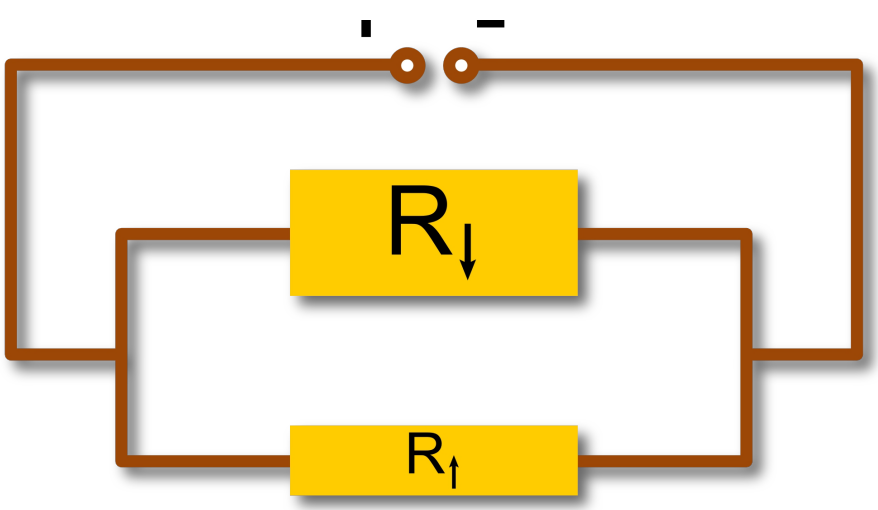

If spin-flip events are negligible current can be considered as carried in-parallel by two spin channels with spins parallel and antiparallel to quantization axis [12]

Introduction

Mott – two current model, 1936.

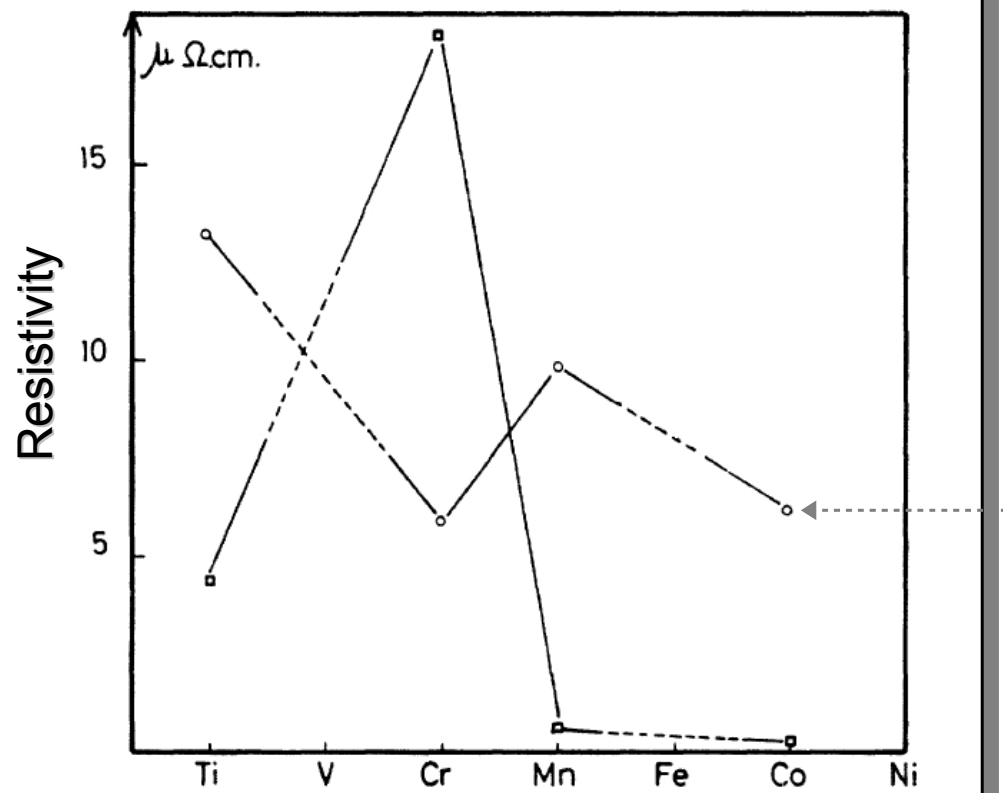

FIG. 3 Residual resistivities $\rho_{\uparrow}^{0}$ and $\rho_{\downarrow}^{0}$ per percent concentration of Ti, Cr, Mn, and Co impurities in Ni. Squares: $\rho_{\uparrow}^{0}$. Circles: $\rho_{\downarrow}^{0}$.

image from: A. Fert and I. A. Campbell, Phys. Rev. Lett. **21**, 1190 (1968)

$$\alpha = \rho_{\downarrow}^{0} / \rho_{\uparrow}^{0}$$

- **Ni** with impurities at low temperatures
- the spin-down channel conductivity can be many times lower than the resistivity of the up-spin channel

$$\alpha_{Co} = 30 \qquad \alpha_{Mn} = 16$$

- the maximum for Cr impurity is associated with the bound state crossing the spin-up Fermi level [10]

spin-down channel

Introduction

Giant Magnetoresistance (GMR) – **Nobel Prize 2007 (A. Fert, P. Grünberg)**

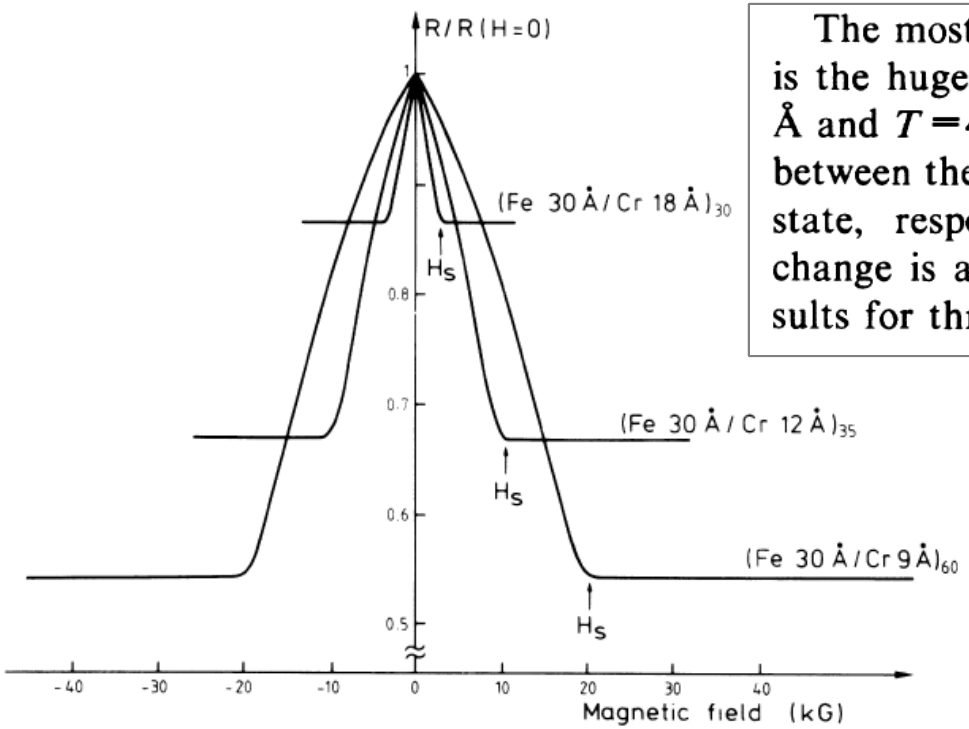

FIG. 3 Magnetoresistance of three Fe/Cr superlattices at 4.2 K. The current and the applied field are along the same [110] axis in the plane of the layers.

The most remarkable result exhibited in Figs. 2 and 3 is the huge value of the magnetoresistance. For $t_{Cr}=9$ Å and $T=4.2$ K, see Fig. 2, there is almost a factor of 2 between the resistivities at zero field and in the saturated state, respectively (in absolute value, the resistivity change is about 23 $\mu\Omega$ cm). By comparison of the results for three different samples in Fig. 3, it can be seen

"In conclusion, we have found a giant magnetoresistance in (001)Fe/(001)/Cr superlattices when, for thin Cr layers (9, 12, and 18 Å), there is **an antiparallel coupling of the neighbor Fe layers** at zero field."- M.N. Baibich *et al*.

image from M.N. Baibich, J.M. Broto, **A. Fert**, F. Nguyen Van Dau, F. Petroff, P. Eitenne, G. Creuzet, A. Friederich, J. Chazelas, Phys. Rev. Lett. **61**, 2472 (1988)

Introduction

Giant Magnetoresistance (GMR) – **Nobel Prize 2007 (A. Fert, P. Grünberg)**

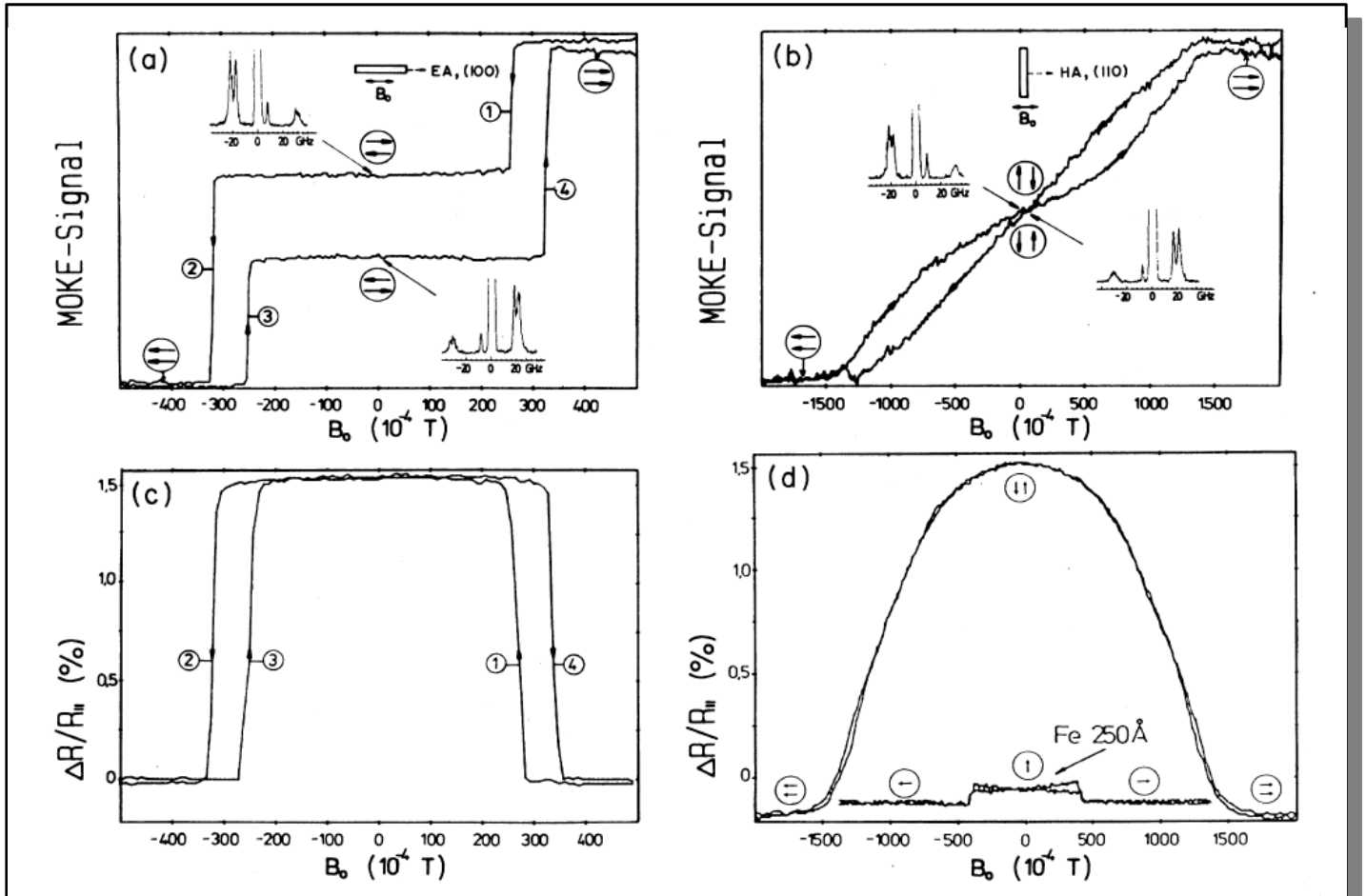

FIG. 2. (a)–(b) MOKE hysteresis curves and (c)–(d) magnetoresistance $\Delta R/R_{\parallel} = (R - R_{\parallel})/R_{\parallel}$ from Fe double layers with antiferromagnetic coupling. Also, (d) displays the anisotropic MR effect of a 250-Å-thick Fe film.

The experimental results reported here show that the **antiparallel alignment of the magnetizations in our double layers produces an appreciable increase of the electrical resistivity**. We propose that this is caused by spin-flip scattering. Electrons in one...

image from G. Binasch, **P. Grünberg**, F. Saurenbach, W. Zinn, Phys. Rev. B **39**, 4828 (1989)

the first interpretation was not correct – see later

Introduction

Giant Magnetoresistance (GMR) – **Nobel Prize 2007 (A. Fert, P. Grünberg)**

VOLUME 61, NUMBER 21 PHYSICAL REVIEW LETTERS 21 NOVEMBER 1988

Giant Magnetoresistance of (001) Fe/(001) Cr Magnetic Superlattices

M. N. Baibich,[a] J. M. Broto, A. Fert, F. Nguyen Van Dau, and F. Petroff
Laboratoire de Physique des Solides, Université Paris-Sud, F-91405 Orsay, France

P. Eitenne, G. Creuzet, A. Friederich, and J. Chazelas
Laboratoire Central de Recherches, Thomson CSF, B.P. 10, F-91401 Orsay, France
(Received 24 August 1988)

RAPID COMMUNICATIONS

PHYSICAL REVIEW B VOLUME 39, NUMBER 7 1 MARCH 1989

Enhanced magnetoresistance in layered magnetic structures with antiferromagnetic interlayer exchange

G. Binasch, P. Grünberg, F. Saurenbach, and W. Zinn
Institut für Festkörperforschung, Kernforschungsanlage Jülich G.m.b.H., Postfach 1913, D-5170 Jülich, West Germany
(Received 31 May 1988; revised manuscript received 12 December 1988)

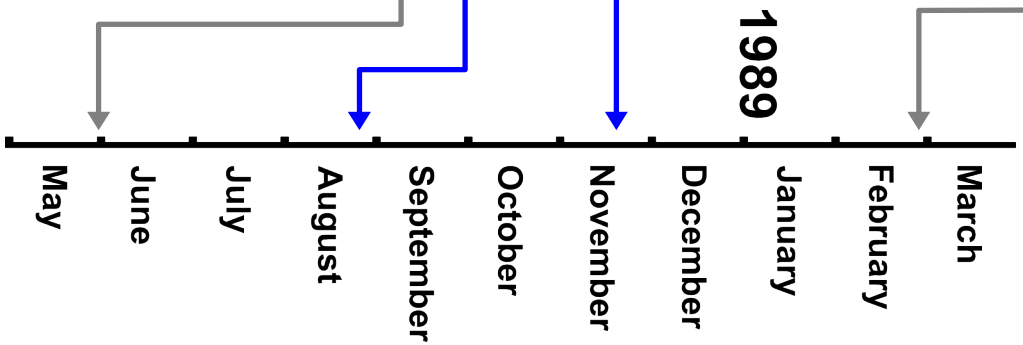

Magnetoresistance

Types of magnetoresistance (incomplete list)

Type of magnetoresistance	Systems	Values	Note
ordinary (OMR)	all conducting materials	approx. 10^{-2} % in metals in RT in up to 2T in high fields (30T) 47% in Cu (at 78K) and 380% in Bi [13]	Lorentz force changes orbits of carriers De Haas-Shubnikov effect – high field oscillations of resistance
anisotropic (AMR)	ferromagnetic materials	several percent at RT (NiCo alloys [14]) in small fields	depends on orientation of current relative to magnetization; high field sensitivity (NiFe)
giant (GMR)	ferromagnetic materials	several dozens percent in small fields [3]	depends on relative orientation of magnetic moments
tunneling (TMR)	ferromagnetic materials	several hundred percent in small fields	depends on the orientation of magnetic moments of electrodes separated by insulating film
colossal (CMR)	transition metal oxides	several hundred percent in several Tesla	phase transition paramagnet-ferromagnet

Magnetoresistance

GMR - the simplistic explanation

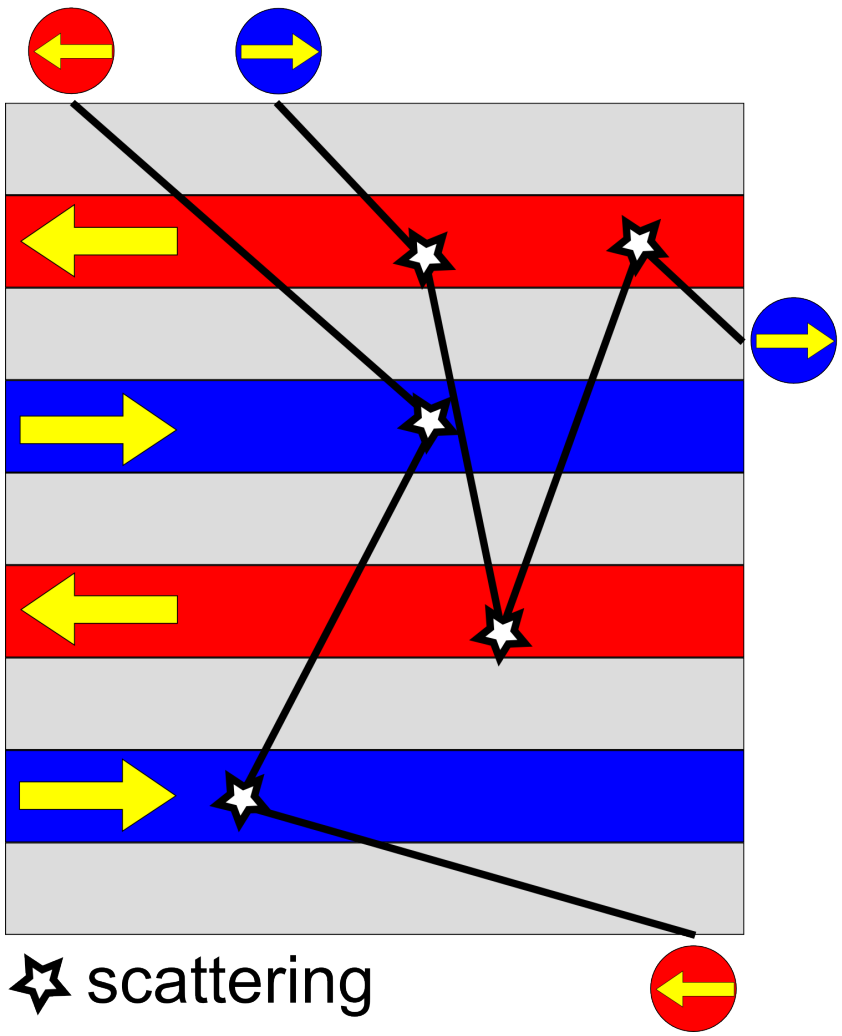

antiparallel – high resistance

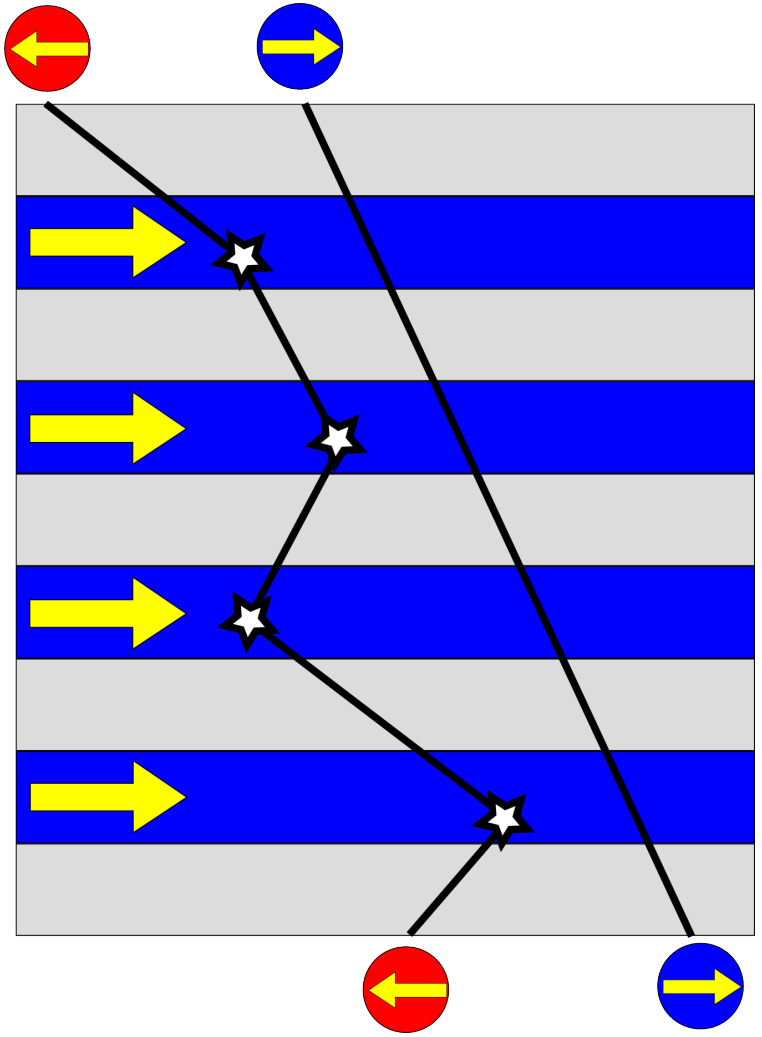

parallel – low resistance

image based on Fig.2 from [17]

Magnetoresistance

GMR - resistor network model [17]

- Mott two spin-channels – two conducting channels do not mix
- resistance of parallel configuration is lower

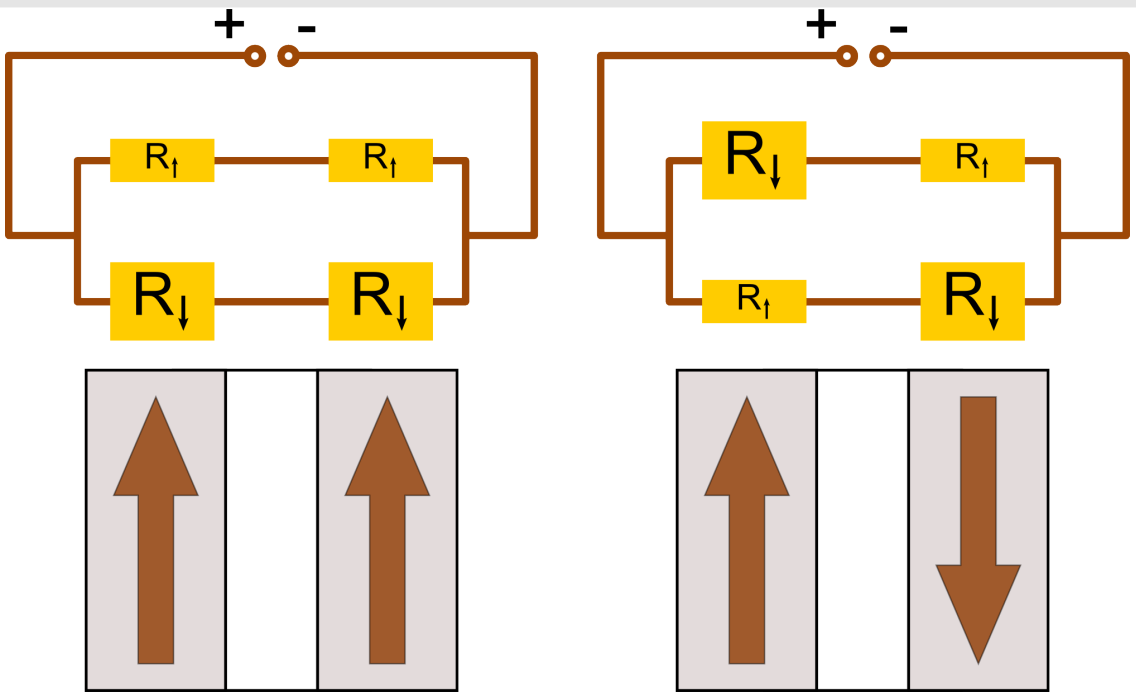

Resistance of parallel configuration

$$\frac{1}{R_P}=\frac{1}{R_\uparrow+R_\uparrow}+\frac{1}{R_\downarrow+R_\downarrow}$$

$$R_P=\frac{2R_\uparrow R_\downarrow}{R_\uparrow+R_\downarrow}$$

Resistance of antiparallel configuration

$$\frac{1}{R_{AP}}=\frac{1}{R_\uparrow+R_\downarrow}+\frac{1}{R_\uparrow+R_\downarrow}$$

$$R_{AP}=\frac{R_\uparrow+R_\downarrow}{2}$$

$$R_\downarrow=(1+a^2)R_\uparrow \quad \rightarrow \quad \frac{R_{AP}}{R_P}-1=\frac{a^4}{4+4a^2}\geq 0 \quad \rightarrow \quad R_{AP}\geq R_P$$

image based on Fig.2 from [17]

Magnetoresistance

Boltzmann transport equation [9,15,16]

The classical theory of transport is based on a statistical distribution function *f* that specifies the probability of finding a particle with its position and momentum within a small range [15] or, which is equivalent*, concentration of carriers with a given momentum in the neighborhood of the given point in space [9].

$$n(r_x, r_x+dx, r_y, r_y+dy, r_z, r_z+dz, v_x, v_x+dv_x, v_y, v_y+dv_y, v_z, v_z+dv_z) = f(\vec{r}, \vec{v})\, dx\, dy\, dz\, dv_x\, dv_y\, dv_z$$

number of particles in dr×dv volume at r,v position in six-dimensional space

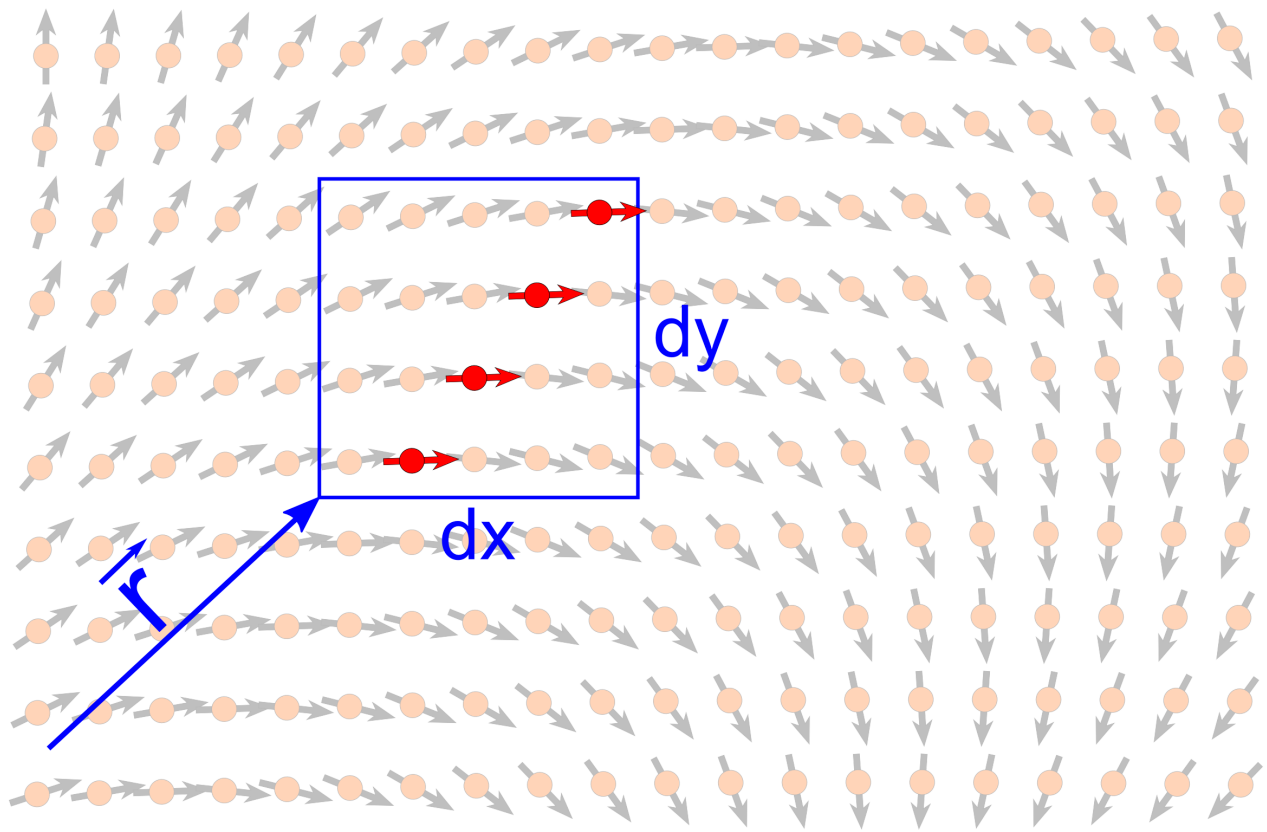

in the 2-D example to the right four particles in the dx×dy volume have v_y velocities in the range from $-dv_y$ to $+dv_y$

*after introducing normalizing factor

Magnetoresistance

Boltzmann transport equation [9,15,16]
The classical theory of transport is based on a statistical distribution function *f* that specifies the probability of finding a particle with its position and momentum within a small range [15] or, which is equivalent*, concentration of carriers with a given momentum in the neighborhood of the given point in space [9].

$$n(r_x, r_x+dx, r_y, r_y+dy, r_z, r_z+dz, v_x, v_x+dv_x, v_y, v_y+dv_y, v_z, v_z+dv_z)=f(\vec{r},\vec{v})\,dx\,dy\,dz\,dv_x\,dv_y\,dv_z$$

- In equilibrium the transition rates between any two states exactly balance [15]
- In the presence of external fields the equilibrium state is disturbed and the scattering tends to return the system to equilibrium
- Some **steady state** is attained in which the effect of external fields is balanced by scattering events
- Scattering "*has the important effect of limiting the extent of the response*" - A.C. Smith *et al.* [15]

*after introducing normalizing factor

Magnetoresistance

Rate of change of the distribution function *f* (*r*,*k*,*t*)* [from A.C. Smith *et al*., 15]:

- the density described by *f* may change because of scattering of phase points into or out of the volume cell dr×dv
- the phase points may flow in or out of the cell due to their spatial velocity and because the velocity changes under the influence of external field (streaming or drift terms)

The carrier (electron) is scattered out of the dxdy volume and it may change its momentum

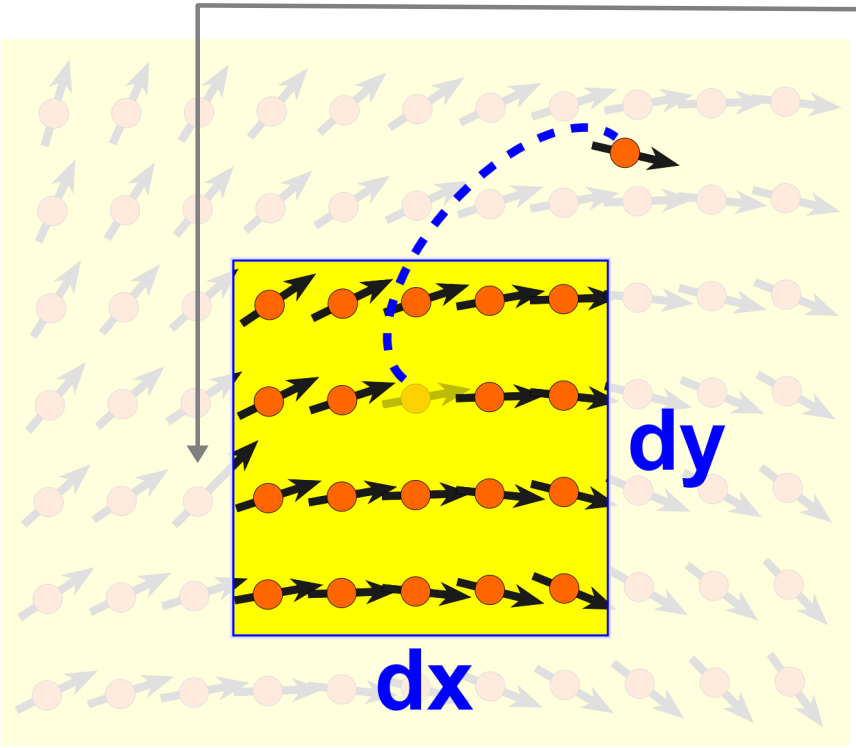

The carrier (electron) is about to enter dxdy volume but his momentum is different than that of carriers in cell; it will not be in the same dx dy $dv_x dv_y$ volume as neighboring (in real space) electrons

view in real space

*not that the function depends on *t* now.

Magnetoresistance

Rate of change of the distribution function *f* (*r*,*k*,*t*)* [from A.C. Smith *et al*., 15]:

- the density described by *f* may change because of scattering of phase points into or out of the volume cell dr×dv
- the phase points may flow in or out of the cell due to their spatial velocity and because the velocity changes under the influence of external field (streaming or drift terms)

Consider the 1-D movement of a phase points along x-direction. The number of points crossing a dy dz area normal to x is given by:

$$\delta n(x)=\int f(x,k)\,dk\,\dot{x}\;dy\,dz=f(x)\dot{x}\;dy\,dz$$

k disappears from here because we integrate over all velocities

note the dot

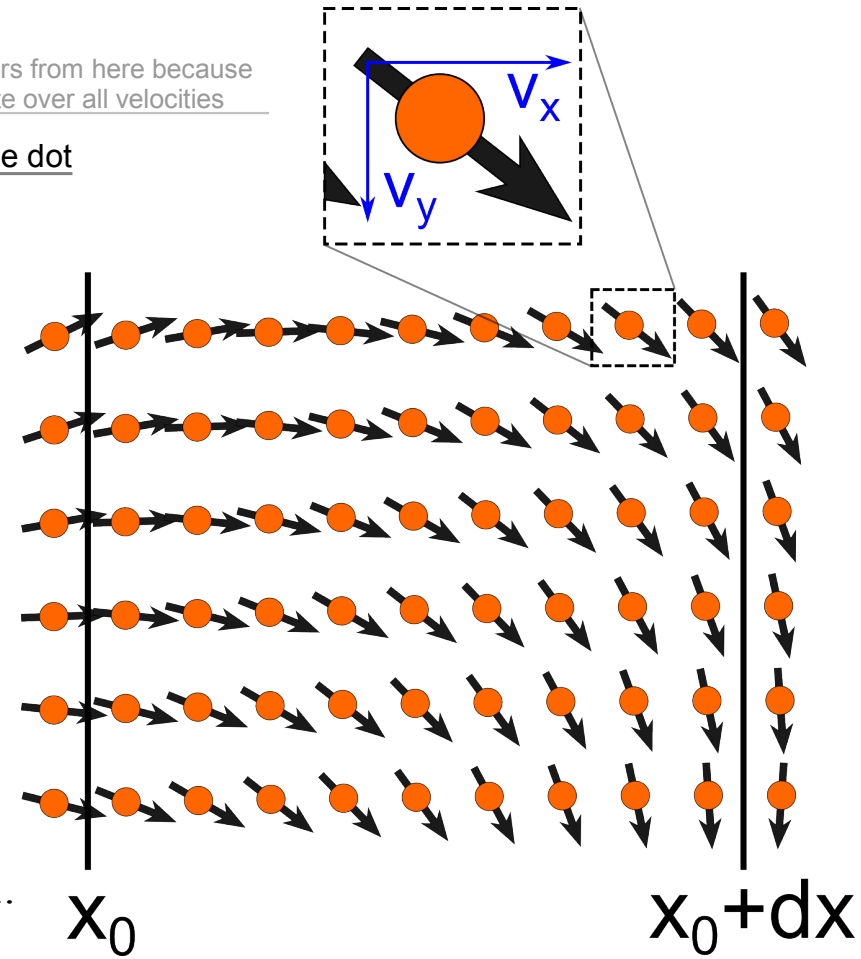

The net flow into the region between x and x+dx is given by:

$$\delta n=[\delta n(x)-\delta n(x+dx)]\;dy\,dz$$
$$=[f(x)\dot{x}(x)-f(x+dx)\dot{x}(x+dx)]\;dy\,dz$$

Which for d*x*→0 is:

$$\delta n=-\left[\frac{\partial}{\partial x}\left(f(x)\dot{x}\right)\right]_{x_0}dx\;dy\,dz$$

In 3-D (change of the number of phase points in dx dy dz volume) we have:

$$\delta n=\left[\frac{\partial}{\partial x}\left(f(x)\dot{x}\right)\right]_{x_0}dx\;dy\,dz+\left[\frac{\partial}{\partial y}\left(f(y)\dot{y}\right)\right]_{y_0}dy\;dx\,dz+\ldots$$

*note that the function depends on *t* now.

Magnetoresistance

Further we have:

$$\nabla\cdot(f\,\vec{v})=\left(i\frac{\partial}{\partial x}+j\frac{\partial}{\partial y}+k\frac{\partial}{\partial z}\right)\cdot\left(i\,f\,\vec{v}_x+j\,f\,\vec{v}_y+k\,f\,\vec{v}_z\right)=\underbrace{\frac{\partial}{\partial x}f\,\vec{v}_x+\frac{\partial}{\partial y}f\,\vec{v}_y+\frac{\partial}{\partial z}f\,\vec{v}_z}_{\text{the last expression of the previous page divided by } dx\,dy\,dz}$$

...and for the change of *f* :

$$\delta n=-\nabla\cdot\left(f(\vec{r})\vec{v}\right)d^3r$$

To get the complete expression (drift of position and momentum/velocity points into 6-dimensional phase space volume $d^3r\,d^3k$) we add together six terms [15]:

$$\delta f(\vec{r},\vec{v},t)=-\left[\nabla_r\cdot\left(f(\vec{r},\vec{k},t)\vec{v}\right)+\nabla_k\cdot\left(f(\vec{r},\vec{k},t)\dot{\vec{k}}\right)\right]d^3r\,d^3k$$

The continuity equation for *f** reads (we cancel $d^3r\,d^3k$ everywhere and work with density of phase points instead of their numbers):

$$\frac{\partial f}{\partial t}=\left(\frac{\partial f}{\partial t}\right)_{scatt}-\nabla_r\cdot(f\,\vec{v})-\nabla_k\cdot\left(f\,\dot{\vec{k}}\right)$$

$$\nabla\cdot(a\vec{b})=\vec{b}\cdot\nabla a+a\nabla\cdot\vec{b}$$

$$\vec{v}=\hbar^{-1}\nabla_k E_n(k)$$

$$\nabla_r\cdot(f\,\vec{v})+\nabla_k\cdot\left(f\,\dot{\vec{k}}\right)=\vec{v}\cdot\nabla_r f+f\,\nabla_r\cdot\vec{v}+\dot{\vec{k}}\cdot\nabla_k f+f\,\nabla_k\cdot\dot{\vec{k}}$$

$$\nabla_r\cdot\vec{v}=\hbar^{-1}\nabla_r\cdot\left[\nabla_k E_n(k)\right]=0$$

since energy E_n does not depend on position ***r***

$$\nabla_k\cdot\dot{\vec{k}}=\nabla_k\cdot\frac{q}{\hbar}\left(\vec{E}+\vec{v}\times\vec{B}\right)=\nabla_k\cdot\left(\frac{q}{\hbar}\vec{v}\times\vec{B}\right)=$$

electric field ***E*** does not depend on position ***r***

$$\frac{q}{\hbar}\nabla_k\cdot\left(\hat{i}\,(B_z v_y-B_y v_z)+\hat{j}\,(-B_z v_x+B_z v_x+B_x v_z)+\hat{k}\,(B_y v_x-B_x v_y)\right)=$$

$$\frac{q}{\hbar^2}\left(\hat{i}\frac{\partial}{\partial k_x}+\hat{j}\frac{\partial}{\partial k_y}+\hat{k}\frac{\partial}{\partial k_z}\right)\cdot$$

$$\left(\hat{i}\,(B_z\frac{\partial E_n(k)}{\partial k_y}-B_y\frac{\partial E_n(k)}{\partial k_z})+\hat{j}\,(-B_z\frac{\partial E_n(k)}{\partial k_x}+B_x\frac{\partial E_n(k)}{\partial k_z})+\hat{k}\,(B_y\frac{\partial E_n(k)}{\partial k_x}-B_x\frac{\partial E_n(k)}{\partial k_y})\right)=$$

$$\frac{q}{\hbar^2}\left(B_z\frac{\partial^2 E_n(k)}{\partial k_y\partial k_x}-B_y\frac{\partial^2 E_n(k)}{\partial k_z\partial k_x}-B_z\frac{\partial^2 E_n(k)}{\partial k_x\partial k_y}+B_x\frac{\partial^2 E_n(k)}{\partial k_z\partial k_y}+B_y\frac{\partial^2 E_n(k)}{\partial k_x\partial k_z}-B_x\frac{\partial^2 E_n(k)}{\partial k_y\partial k_z}\right)=0$$

0 0 0

$$\frac{\partial f}{\partial t}=\left(\frac{\partial f}{\partial t}\right)_{scatt}-\vec{v}\cdot\nabla_r f-\dot{\vec{k}}\cdot\nabla_k f$$

*we do not write further the explicit dependence of *f* on ***r***, ***v***, and ***t***.

Magnetoresistance

$$\frac{\partial f}{\partial t} = \left(\frac{\partial f}{\partial t}\right)_{scatt} - \vec{v}\cdot\nabla_r f - \dot{\vec{k}}\cdot\nabla_k f$$

Boltzmann transport equation

- "*derived under the condition that the fictitious particle representing electron executes a classical motion*" [15]
- not valid for large external fields and when band-to-band transitions occur

The scattering term is due to: lattice vibrations, impurities, electron-electron scattering, electron-magnon scattering, vacancies, grain boundaries dislocations etc.

In steady state *f* is constant and we have:

$$\left(\frac{\partial f}{\partial t}\right)_{scatt} - \underbrace{\vec{v}\cdot\nabla_r f}_{\text{diffusion}} - \underbrace{\dot{\vec{k}}\cdot\nabla_k f}_{\text{effect of fields}} = 0$$

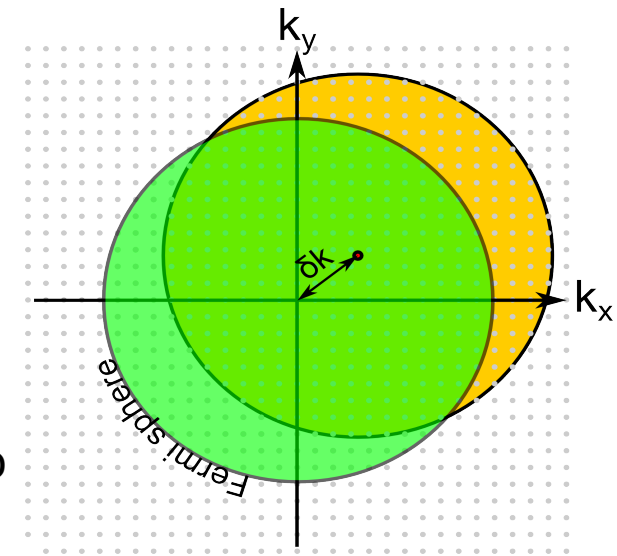

The relaxation time approximation:
In general it is not possible to calculate scattering contribution to the change of *f*. In many applications it is useful to assume that disturbed system returns to equilibrium exponentially in time* [9]:

$$\left(\frac{\partial f}{\partial t}\right)_{scatt} = -\frac{f_k - f_k^0}{\tau_k}$$

relaxation time (in general different for each Bloch state)

$$f_k(t) = f_k^0 + \Delta f_k \exp(-t/\tau_k)$$

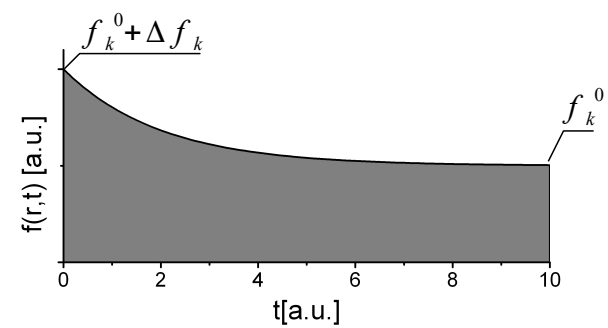

*this approximation is valid for pure metals for temperatures exceeding Debye temperature and for contaminated metals (or those with defects) for all temperatures [9]

Magnetoresistance

Linearized Boltzmann equation

The distribution function can in general be expanded in powers of the driving field [18]:

$$f = f^{0} + \left(\frac{\partial f}{\partial E}\right)\vec{E} + \left(\frac{\partial^2 f}{\partial E^2}\right)\vec{E}^{2} + \ldots$$

, with f^0 given for electrons by Fermi-Dirac statistics [9]:

$$f_k^{0} = \frac{1}{\exp(E_k - E_F)/k_b T + 1}$$

"*When the electric field is small, only a small amount of current flows. The system is only slightly out of equilibrium.*" [19]. The distribution function can be written as:

$$f = f^{0} + f^{1}$$

f^{1} is a small change

Magnetoresistance

Giant magnetoresistance from Boltzmann equation*

Investigating electron transport in thin films one can assume that the system is infinitely extended in xy-plane so that the distribution function depends only on z-coordinate (perpendicular to the film plane).

Using two-channel model of Mott the distribution function is decomposed into two parts:

-equilibrium distribution function $f_0(z,v)$ – in zero electric field

-small change g, induced by external field, that depends on electrons spin

$$f^{\uparrow(\downarrow)}(z,\vec{v}) = f_0(\vec{v}) + g^{\uparrow(\downarrow)}(z,\vec{v})$$

Substituting the above distribution function into linearized Boltzmann equation in relaxation time approximation we obtain the expression for g [20]

$$\frac{\partial g^{\uparrow(\downarrow)}(z,\vec{v})}{\partial z} + \frac{g^{\uparrow(\downarrow)}(z,\vec{v})}{\tau^{\uparrow(\downarrow)} v_z} = \frac{e\vec{E}}{m v_z}\frac{\partial f_o(\vec{v})}{\partial v_x}$$

m, e – electron effective mass and charge

- relaxation times are spin dependent (spin channels)
- g is divided into two parts depending on the sign of v_z component of velocity

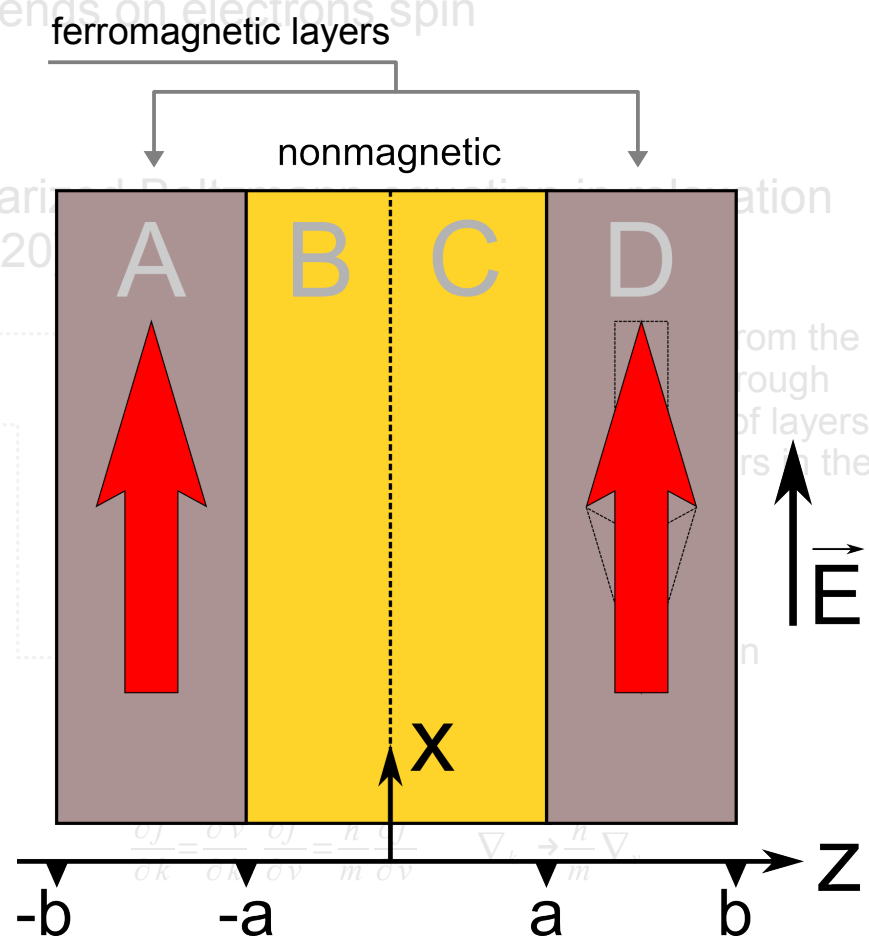

*theory developed by J. Barnaś and coworkers [20]

Magnetoresistance

Giant magnetoresistance from Boltzmann equation*

Investigating electron transport in thin films one can assume that the system is infinitely extended in xy-plane so that the distribution function depends only on z-coordinate (perpendicular to the film plane).

Using two-channel model of Mott the distribution function is decomposed into two parts:

-equilibrium distribution function $f_0(z,v)$ – in zero electric field

-small change *g*, induced by external field (electric), that depends on electrons spin

$$f^{\uparrow(\downarrow)}(z,\vec{v}) = f_0(\vec{v}) + g^{\uparrow(\downarrow)}(z,\vec{v})$$

Substituting the above distribution function into linearized Boltzmann equation in relaxation time approximation we obtain the expression for *g* [20]:

$$\frac{\partial g^{\uparrow(\downarrow)}(z,\vec{v})}{\partial z} + \frac{g^{\uparrow(\downarrow)}(z,\vec{v})}{\tau^{\uparrow(\downarrow)} v_z} = \frac{e\vec{E}}{m v_z}\frac{\partial f_o(\vec{v})}{\partial v_x}$$

m, e – electron effective mass and charge

Note that magnetoresistance results from the presence of external magnetic field through the orientation of magnetic moments of layers. Magnetic field does not explicitly occur in the model.

Note that previously we had Boltzmann equation in r,k-space

$$p = m v = \hbar k$$

$$\frac{\partial f}{\partial k} = \frac{\partial v}{\partial k}\frac{\partial f}{\partial v} = \frac{\hbar}{m}\frac{\partial f}{\partial v} \qquad \nabla_k \rightarrow \frac{\hbar}{m}\nabla_v$$

- relaxation times are spin dependent (spin channels)
- *g* is divided into two parts depending on the sign of v_z component of velocity

*theory developed by J. Barnaś and coworkers [20]

Magnetoresistance

The general solution can be written as [20]:

$$g_{\pm}^{\uparrow(\downarrow)}(z,\vec{v}) = \frac{e\vec{E}\tau^{\uparrow(\downarrow)}}{m}\frac{\partial f_o(\vec{v})}{\partial v_x} \times \left[1 + F_{\pm}^{\uparrow(\downarrow)}(v)\exp\left(\frac{\mp z}{\tau^{\uparrow(\downarrow)}|v_z|}\right)\right]$$

4 arbitrary functions to be determined from boundary conditions

Boundary conditions (BCs) – in steady state the current flowing in the conductor is continuous
At the interface at z=-a between the ferromagnetic film and the spacer BC can be written in the form:

$$g_{A-}^{\uparrow(\downarrow)}(-a,\vec{v}) = T^{\uparrow(\downarrow)} g_{B-}^{\uparrow(\downarrow)}(-a,\vec{v}) + R^{\uparrow(\downarrow)} g_{A+}^{\uparrow(\downarrow)}(-a,\vec{v}),$$

where *T* and *R* are coefficients of a non-diffusive transmission and a reflection (conserving momentum, specular) of electrons.

- the above condition states that in the vicinity of interface the current of electrons flowing in -z direction consists of electrons that came from region B and those which were heading in +z direction and were reflected back to region B
- fraction (1-*T*) of electrons is scattered diffusely

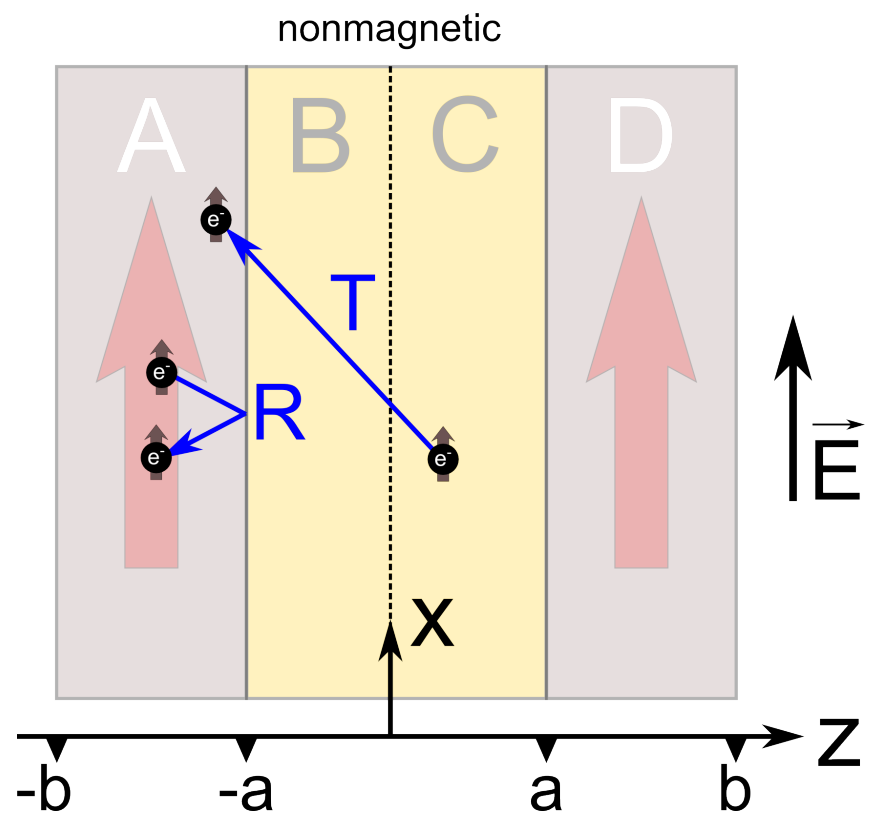

Magnetoresistance

The general solution can be written as [20]:

$$g_{\pm}^{\uparrow(\downarrow)}(z,\vec{v}) = \frac{e\vec{E}\tau^{\uparrow(\downarrow)}}{m}\frac{\partial f_o(\vec{v})}{\partial v_x} \times \left[1 + F_{\pm}^{\uparrow(\downarrow)}(v)\exp\left(\frac{\mp z}{\tau^{\uparrow(\downarrow)}|v_z|}\right)\right]$$

4 arbitrary functions to be determined from boundary conditions

Similar Fuchs* BCs are introduced for outer interfaces with specularity factors depending generally on spin:

$$g_{A+}^{\uparrow(\downarrow)}(z,\vec{v}) = p_A^{\uparrow(\downarrow)} g_{A-}^{\uparrow(\downarrow)}(z,\vec{v}) \qquad z=-b$$

- the condition states that in the vicinity of the outer interface electrons traveling into the multilayer are those reflected from the interface
- the electrons which are diffusely reflected do not contribute to conductivity along the film (their net contribution is zero)
- any angle dependence of the specularity is neglected for simplicity [20]

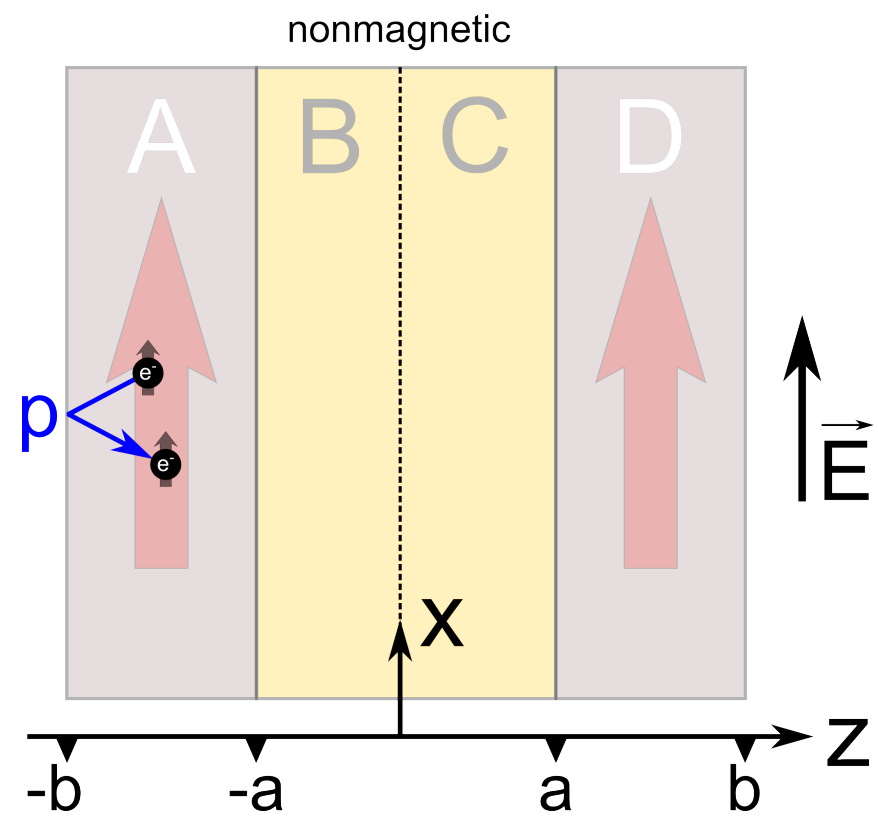

*remember Fuchs-Sondheimer theory of the resistivity of thin films

Magnetoresistance

At the fictitious interface at z=0 one can write [20]:

$$g_{C+}^{\uparrow(\downarrow)}(z,\vec{v})=\cos^2(\theta/2)g_{B+}^{\uparrow(\downarrow)}(z,\vec{v})+\sin^2(\theta/2)g_{B+}^{\downarrow(\uparrow)}(z,\vec{v})$$
$$g_{B-}^{\uparrow(\downarrow)}(z,\vec{v})=\cos^2(\theta/2)g_{C-}^{\uparrow(\downarrow)}(z,\vec{v})+\sin^2(\theta/2)g_{C\mp}^{\downarrow(\uparrow)}(z,\vec{v}),$$

Note that all terms are proportional to cos(θ)

$$2\cos^2(\theta/2)-1=\cos(\theta)$$
$$1-2\sin^2(\theta/2)=\cos(\theta)$$

which assures an agreement with observed resistance changes versus *θ*.
The total current (per unit length along the y axis; electric field is along x axis) is given by:

$$I=e\int dz\int d^3v\left[g^{\uparrow}(\vec{v},z)+g^{\downarrow}(\vec{v},z)\right]$$ a sum of two spin-channels currents

The equations were solved numerically

- the amplitude of magnetoresistance is given by

$$GMR=\frac{\rho^{\uparrow\downarrow}-\rho^{\uparrow\uparrow}}{\rho^{\uparrow\uparrow}}$$

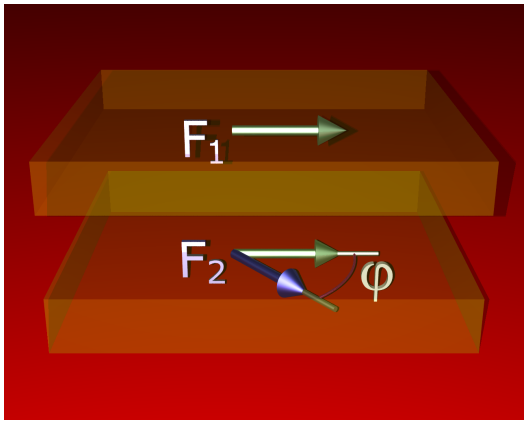

To better analyze the results additional parameters are introduced to describe:

- the spin asymmetry of the diffusive scattering of electrons at interfaces

$$N_s=(1-T^{\uparrow})/(1-T^{\downarrow})$$

- spin asymmetry of the bulk scattering rate in the ferromagnetic material

$$N_b=\lambda^{\uparrow}/\lambda^{\downarrow}$$

λ - electron mean free paths

Magnetoresistance

The main results of the analysis of Barnaś *et al*. [20] can be summarized as follows [21]:

- GMR increases monotonically with mean free path λ if the interface scattering dominates
- GMR displays clear maximum versus λ if the bulk scattering dominates

Assumptions:

- $p_A^{\uparrow}=p_A^{\downarrow}=p_D^{\uparrow}=p_A^{\downarrow}=p$ – Fuchs specularity factors
- $r=s=t=1$ conductivities of all layers are equal
- $D^{\uparrow(\downarrow)}=(1-T^{\uparrow(\downarrow)})=0$ - *"the omission of specular reflection at the interfaces."*

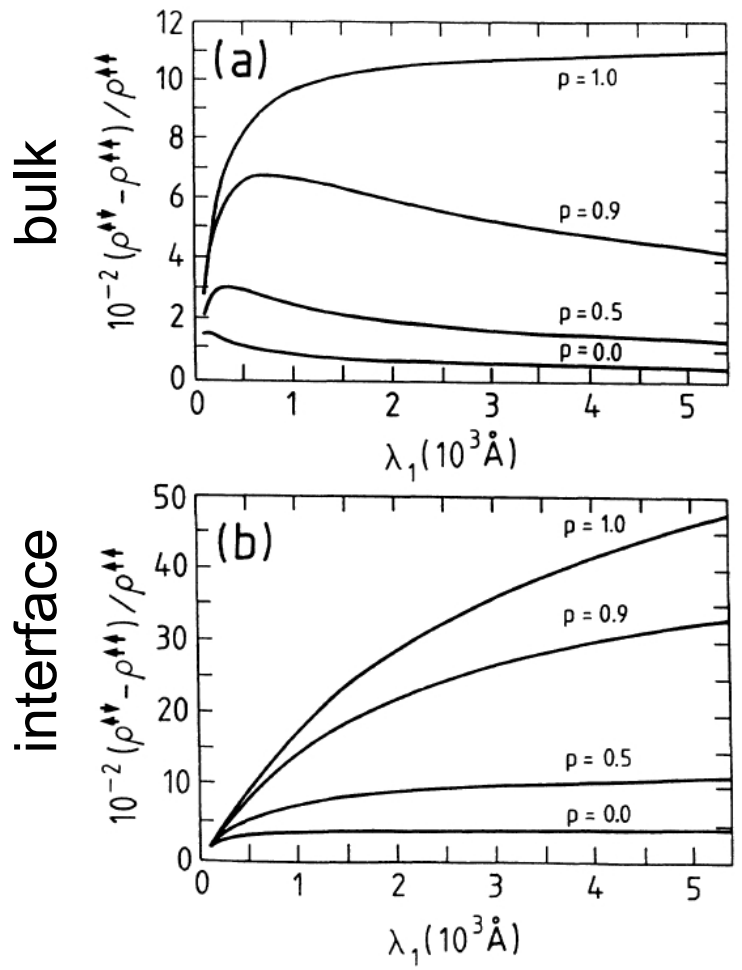

FIG. 2. (a) Bulk and (b) interface contribution to the magnetoresistivity in double layers with $d=100$ and 10 Å for different values of the specularity factor p. The curves in (a) have been calculated for $N_b=2$, $D^{\uparrow}=0$, and $r=s=t=1$, whereas the curves in (b) for $N_s=6$, $D^{\uparrow}=0.5$, $N_b=1$, and $r=s=t=1$.

image from: J. Barnaś, A. Fuss, R.E. Camley, P. Grunberg, W. Zinn, Phys. Rev. B **42**, 8110 (1990)

Magnetoresistance

The main results of the analysis of Barnaś *et al*. [20] can be summarized as follows [21]:

- GMR decreases monotonically with the thickness of ferromagnetic layer if the interface scattering dominates
- GMR shows a distinct maximum versus thickness of the ferromagnetic layers if the bulk scattering dominates (if the thickness of the ferromagnetic layer exceeds λ part of it becomes inactive in GMR but still contributes to conductivity [21])

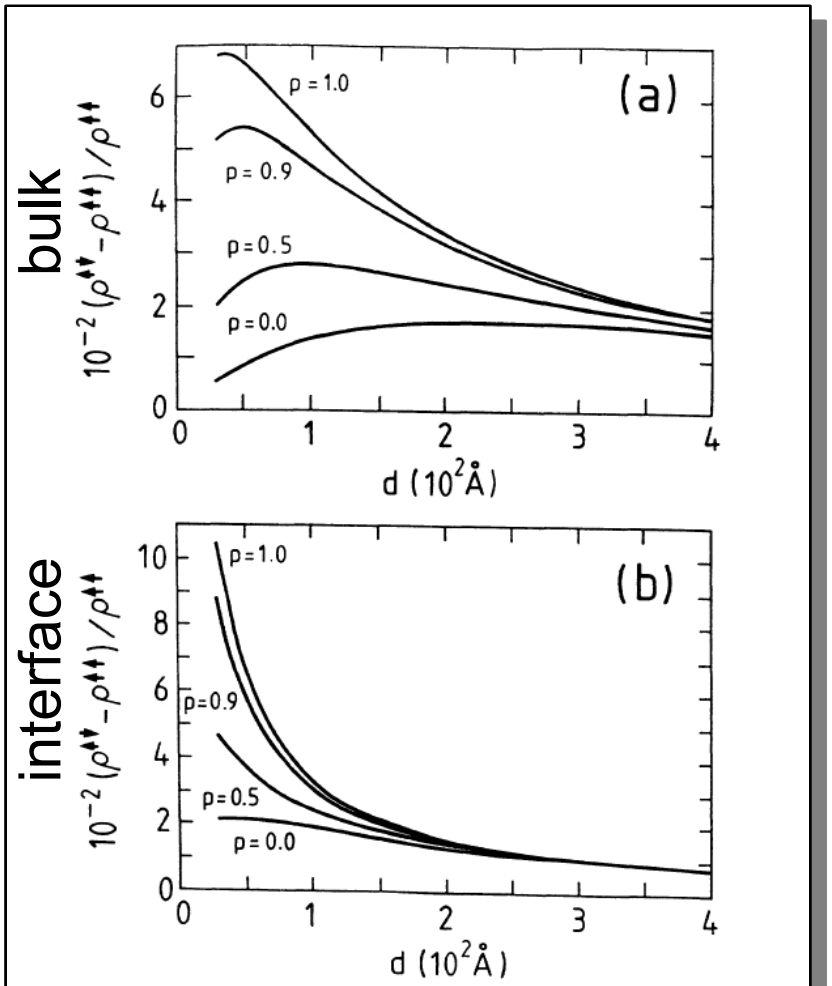

FIG. 3. (a) Bulk and (b) interface contribution to the magnetoresistivity in double layers vs thickness of the ferromagnetic layers. The curves are calculated for the specularity factors as indicated. The interlayer thickness is assumed to be constant, $d_0 = 10$ Å. The other parameters assumed in numerical calculations are (a) $N_b = 2$, $D^{\uparrow} = 0$, $\lambda_1 = 200$ Å, and $r = s = t = 1$; (b) $N_s = 6$, $D^{\uparrow} = 0.5$, $N_b = 1$, $\lambda_1 = 200$ Å, and $r = s = t = 1$.

image from: J. Barnaś, A. Fuss, R.E. Camley, P. Grunberg, W. Zinn, Phys. Rev. B **42**, 8110 (1990)

Magnetoresistance

The main results of the analysis of Barnaś *et al*. [20] can be summarized as follows [21]:

- GMR increases monotonically with mean free path λ if the interface scattering dominates
- GMR displays clear maximum versus λ if the bulk scattering dominates
- GMR decreases monotonically with the thickness of ferromagnetic layer if the interface scattering dominates
- GMR shows a distinct maximum versus thickness of the ferromagnetic layers if the bulk scattering dominates (if the thickness of the ferromagnetic layer exceeds λ part of it becomes inactive in GMR but still contributes to conductivity [21])
- GMR increases with the increase of repetition number of basic bilayers (ferromagnet/nonmagnetic spacer) – number of GMR active interfaces within λ increases (additionally in thick multilayers the influence of outer surfaces of the system decreases)

Magnetoresistance

Angular dependence of GMR

$$\Delta R \propto \cos(\theta)$$

- in the limit of quantum transport (QT) deviations from the dependence occur due to interference of electron waves reflected from interfaces and/or surfaces [23]
- in QT limit the dependence is proportional to cosine if the structure is symmetrical and the crystal potential is independent of spin
- in the case of current perpendicular to plane geometry (CPP) the significant deviations were observed too [23]

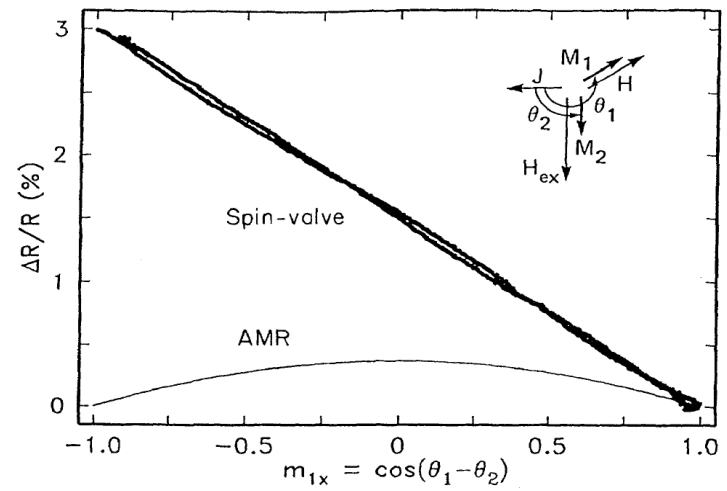

FIG. 2. Relative change in resistance vs the cosine of the relative angle between the magnetizations of the two NiFe layers of Si/(60-Å NiFe)/(26-Å Cu)/(30-Å NiFe)/(60-Å FeMn)/(20-Å Ag). Inset shows the orientation of the current J, exchange field H_{ex}, applied field H, and magnetizations M_1 and M_2.

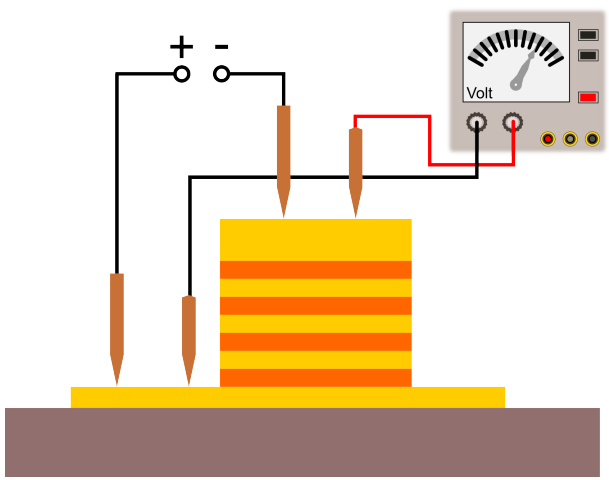

CPP geometry

image from B. Dieny, V.S. Speriosu, S.S.P. Parkin, B.A. Gurney, D.R. Wilhoit, D. Mauri, Phys. Rev. B **43**, 1297 (1991)

Magnetoresistance

Angular dependence of GMR

- knowing field dependence of magnetic moments configuration one can approximately predict the shape (*not the amplitude!*) of *R*(*H*) dependence

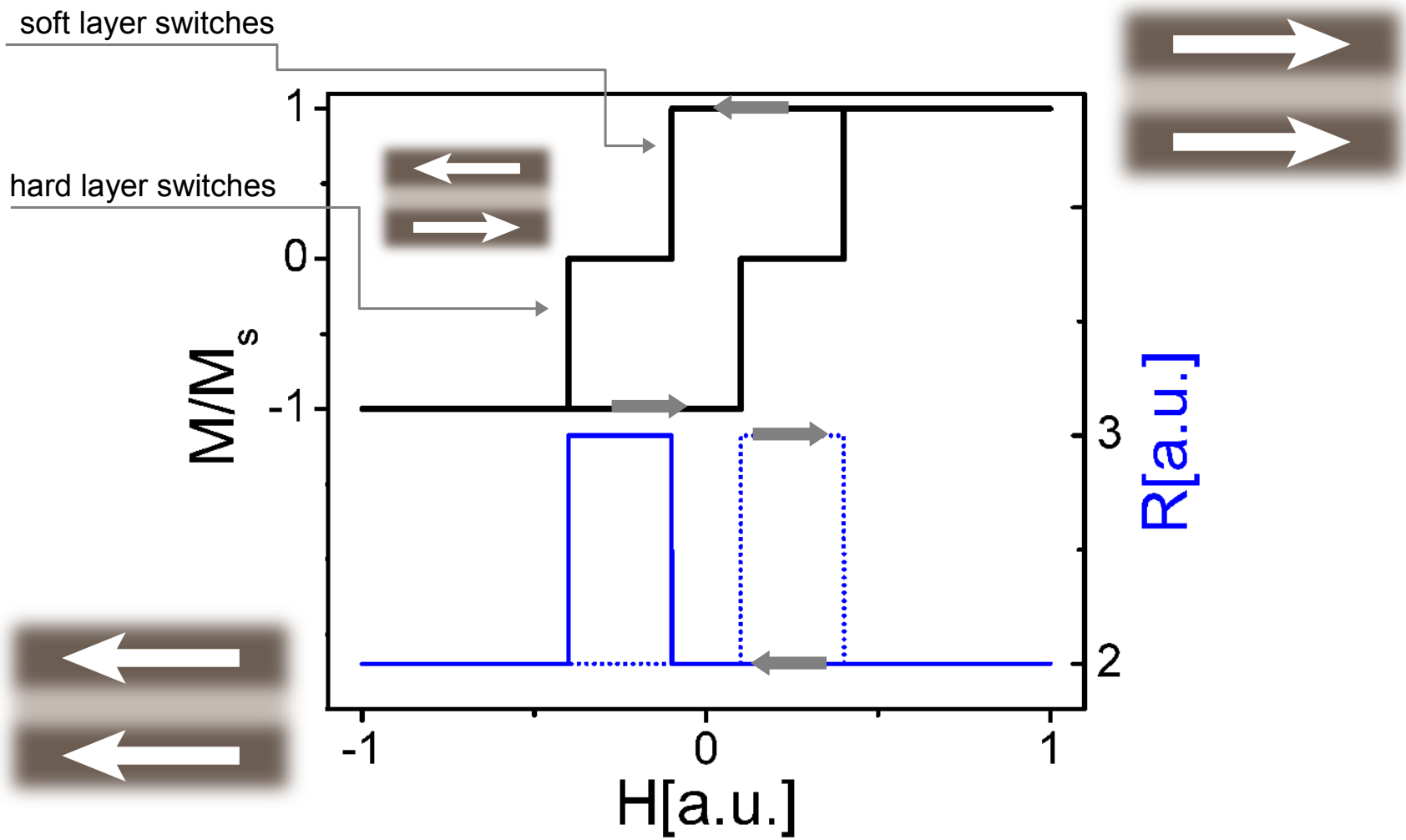

example: GMR of spin valve with two layers of different switching fields

Magnetoresistance

Angular dependence of GMR

- Co(10nm)/Au(6nm)/Co(10nm)
- note the increase of GMR amplitude with decreasing temperature (increase of mean free path and a decreased phononic contribution) from 1.2 to1.7%
- magnetic layers have different magnetic moments so after switching of the soft layer the net magnetization is different from zero

A digression:

"All these features can be used for verification of the theoretical predictions with the experimental results. However, the most reliable one seems to be the temperature dependence of the effect. This follows from the fact that <u>the relevant experiments are performed on one single sample</u>. In the case of other features one has to compare data obtained on different samples." J. Barnaś *et al.* [20]

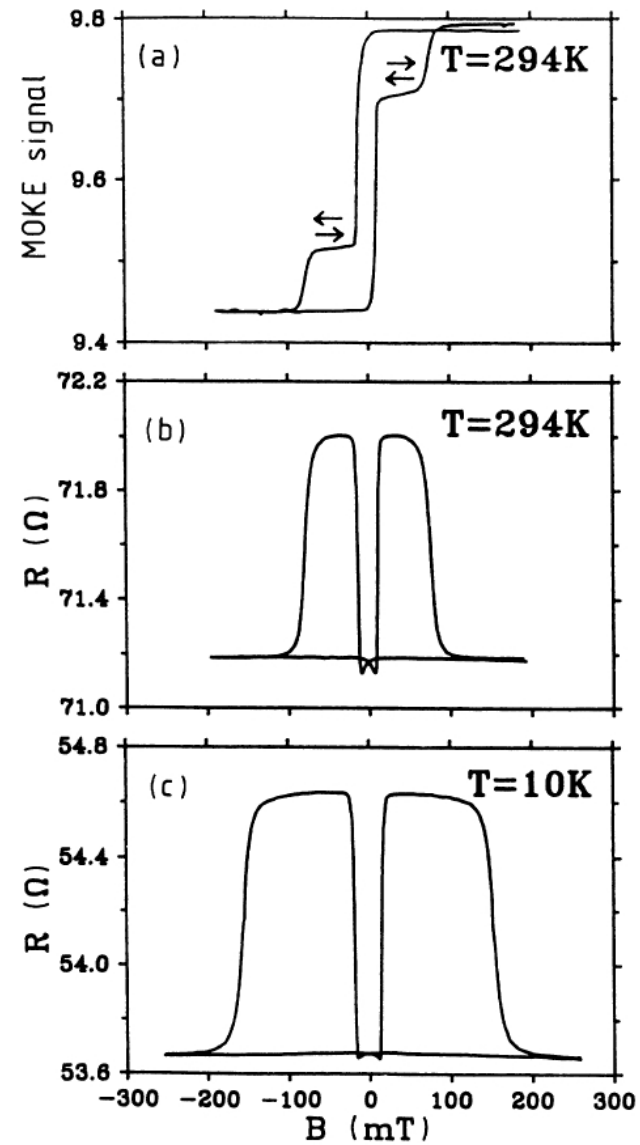

FIG. 9. (a) MOKE-signal and (b) and (c) resistance of the Co/Au/Co structure with the Co-film thickness $d = 100$ Å and the Au-interlayer thickness $d_0 = 60$ Å.

image from: J. Barnaś, A. Fuss, R.E. Camley, P. Grunberg, W. Zinn, Phys. Rev. B **42**, 8110 (1990)

Magnetoresistance

RKKY-like interlayer coupling

- two Fe layers separated by a Cr wedge-shaped spacer; scanning electron microscopy with polarization analysis (SEMPA)
- measurement on a single specimen!
- up to six oscillations in coupling were observed

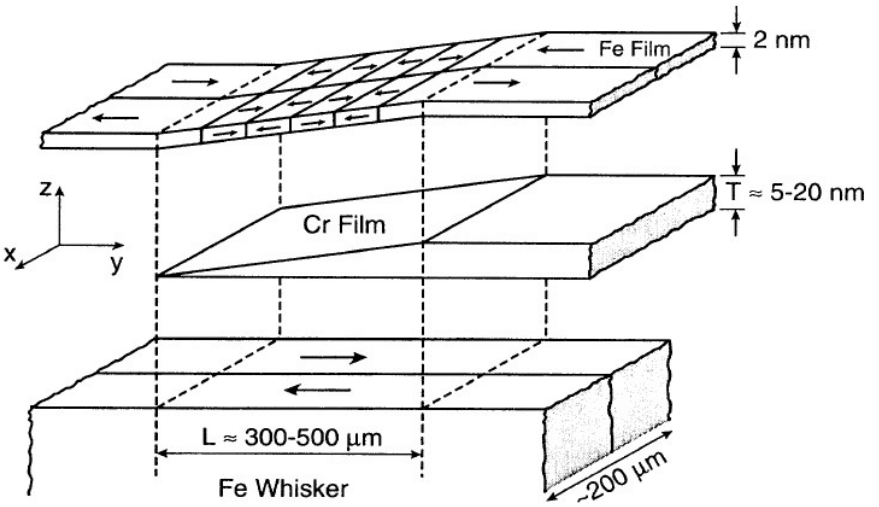

FIG. 1. A schematic exploded view of the sample structure showing the Fe(100) single-crystal whisker substrate, the evaporated Cr wedge, and the Fe overlayer. The arrows in the Fe show the direction of the magnetization in each domain. The z scale is expanded approximately 5000 times; the actual wedge angle is of order 10^{-3} deg.

Obtaining wedge-shaped films:

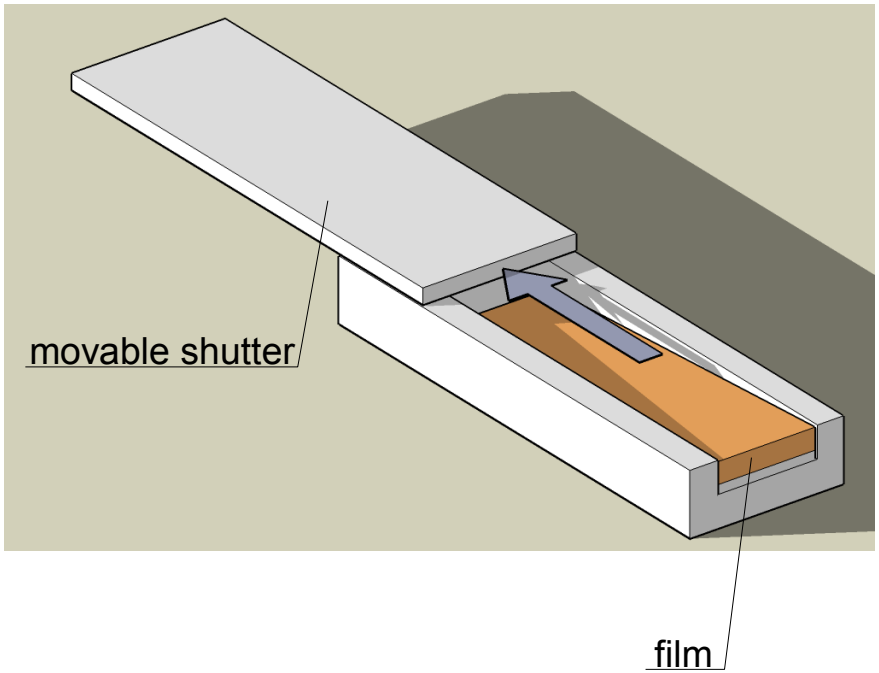

image from J. Unguris, R. J. Celotta, and D. T. Pierce Phys. Rev. Lett. **67**, 140 (1991)

Magnetoresistance

RKKY-like interlayer coupling

- two Fe layers separated by a Cr wedge-shaped spacer; scanning electron microscopy with polarization analysis (SEMPA)
- measurement on a single specimen!
- up to six oscillations in coupling were observed
- different periods of coupling depending on temperature of the substrate during the film growth: samples grown at elevated temperature are of better quality and the magnetization of the upper Fe layer changes with each atomic-layer change in Cr thickness
- "lower quality" samples display only RKKY-like coupling

grown at elevated temperatures (200-300°C)

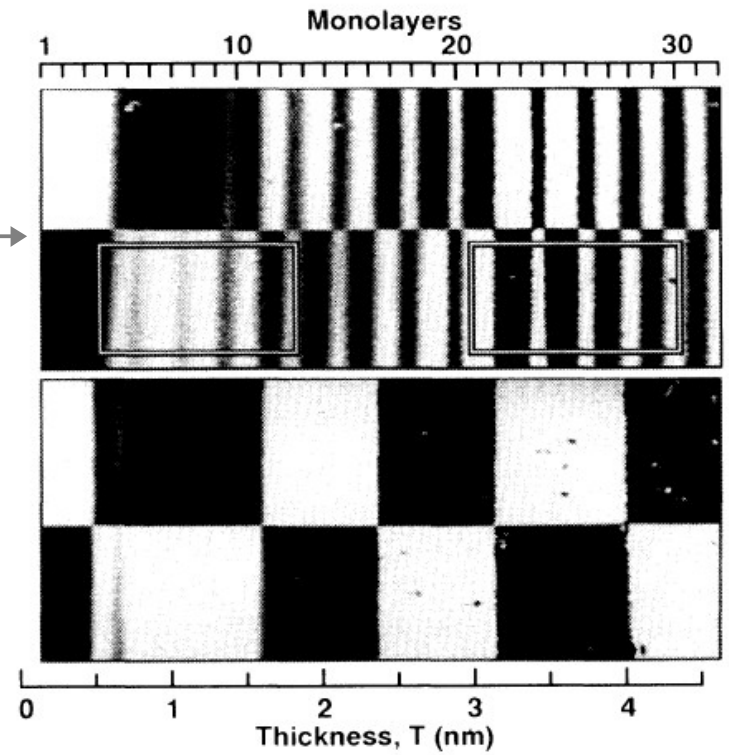

FIG. 3. The difference in the magnetic coupling of the Fe layers in the Fe/Cr/Fe sandwich for the Cr wedge grown (2.7 ML/min) on a substrate at room temperature (lower panel) and grown (7.2 ML/min) on a substrate at elevated temperature (upper panel) is clear in these SEMPA M_y images. The images in the upper and lower panels represent areas 300×280 and 350×290 μm, respectively.

image from J. Unguris, R. J. Celotta, and D. T. Pierce Phys. Rev. Lett. **67**, 140 (1991)

Magnetoresistance

RKKY-like interlayer coupling

Magnetic impurity in a conducting medium induces spatial fluctuations of spin polarization of s-electrons about the impurity [9]

- the oscillatory term of wave number 2 k_F falls off like r^{-3} at large distances

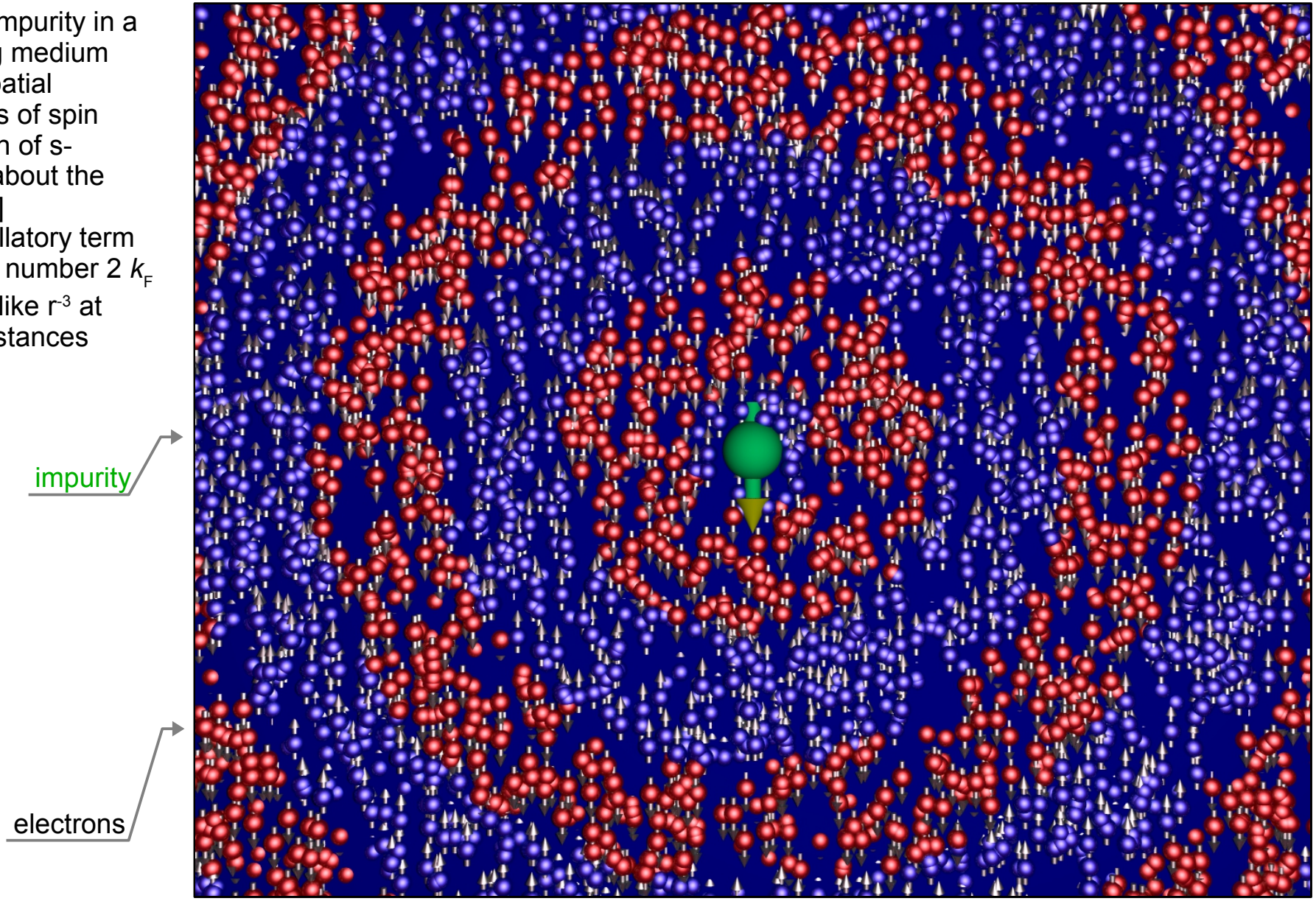

Magnetoresistance

RKKY-like interlayer coupling

Magnetic impurity in a conducting medium induces spatial fluctuations of spin polarization of s-electrons about the impurity [9]

- the oscillatory term of wave number 2 k_F* falls off like r^{-3} at large distances
- the second impurity placed in the vicinity experiences interaction with the first impurity
- depending on the distance between impurities the interactions may be **ferromagnetic** or **antiferromagnetic**

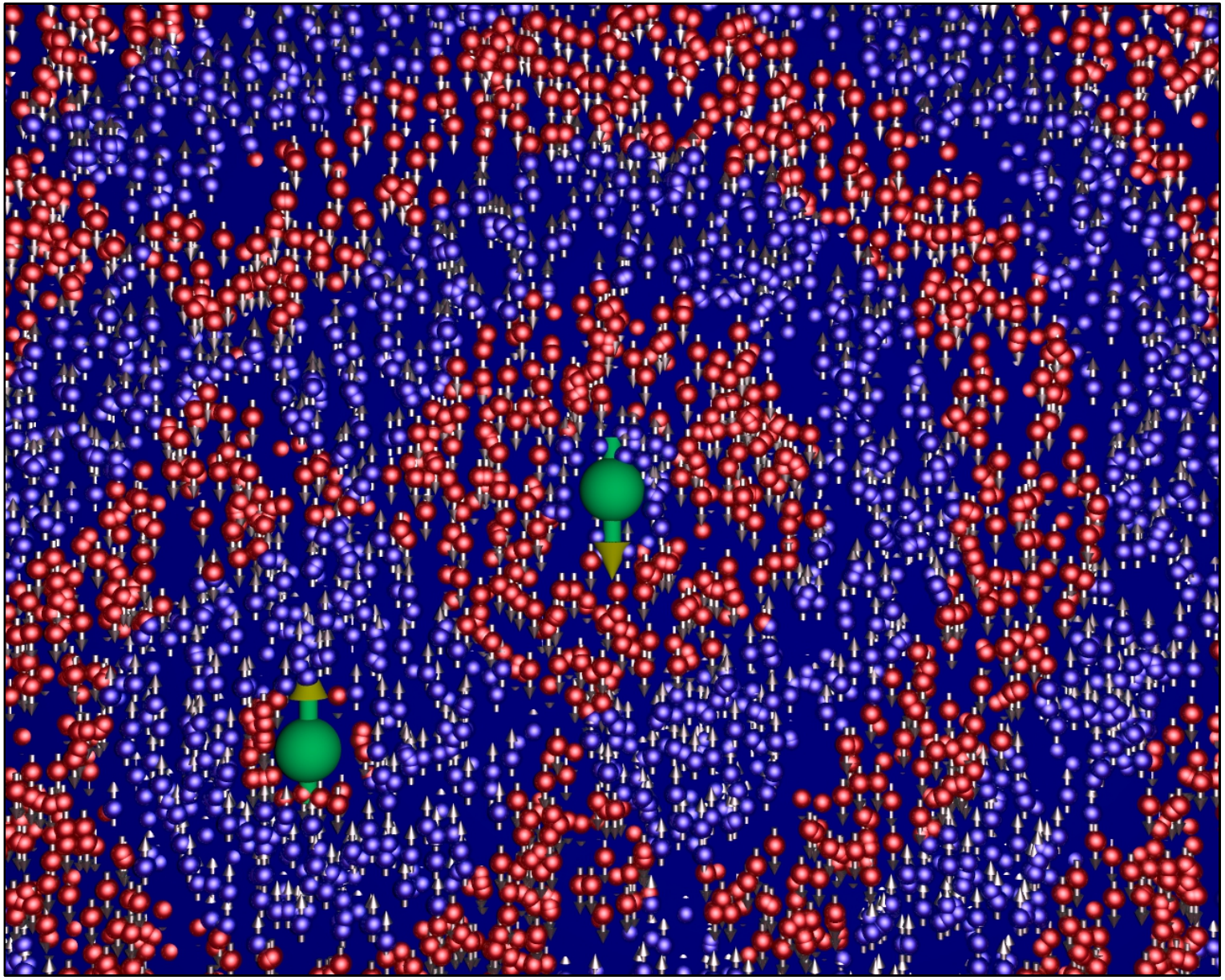

*Fermi wave vector

Magnetoresistance

RKKY-like interlayer coupling

Magnetic impurity in a conducting medium induces spatial fluctuations of spin polarization of s-electrons about the impurity [9]

- the oscillatory term of wave number 2 k_F falls off like r^{-3} at large distances
- the second impurity placed in the vicinity experiences interaction with the first impurity
- depending on the distance between impurities the interactions may be **ferromagnetic** or **antiferromagnetic**

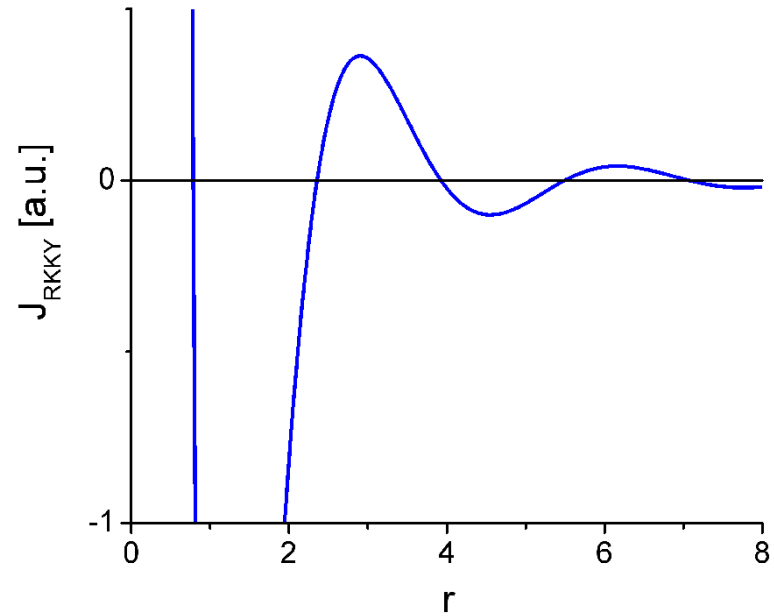

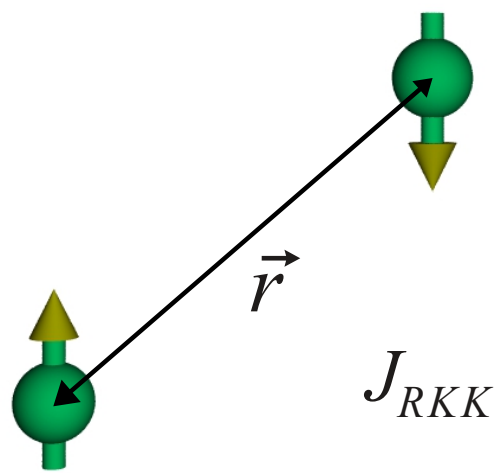

$$J_{RKKY} \propto \frac{1}{r^3} \cos\left(2 k_F r\right)$$

Magnetoresistance

RKKY-like interlayer coupling

schematic drawing of a RKKY spin polarization due to single atom thick (11×11atoms) layer of impurities*

A plane composed of exchange coupled impurities creates spatial oscillations of spin polarization in the direction perpendicular to its surface

- if the moments are strongly coupled ferromagnetically they form a ferromagnetic layer
- a similar, parallel, layer or multilayer placed a certain distance away experiences ferromagnetic or antiferromagnetic coupling depending on a distance from the first layer

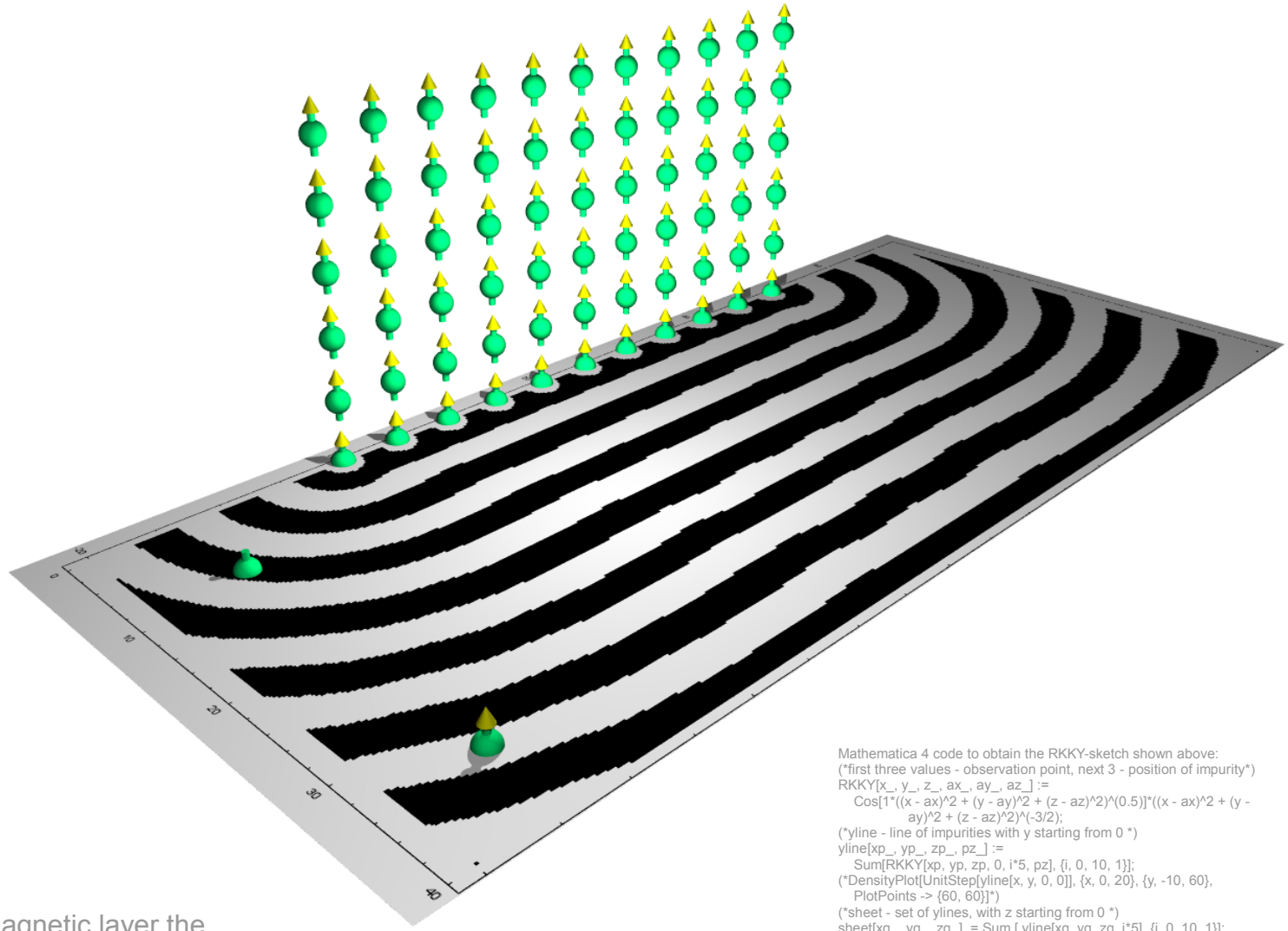

Mathematica 4 code to obtain the RKKY-sketch shown above:

```
(*first three values - observation point, next 3 - position of impurity*)
RKKY[x_, y_, z_, ax_, ay_, az_] :=
   Cos[1*((x - ax)^2 + (y - ay)^2 + (z - az)^2)^(0.5)]*((x - ax)^2 + (y -
        ay)^2 + (z - az)^2)^(-3/2);
(*yline - line of impurities with y starting from 0 *)
yline[xp_, yp_, zp_, pz_] :=
   Sum[RKKY[xp, yp, zp, 0, i*5, pz], {i, 0, 10, 1}];
(*DensityPlot[UnitStep[yline[x, y, 0, 0]], {x, 0, 20}, {y, -10, 60},
   PlotPoints -> {60, 60}]*)
(*sheet - set of ylines, with z starting from 0 *)
sheet[xq_, yq_, zq_]  = Sum [ yline[xq, yq, zq, i*5], {i, 0, 10, 1}];
DensityPlot[UnitStep[sheet[x, y, 25]], {x, 0, 40}, {y, -20, 70},
  PlotPoints -> {200, 200*   9/4  }, AspectRatio -> 9/4, Mesh -> False,
  ImageSize -> 600]
```

in case of quasi-infinite/real ferromagnetic layer the lines delimiting areas of opposite spin polarization would not be bowed except at the ends

*the drawing shows the sign of the coupling (black and gray correspond to positive and negative spin polarization)

Magnetoresistance

RKKY-like interlayer coupling

Theoretical considerations show that the coupling between **two ferromagnetic layers** is inversely proportional to the square of the spacer thickness [30]

$$J_{RKKY} \propto \frac{1}{r^2}$$

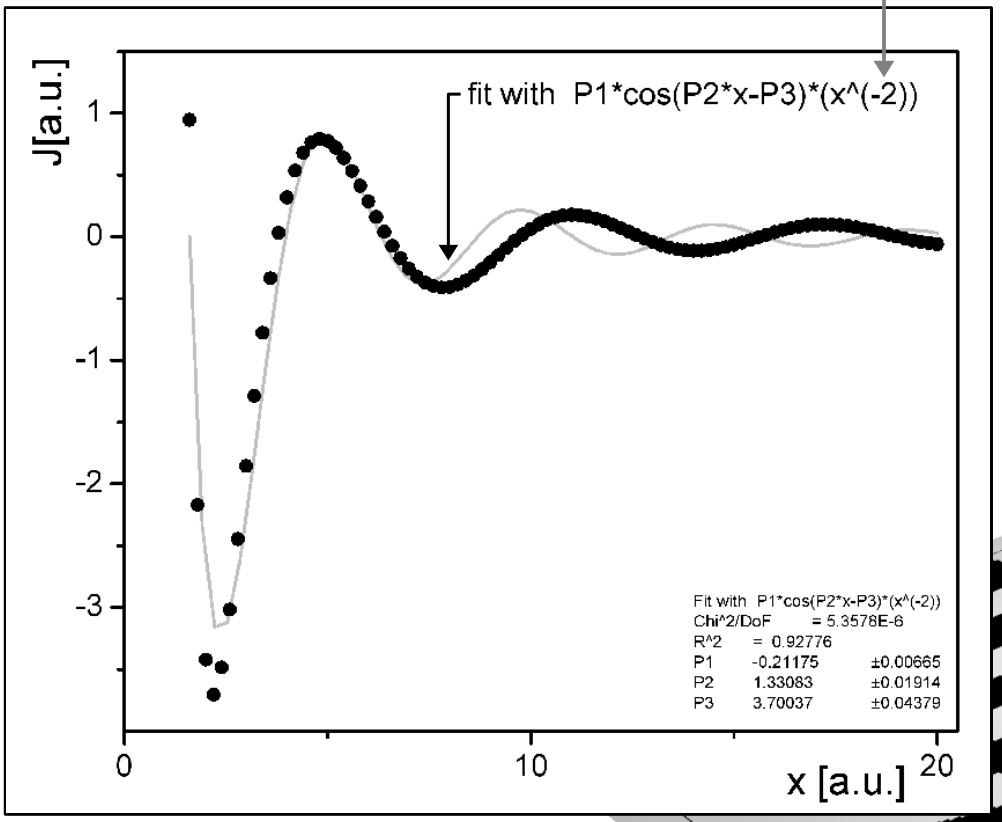

the coupling along AB line

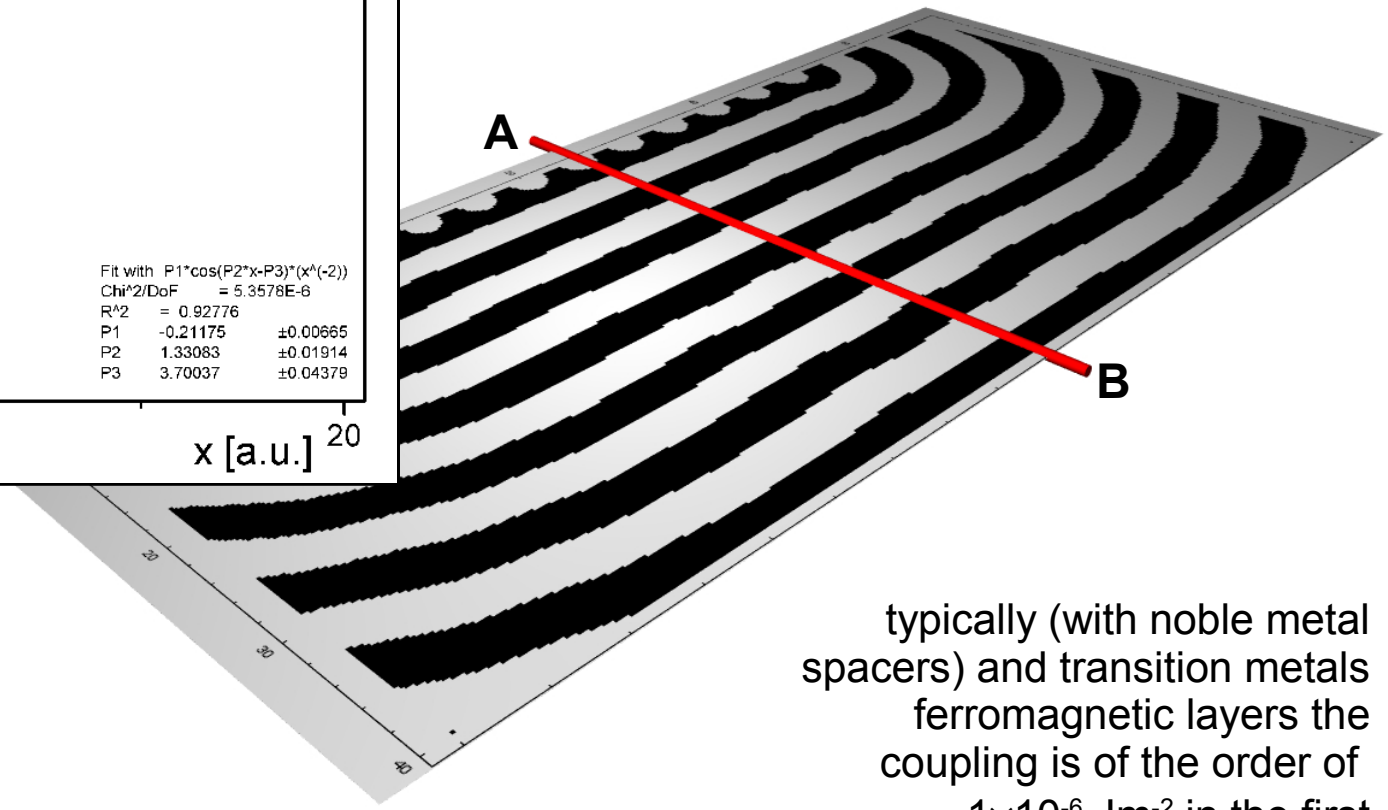

typically (with noble metal spacers) and transition metals ferromagnetic layers the coupling is of the order of 1×10^{-6} Jm^{-2} in the first antiferromagnetic maximum

*the drawing shows the sign of the coupling (black and gray correspond to positive and negative spin polarization)

Magnetoresistance

RKKY-like interlayer coupling

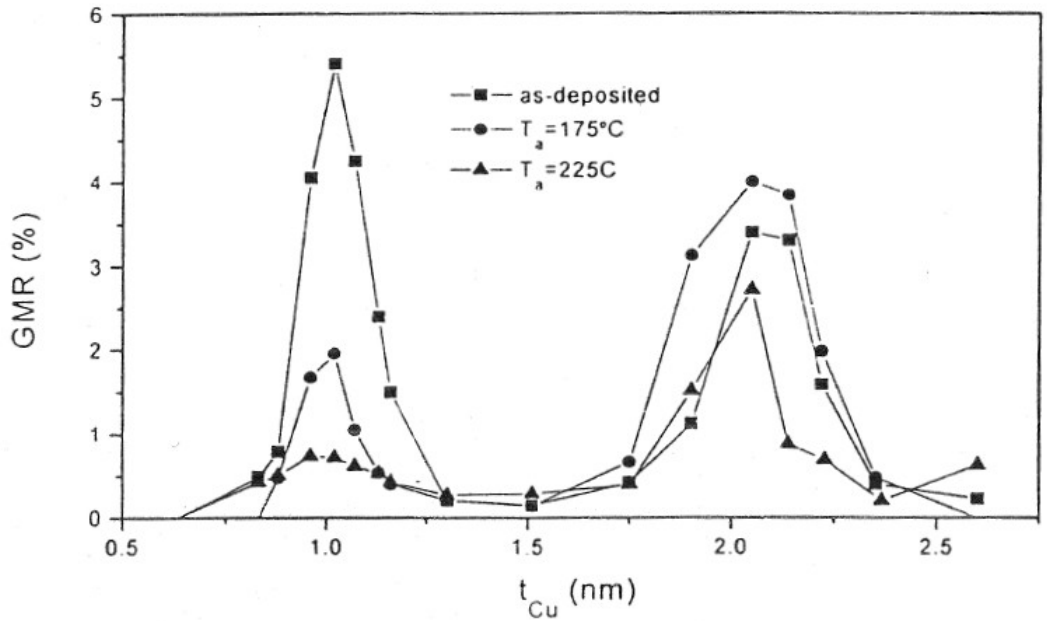

Fig. 1. GMR as a function of the Cu sublayer thickness for the as deposited and annealed samples.

- Si(100)/Cu(20nm)[$Ni_{83}Fe_{17}$(2nm)/Cu(t_{Cu})]$_{100}$
- GMR reflects the oscillatory character of the RKKY-like coupling between permalloy layers
- in MLs with identical magnetic layers (the same switching fields) GMR can be observed only for spacer thicknesses corresponding to antiferromagnetic coupling; otherwise the magnetic field does not change relative orientation of magnetic moments of neighboring layers

image from: F. Stobiecki, T. Luciński, R. Gontarz, M. Urbaniak, Materials Science Forum 287, 513 (1998)

Magnetoresistance

RKKY-like interlayer coupling

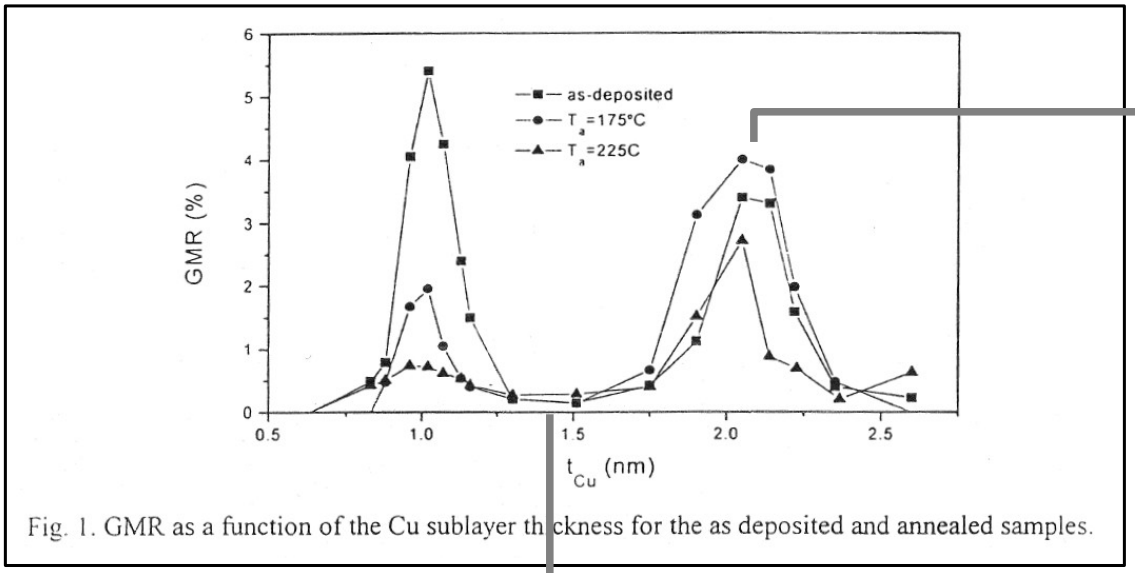

Fig. 1. GMR as a function of the Cu sublayer thickness for the as deposited and annealed samples.

AF-coupling

F-coupling

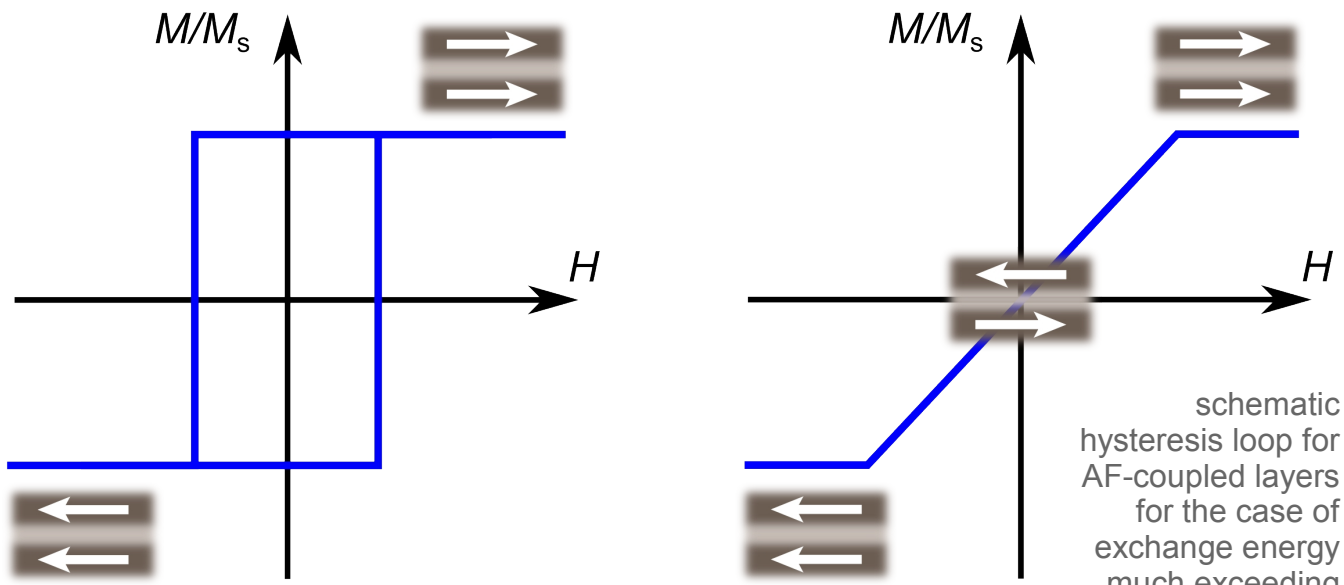

schematic hysteresis loop for AF-coupled layers for the case of exchange energy much exceeding magnetic anisotropy

image from: F. Stobiecki, T. Luciński, R. Gontarz, M. Urbaniak, Materials Science Forum 287, 513 (1998)

Magnetoresistance

Inverse CPP GMR [31]

- "*Fe doped with V gains negative spin asymmetry for bulk scattering*" - the up-spin channel is characterized by higher resistivity

$$\rho_{\uparrow(\downarrow)} = \rho_{bulk}(1 \mp \beta)$$

- similarly the interface resistivity depends on spin orientation – factor γ (positive)
- in $(FeV/Cu/Co/Cu)_{20}$ multilayers the resistance of saturated system (all magnetizations pointing in one direction) may be higher than for the case of antiparallel orientation of magnetizations in neighboring magnetic layers
- depending on the FeV layer thickness the **GMR can be either normal or inverse**; at small FeV layer thicknesses the interface scattering dominates resulting in normal GMR
- the crossover thickness of FeV layers lies between 2 and 3 nm

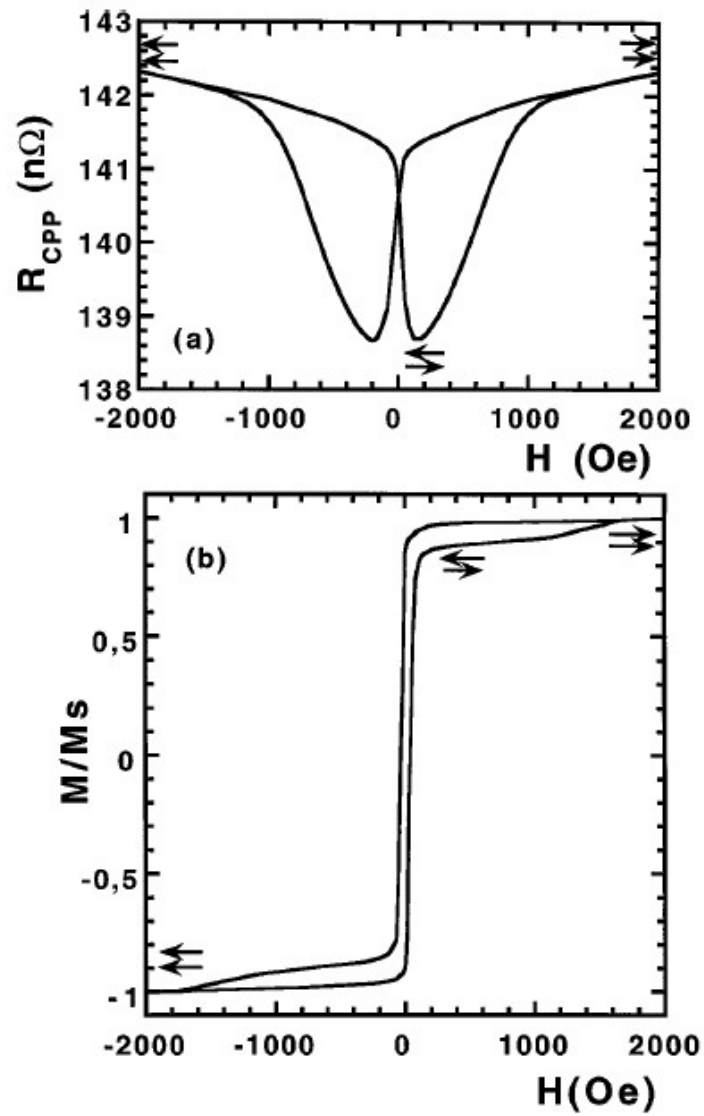

FIG. 1. Magnetoresistance (a) and magnetization (SQUID) (b) curves at 4.2 K for a $(Fe_{72}V_{28}$ 6 nm/Cu 2.3 nm/Co 0.4 nm/Cu 2.3 nm$)_{20}$ multilayer.

image from: S.Y. Hsu, A. Barthélémy, P. Holody, R. Loloee, P. A. Schroeder, A. Fert, Phys. Rev. Lett. **78**, 2652 (1997)

Magnetoresistance

Typical GMR systems

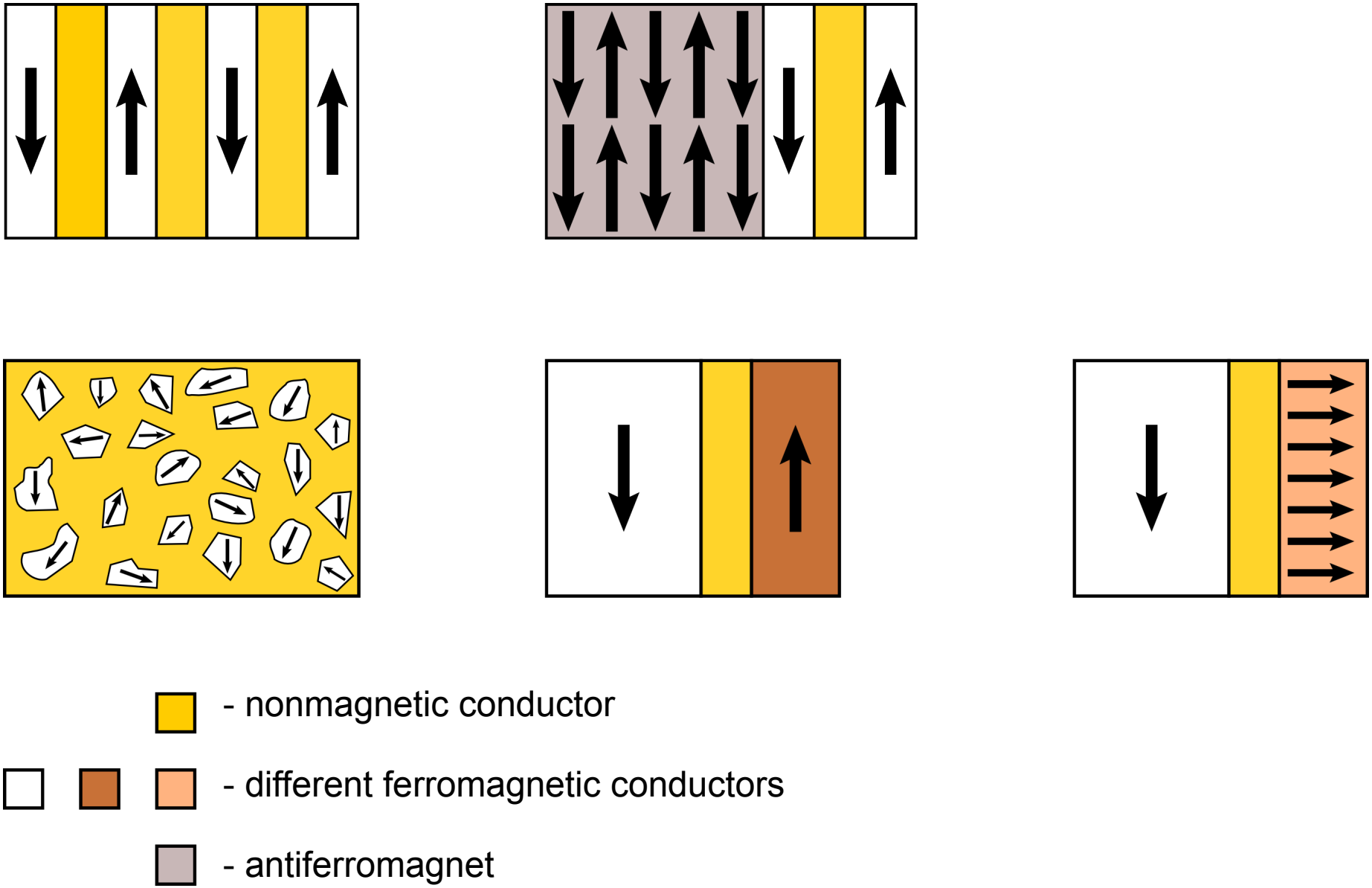

Magnetoresistance

Typical GMR systems

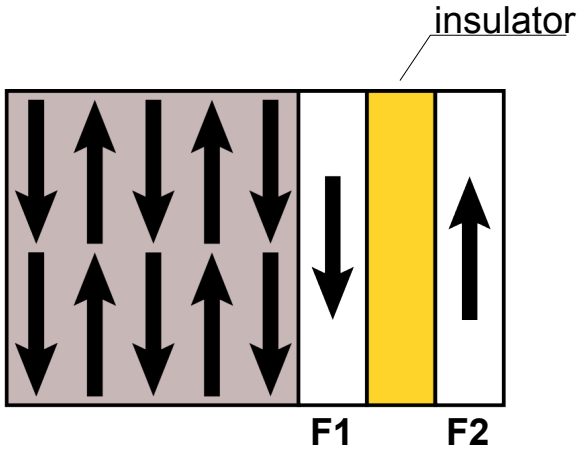

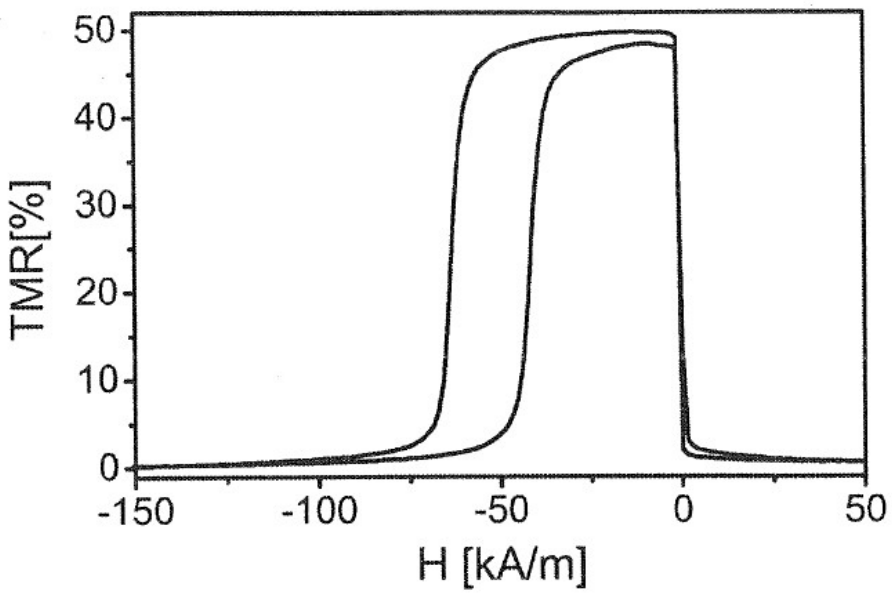

Fig. 6 The room temperature TMR curve of Cu(30 nm)/$Ni_{80}Fe_{20}$(4 nm)/$Mn_{83}Ir_{17}$(15 nm)/$Co_{70}Fe_{30}$ (2 nm)/Al(1.4 nm) + Ox/$Ni_{80}Fe_{20}$(4 nm)/Ta(3 nm)/ Cu(55 nm)/Au (20 nm) multilayer.

GMR (or TMR*) in systems with exchange bias

- magnetization of ferromagnetic layer F1 “fixed” by the anisotropy of the antiferromagnetic layer
- magnetization of the F2 layer is “free” to rotate in external magnetic field
- both conducting and insulating spacer may be used
- very high field sensitivities of the effect achievable

image from: M. Urbaniak, J. Schmalhorst, A. Thomas, H. Brückl, G. Reiss, T. Luciński, F. Stobiecki Phys. Stat. Sol. (a) **199**, 284 (2003)

*tunneling magnetoresistance

Magnetoresistance

Typical GMR systems

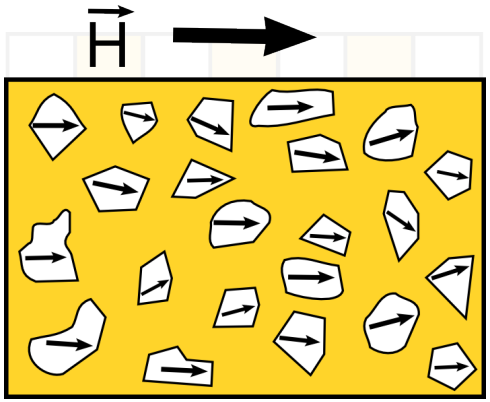

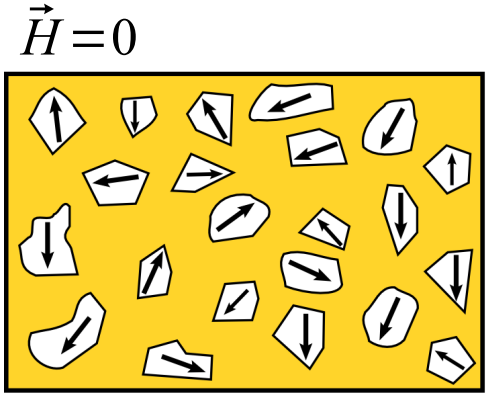

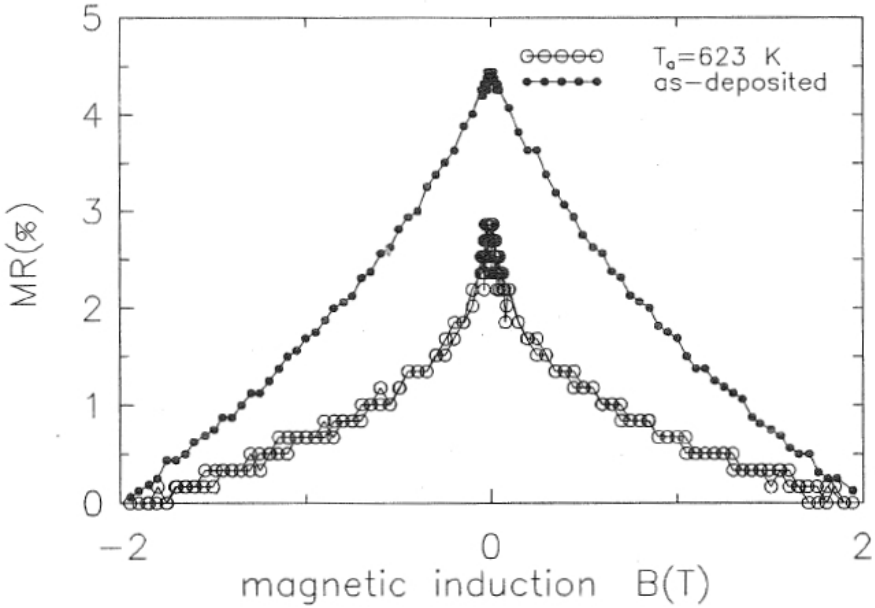

Fig. 1. Exemplary magnetoresistive curves obtained for 76 nm thick $Co_{20}Ag_{80}$ film in as-deposited state and after annealing at 623 K

directions of the magnetic moments within the grain depend on external field and on the effective magnetic anisotropy of the grain (shape, magnetocrystalline etc.) and on interactions with other grains.

Granular GMR (G^2MR)

- magnetic grains in nonmagnetic matrix (content below percolation threshold)
- resistance saturates in high fields

- nonmagnetic conductor
- different ferromagnetic conductors
- antiferromagnet

image from: M. Urbaniak, I. Gościańska, H. Ratajczak, Phys. Stat. Sol. (a) **160**, 121 (1997)

Magnetoresistance

Typical GMR systems

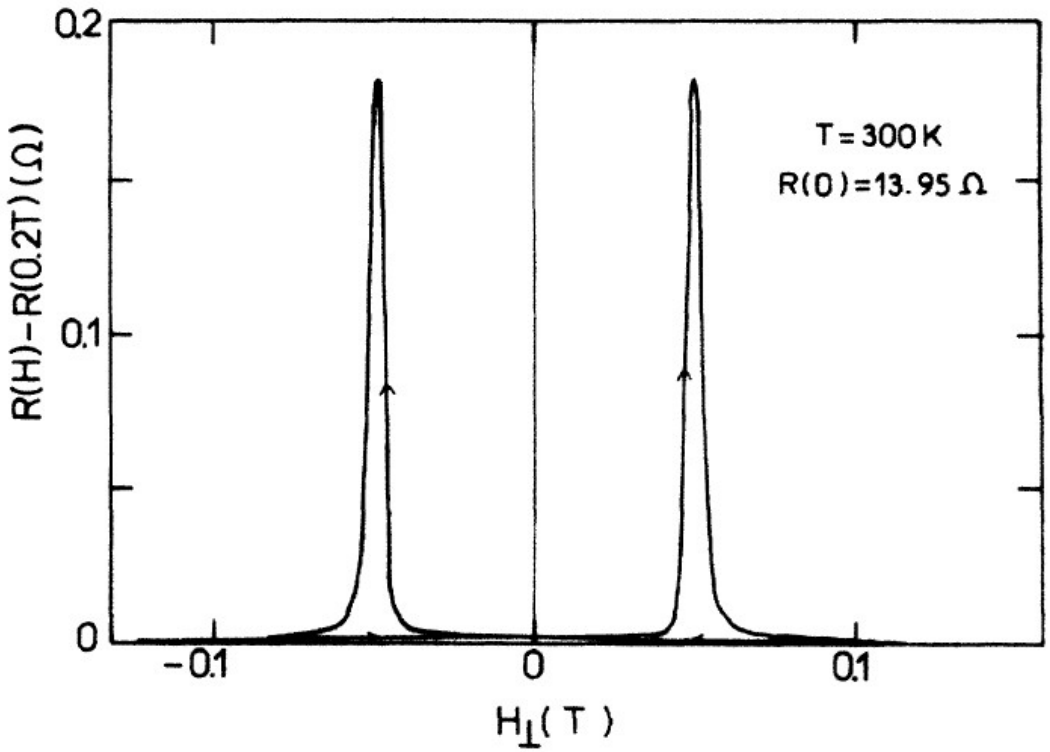

FIG. 3. Room-temperature perpendicular magnetoresistance of sample 3: Au/Co (0.76 nm)/Au (3 nm)/Co (0.76 nm)/Au. The coercive field is H_c=493 G and $\delta R_c/R$=1.3%.

GMR in systems with perpendicular magnetic anisotropy

- two Co layers with slightly different coercive fields
- **first observation of GMR** – before "Nobel papers" by A. Fert and P. Grünberg; the explanation (three different mechanisms proposed) of the effect was not correct

- different ferromagnetic conductors
- antiferromagnet

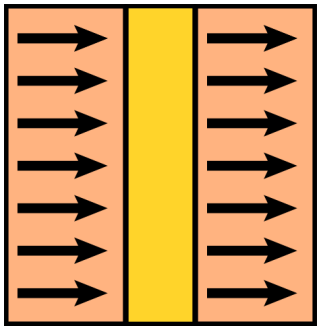

image from: E. Vélu, C. Dupas, D. Renard, J.P. Renard, J. Seiden, Phys. Rev. B **37**, 668 (1988)

Magnetoresistance

Typical GMR systems

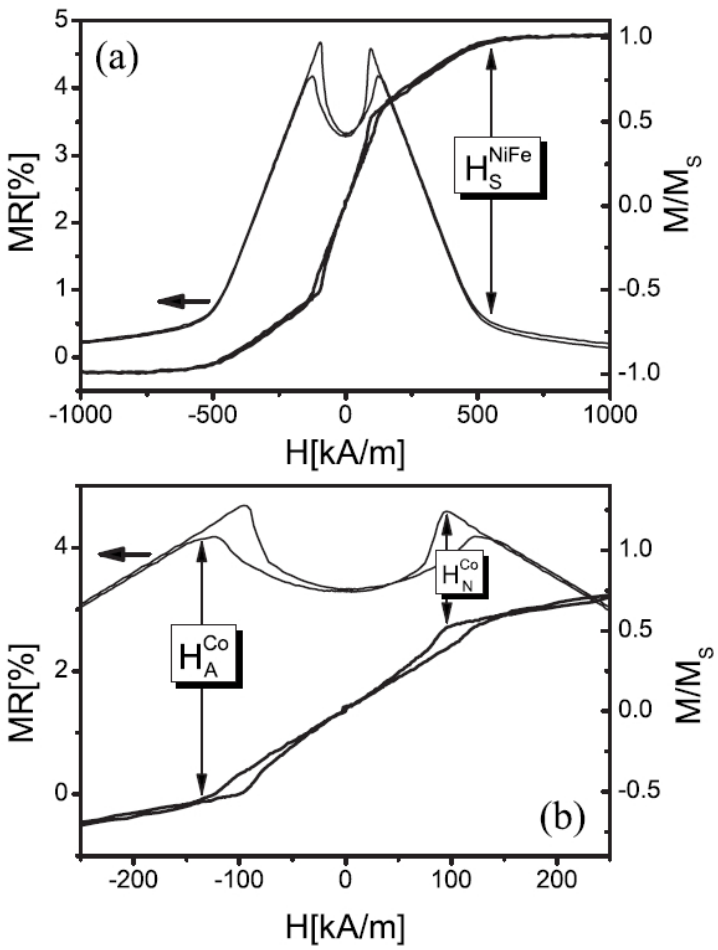

FIG. 1. The magnetization hysteresis and the current-in-plane magnetoresistance of sputtered $[Ni_{80}Fe_{20}(2\ nm)/Au(2.4\ nm)/Co(1.1\ nm)/Au(2.4\ nm)]_{10}$ ML measured with the magnetic field applied perpendicularly to the sample plane (source: Ref. 3). Panel (b) shows a small field range. H_S^{NiFe} denotes a saturation field of the NiFe layers; H_N^{Co} and H_A^{Co} denote nucleation and annihilation fields of the Co domain structure, respectively.

GMR in systems with alternating direction of magnetic anisotropy

- maximal angle between magnetic moments of neighboring magnetic layers approx. 90 deg
- in MIs the domain structure of one layer can influence the reversal of the second layer
- approx. linear* dependence of resistance on the applied perpendicular field strength – sensor applications

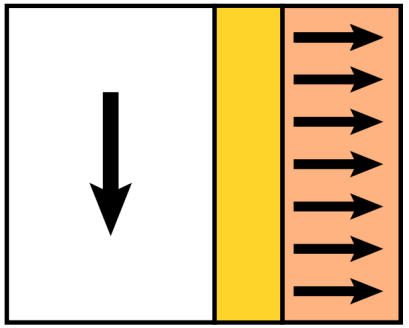

image from: M. Urbaniak, J. Appl. Phys. **104**, 094909 (2008)

*here in the field range approx. 150-400 kA/m, i.e., in the range in which Co layers are magnetically saturated

Magnetoresistance

Switching of magnetic moments by a spin-torque [24]

- spin polarized electrons can transfer their magnetic moment to ferromagnetic layer
- the layer oscillates or switches (changes its magnetization orientation)
- the smaller memory cells require in general higher magnetic field to switch magnetization direction. "*This has an implication on the length of the selection transistor, which has to be large to enable sufficient current for the reversal of the FL magnetization. As a consequence, it becomes difficult to achieve large storage capacity using field switching*" Sbiaa *et al.* [24]
- spin torque transfer random access memories* (STT-RAM) do not require electrodes providing magnetic field – simpler fabrication

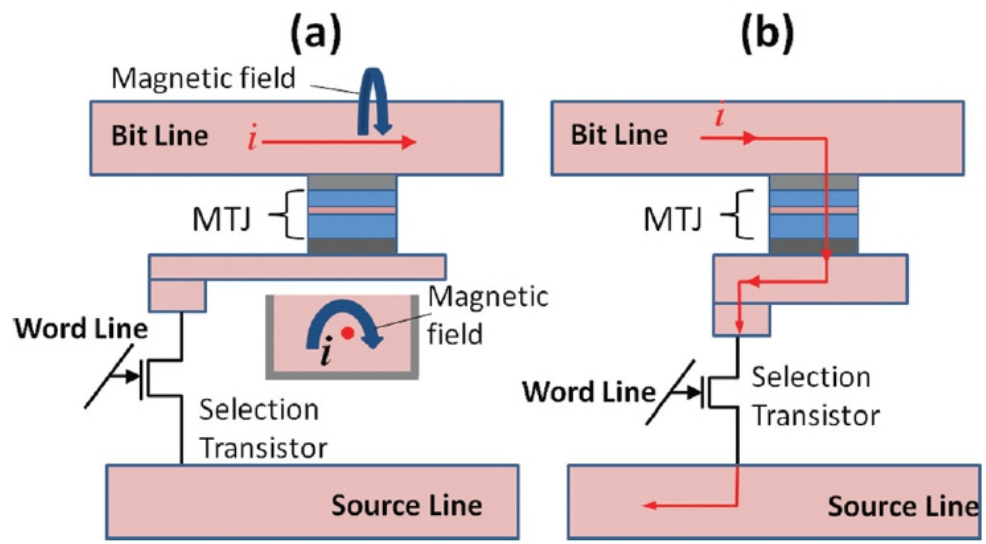

FIG. 1. (Color online) Cell structure including bit and word lines for field switching MRAM (left) and spin transfer torque RAM (right).

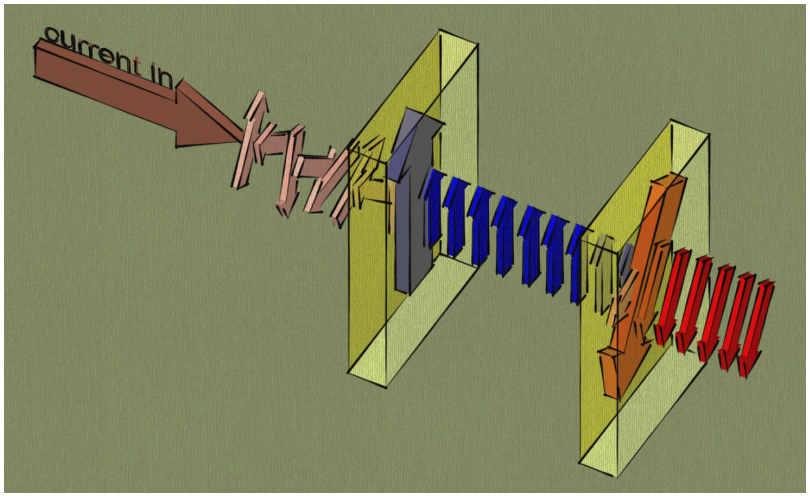

image from R. Sbiaa, S.Y.H. Lu, R. Law, H. Meng, R. Lye, H.K. Tan, J. Appl. Phys. **109**, 07C707 (2011)

*see next lecture

Magnetoresistance

Electric field-induced magnetization reversal [25]

- Ta (5)/Ru (10)/Ta (5)/$Co_{0.2}Fe_{0.6}B_{0.2}$ (0.9)/MgO(1.4)/$Co_{0.2}Fe_{0.6}B_{0.2}$ (1.8)/Ta (5)/Ru(5) is deposited by rf magnetron sputtering on an Al_2O_3 substrate (nanometers)
- CoFeB layers possess a perpendicular magnetic anisotropy
- application of the electric field (through bias voltage) temporarily changes the effective anisotropy of CoFeB
- the magnetization reversal takes place when bias voltage pulse duration is equal to half period of magnetization precession
- it is hoped that electric field-induced switching will require less energy to write a single bit of information than conventional methods (magnetic field or STT); sub pJ energies are sufficient to switch magnetization of a TMR stack with SST [26]

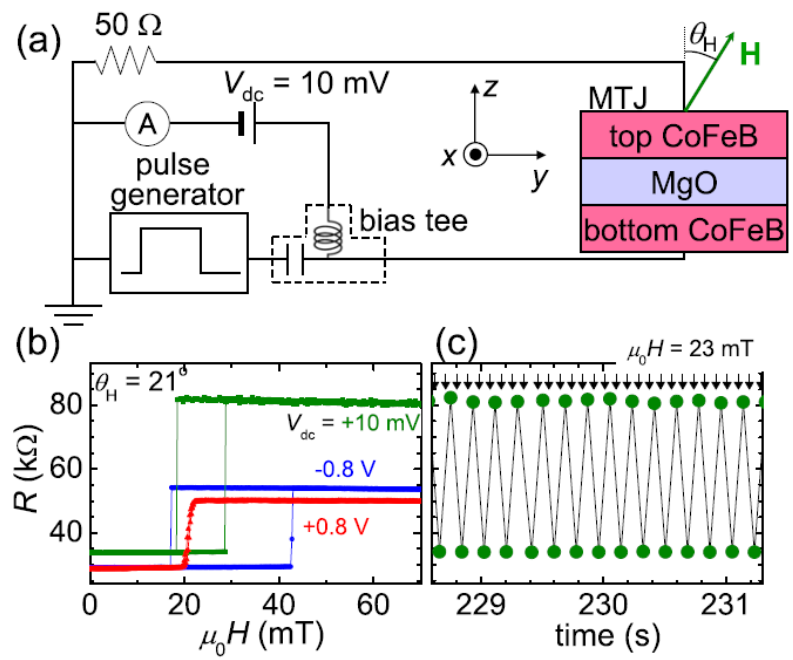

FIG. 2. (a) Schematic of experimental setup. (b) Minor resistance versus magnetic field curves as a function of dc bias voltage. The magnetic field is applied along $\theta_H = 21°$. (c) Resistance measured after the application of voltage pulses of 0.9 V with 1.8 ns duration. Arrows indicate the time at which voltage pulse is applied. The applied magnetic field is 23 mT along $\theta_H = 21°$ and dc bias for measurements is 10 mV.

image from S. Kanai, M. Yamanouchi, S. Ikeda, Y. Nakatani, F. Matsukura, H. Ohno, Appl. Phys. Lett. **101**, 122403 (2012)

Bibliography

[1] wikipedia.org
[2] I.A.Campbell, A.Fert, in “Ferromagnetic Materials” 1982
[3] E. Y. Tsymbal, D. G. Pettifor, *Perspectives of Giant Magnetoresistance*, published in Solid State Physics, ed. by H. Ehrenreich and F. Spaepen, Vol. 56 (Academic Press, 2001) pp.113-237
[4] R. Wawryk, J. Rafalowicz, Cz. Marucha, K. Balcerek, International Journal of Thermophysics **15**, 379 (1994)
[5] R.A. Matula, J.Phys.Chem.Ref.Data **8**, 1147 (1979)
[6] J. Rudny, chapter 3 in *Cienkie warstwy metaliczne* edited by W. Romanowski, PWN, Warszawa 1974
[7] H.-D. Liu, Y.-P. Zhao, G. Ramanath, S.P. Murarka, G.-C. Wang, Thin Solid Films **384**, 151 (2001)
[8] B. Raquet, M. Viret, E. Sondergard, O. Cespedes, R. Mamy, Phys. Rev. B **66**, 024433 (2002)
[9] J.M. Ziman, *Principles of the Theory of Solids*, Cambridge University Press 1972
[10] A. Fert and I. A. Campbell, Phys. Rev. Lett. **21**, 1190 (1968)
[11] J. Sólyom, *Fundamentals of the Physics of Solids*, vol.I, Springer-Verlag Berlin Heidelberg 2007
[12] B.Dieny, *Models in spintronics*, 2009 European School on Magnetism, Timisoara
[13] A.N. Gerritsen, *Metallic Conductivity* in Encyclopedia of Physics, vol.XIX, *Electrical Conductivity I*, Springer 1956
[14] Th.G.S.M. Rijks, R. Coehoorn, M.J.M. De Jonge, Phys. Rev. B **51**, 283 (1995)
[15] A.C. Smith, J.F. Janak, R.B. Adler, *Electronic Conduction in Soilds*, McGraw-Hill, 1967
[16] Ch. Kittel, *Introduction to Solid State physics*, John Wiley & Sons, 2005
[17] S.M Thompson, J. Phys. D: Appl. Phys. **41**, 093001 (2008)
[18] K. Esfarjani, Semiclassical Transport, lecture notes, 2010
[19] G.D. Mahn, Many-Particle Physics, Plenum Press, 1990
[20] J.Barnaś, A. Fuss, R.E. Camley, P. Grunberg, W. Zinn, Phys. Rev. B **42**, 8110 (1990)
[21] A. Fert, P. Bruno, *Interlayer Exchange Coupling and Magnetoresistance in Multilayers* in Ultarthin Magnetic Structures II, ed. by B. Heinrich, J.A.C. Bland, Springer 1994
[22] B. Dieny, V.S. Speriosu, S.S.P. Parkin, B.A. Gurney, D.R. Wilhoit, D. Mauri, Phys. Rev. B **43**, 1297 (1991)
[23] J. Barnaś, O. Baksalary, A. Fert, Phys. Rev. B **56**, 6079 (1997)
[24] R. Sbiaa, S.Y.H. Lu, R. Law, H. Meng, R. Lye, H.K. Tan, J. Appl. Phys. **109**, 07C707 (2011)
[25] S. Kanai, M. Yamanouchi, S. Ikeda, Y. Nakatani, F. Matsukura, H. Ohno, Appl. Phys. Lett. **101**, 122403 (2012)
[26] S. Kanai, Y. Nakatani, M. Yamanouchi, S. Ikeda, F. Matsukura, and H. Ohno, Appl. Phys. Lett. **103**, 072408 (2013)

Bibliography

[27] J. Unguris, R. J. Celotta, and D. T. Pierce Phys. Rev. Lett. **67**, 140 (1991)
[28] M.N. Baibich, J.M. Broto, A. Fert, F. Nguyen Van Dau, F. Petroff, P. Eitenne, G. Creuzet, A. Friederich, J. Chazelas, Phys. Rev. Lett. **61**, 2472 (1988)
[29] G. Binasch, P. Grünberg, F. Saurenbach, W. Zinn, Phys. Rev. B **39**, 4828 (1989)
[30] M. Getzlaff, Fundamentals of Magnetism, Springer 2008
[31] S.Y. Hsu, A. Barthélémy, P. Holody, R. Loloee, P. A. Schroeder, A. Fert, Phys. Rev. Lett. **78**, 2652 (1997)
[32] E. Vélu, C. Dupas, D. Renard, J.P. Renard, J. Seiden, Phys. Rev. B **37**, 668 (1988)
[33] F. Stobiecki, T. Luciński, R. Gontarz, M. Urbaniak, Materials Science Forum **287**, 513 (1998)
[34] G. Ibach, Physics of Surfaces and Interfaces, Springer 2006
[35] H. Alloul , Introduction to the Physics of Electrons in Solids, Springer 2011

Acknowledgment

During the preparation of this, and other lectures in the series "*Magnetic materials in nanoelectronics – properties and fabrication*" I made an extensive use of the following software for which I wish to express my gratitude to the authors of these very useful tools:

- OpenOffice www.openoffice.org
- Inkscape inkscape.org
- POV-Ray www.povray.org
- Blender www.blender.org
- SketchUp sketchup.com.pl

I also used "Fizyczne metody osadzania cienkich warstw i metody analizy powierzchniowej" lectures by Prof. F. Stobiecki which he held at Poznań University of Technology in 2011.

version 2014.04.08

Special thanks are due to Google team as I used the search engine extensively.